7-15-2011 12:00 AM

The Regulation of Cell Division and Neurogenesis by the Chromatin Remodeling Protein ATRX

Kieran L. Ritchie
The University of Western Ontario

Supervisor
Dr. Nathalie Berube
The University of Western Ontario

Graduate Program in Biochemistry
A thesis submitted in partial fulfillment of the requirements for the degree in Doctor of Philosophy

THE REGULATION OF CELL DIVISION AND NEUROGENESIS BY THE CHROMATIN REMODELING PROTEIN ATRX

(Spine title: Regulation of Cell Division and Neurogenesis by ATRX)

(Thesis format: Integrated Article)

by

Kieran Lawren Ritchie

Graduate Program in Biochemistry

A thesis submitted in partial fulfillment
of the requirements for the degree of
Doctor of Philosophy

The School of Graduate and Postdoctoral Studies
The University of Western Ontario
London, Ontario, Canada

THE UNIVERSITY OF WESTERN ONTARIO
School of Graduate and Postdoctoral Studies

CERTIFICATE OF EXAMINATION

Supervisor

Dr. Nathalie Bérubé

Supervisory Committee

Dr. Fred Dick

Dr. Joe Torchia

Examiners

Dr. Susan Meakin

Dr. David Litchfield

Dr. Dale Laird

Dr. Mike Hendzel

The thesis by

Kieran Lawren Ritchie

entitled:

THE REGULATION OF CELL DIVISION AND NEUROGENESIS BY THE CHROMATIN REMODELING PROTEIN ATRX

is accepted in partial fulfillment of the
requirements for the degree of
Doctor of Philosophy

Date

Chair of the Thesis Examination Board

Abstract

Mutations in the human *ATRX* gene cause alpha-thalassemia mental retardation X-linked (ATR-X) syndrome associated with severe cognitive and behavioural deficits, seizures, and microcephaly, indicating that *ATRX* is an essential factor in the normal development of the central nervous system (CNS). Conditional inactivation of *Atrx* in the developing mouse forebrain leads to a reduction in cerebral cortical size, elevated levels of p53-dependent neuronal apoptosis, and cortical dysgenesis, confirming a broad requirement for *Atrx* in mammalian brain development. The mammalian *ATRX* gene encodes a member of the Snf2 family of chromatin remodeling proteins and was originally defined as a transcriptional regulator, however at the commencement of this research project no ATRX gene targets had yet been linked to CNS development. In contrast, ATRX is highly enriched at pericentromeric heterochromatin in somatic and germ cells where it is required for normal meiotic cell division, however a requirement for ATRX in mitotic cell division has not yet been reported. In chapters two and three, I investigated this by using RNAi to deplete ATRX levels in a human cancer cell line and found that cells depleted of ATRX showed mitotic dysfunction including chromosome congression and alignment defects and chromosome bridging, and reduced centromeric sister chromatid cohesion and elevated levels of cytokinetic failure and multinucleation. Furthermore, mitotic neuronal progenitor cells from the embryonic *Atrx*-null mouse forebrain display mitotic dysfunction *in vitro* and *in vivo*, suggesting that the requirement for ATRX in normal cortical development and mitotic cell division might be linked. Binary control of neuronal progenitor proliferation or differentiation is considered the primary mechanism of mammalian cortical neurogenesis in the developing brain, and is thought to be determined primarily by the regulation of asymmetric progenitor cell division. In chapter four I report that apical neuronal progenitors of the *Atrx*-null forebrain display a disruption in the balance of symmetric to asymmetric cell divisions, leading to an altered complement of differentiated neurons in the postnatal cortex, providing a novel requirement for ATRX in cortical development. Taken together, this data present a novel role for the chromatin remodeling protein ATRX in mitotic cell division and cortical neurogenesis.

Keywords

ATRX, ATR-X, Mitosis, Cytokinesis, Neurogenesis, Snf2, Chromatin remodeling, Cell Division, Neurodevelopment, Pericentromeric heterochromatin

Co-Authorship Statement

I participated in the design of all experiments presented in this thesis, and conducted all of the experiments with the exception of the following:

In chapter two, the western blot represented in Figure 2-1B was conducted by C Seah. The microscopy and quantification represented in Figure 2-1D,E was conducted by J Moulin and NG Bérubé. The immunofluorescence represented in figure 2-5A was conducted by C Seah. The flow cytometry represented in Figure 2-2B was performed by C Isaac.

In chapter three, the RNA interference and imaging represented in Figure 3-1 was conducted by J Moulin and NG Bérubé. The immunofluorescence staining represented in Figure 3-5 was conducted by LA Watson.

Acknowledgements

All of the work presented in this thesis would never have been possible without the dedication of many talented researchers and support staff in the Bérubé lab, the Victoria Research Labs, and London Regional Cancer Centre.

First and foremost I thank my supervisor Dr. Nathalie Bérubé for her guidance and support. Her tireless effort was a great benefit to me from the day I stepped into the lab and into the amazing world of biomedical research.

My supervisory committee of Dr. Frederick Dick and Dr. Joseph Torchia gave me immensely valuable perspectives on my research, and their expertise was a great asset in guiding me along this challenging but rewarding path.

I met and worked with many amazing and talented people during my time at the VRL. A special thanks to Claudia Seah, Yan Jiang, and Xu Wang who somehow found the time to tutor, train, explain, supervise, correct, and help me for the past 6 years. I'm glad to have worked alongside a number of great trainees, all of whom have given me great memories I will always fondly remember, especially Mike, Kristin, Ashley, Deanna, and Kris from the Bérubé lab, Courtney, Srikanth, Matt, Christian, and Craig.

Dedication

For my family. My father Don, my mother Susan, my brother Matthew, and my wife Anju. None of this would ever have been possible without your endless love and support.

Table of Contents

List of Figures

List of Appendices

List of Abbreviations

Abbreviation	Meaning
γ-TuRC:	γ-tubulin ring complex
ADD:	ATRX-DNMT3-DNMT3L
ANOVA:	Analysis of Variance
AO:	Anaphase onset
APC/C:	Anaphase-promoting complex/cyclosome
ASPM:	Abnormal spindle-like microcephaly-associated
ATCC:	American type culture collection
ATM:	Ataxia telangiectasia mutated
ATP:	Adenosine triphosphate
ATPase:	Adenosine triphosphatase
ATR:	Ataxia and telangiectasia and Rad3 related
ATRX, ATR-X:	Alpha thalassemia/mental retardation X-Linked
BSA:	Bovine Serum Albumin
BUB1:	Budding inhibited by benzimidazoles 1
BUBR1:	BUB1 related kinase
C-terminal:	Carboxy terminal
CAF-1:	Chromatin assembly factor 1
CDC:	Cell division cycle
CDK5RAP2:	Cyclin-dependent kinase 5 regulatory-associated protein 2
CdLS:	Cornelia DeLange syndrome
cDNA:	Complimentary DNA
CDS:	Coding sequence
CDK:	Cyclin-dependent kinase

CENP(C/E/F/J):	Centromere-associated protein (C/E/F/J)
CHD1:	Chromodomain helicase DNA-binding protein 1
CitK:	Citron kinase
Co-IP:	Co-immunoprecipitation
CMF-PBS:	Calcium magnesium free PBS
CNS:	Central nervous system
CP:	Cortical plate
CREST:	Calcinosis, Raynaud's phenomenon, esophageal dismotility, sclerodactyly, and telangiectasia
CSD:	Chromoshadow domain
Ct:	threshold cycle
d:	days
DAPI:	4'6-diamidino-2-phenylindole
DMEM:	Dulbecco's modified eagle's medium
DNA:	Deoxyribonucleic acid
DNMT(3A/B):	DNA methyltransferase (3A/B)
DNMT3L:	DNA methyltransferase 3-like
dNTPs:	Deoxyribonucleotide triphosphate
DTT:	Dithiothreitol
E:	Embryonic day
ECL:	Enhanced chemiluminescence
EDTA:	Ethylenediamine tetracetic acid
EDTA:	Ethylene gycol tetraacetic acid
ESCs:	Embryonic stem cells
ESCO2:	Establishment of cohesion homolog 2
EtOH:	Ethyl hydroxide

FBS:	Fetal bovine serum
G1:	Growth phase 1
G2:	Growth phase 2
G4:	G-quadruplex
GAPDH:	Glyceraldehyde 3 phosphate dehydrogenase
GEF:	Guanine exchange factor
GFP:	Green fluorescent protein
GTPase:	Guanosine triphosphatase
h:	Hours
H2B:	Histone 2B
H3K4me0:	Histone H3 lysine 4 unmethylated
H3K4me3:	Histone 3 lysine 4 trimethylation
H3K9me3:	Histone 3 lysine 9 trimethylation
H3S10:	Histone 3 serine 10
HEPES:	4-(2-hydroxyethyl)-1-piperazineethanesulfonic acid
HG:	HeLa-H2B-GFP
HIRA:	Histone cell cycle regulation defective homolog A
HP1 (α/β/γ):	Heterochromatin binding protein 1 (α/β/γ)
HRP:	Horseradish peroxidase
ISWI:	Imitation switch
JNK:	c-Jun-N-terminal kinase
kb:	Kilobase
KCl:	Potassium chloride
kDa:	Kilodalton
LV:	Lateral ventricle

MII:	Metaphase II
MAPK:	Mitogen activated protein kinase
MAPKAP:	MAPK-activated protein
mATRX:	Mouse ATRX
mb:	Megabases
MCPH:	Microcephaly, primary autosomal microcephaly
MCPH1:	Microcephalin
MeCP2:	Methyl-CpG binding protein 2
MEFs:	Mouse embryonic fibroblasts
mESCs:	Mouse ESCs
MOT1:	Modifier of transcription 1
MPF:	Mitosis promoting factor
mRNA:	Messenger RNA
n:	number
NA:	numerical aperture
NaCl:	Sodium chloride
NE:	Neuroepithelium
NEBD:	Nuclear envelope breakdown
NIPBL:	Nipped-B-like
NP:	Neural progenitor
NPC:	Neural progenitor cell
NuRD:	Nucleosome remodeling and deacetylase
OCT:	Optimal cutting temperature
PAGE:	Polyacrylamide gel electrophoresis
PAR-3:	Partitioning defective 3 homolog

PBS:	Phosphate buffered saline
PCH:	Pericentromeric heterochromatin
PCR:	Plymerase chain reaction
PFA:	Paraformaldehyde
PHB2:	Prohibitin 2
PHD:	Plant homeodomain
PHEM buffer:	PIPES, HEPES, EDTA, $MgCl_2$ buffer
PI:	Propidium iodide
PI3K:	Phosphoinositide 3-kinase
PLK1:	Polo-like kinase 1
PML-NB:	Promyelocytic leukemia nuclear body
PMSF:	Phenylmethylsulfonyl fluoride
PNS:	Peripheral nervous system
Poly(A):	Polyadenylation
qRT-PCR:	Quantitative real time PCR
rATRX:	Recombinant ATRX
RIPA:	Radioimmunoprecipitation assay
RNA:	Ribonucleic acid
RSC:	Remodels the structure of chromatin
RT:	Reverse transcriptase
S:	Synthesis phase
SAC:	Spindle assembly checkpoint
SDS:	Sodium dodecyl sulphate
SF2:	Superfamily 2
Sgo:	Shugoshin

shRNA:	short hairpin RNA
siRNA:	small interfering RNA
SMC:	Structural maintenance of chromosomes
SNAP:	Soluble *N*-ethylmaleimide-sensitive fusion protein-attachment protein
SNARE:	SNAP receptor
Snf2:	Sucrose non-fermenting 2
Suv39H1:	Supressor of variegation 3-9 homolog 1
SVZ:	Subventricular zone
SWI/SNF:	Switching defective/sucrose non-fermenting
t-SNARE:	Target SNARE
v:	version
vSNARE:	Vesicle SNARE
VZ:	Ventricular zone
VNTR:	Variable nucleotide tandem repeat
Wapl:	Wings apart-like

Chapter 1

1 Introduction

1.1 General Introduction

Mitotic cell division (Mitosis) is one of the most fundamental processes in the life cycle of every eukaryotic cell. In essence, the objective of mitosis is to transmit a replicated copy of the parental genome to two daughter cells. However, with the emergence of multicellular organisms, with diverse tissues and organs, mitotic cell division is no longer solely a process of genetic replication, but is a critical aspect of the global developmental process. Progenitor cells can give rise to a variety of different cell types within a tissue, a process that is often governed by asymmetric (or 'unequal') cell division (Horvitz and Herskowitz, 1992). Many studies have shown that asymmetric cell division in the developing mammalian brain is critical for normal brain development, and it is believed that disturbances in this process underlie some human intellectual disability disorders [Reviewed in (Kaindl et al., 2009)]. Mutations in the *ATRX* gene cause a mental retardation syndrome called alpha thalassemia mental retardation X-linked (ATR-X). Studies in the mouse have confirmed a requirement for ATRX in normal brain development, however the precise role of ATRX in neurodevelopment is largely unknown, and is the topic of this thesis.

1.2 The *ATRX* Gene and Protein

1.2.1 The *ATRX* Gene Encodes a Member of the Snf2 Family of Chromatin Remodeling Proteins

The human *ATRX* gene contains 36 exons spanning over 300 kilobases (kb) of genomic DNA on the X chromosome (Xq13.3) (Gibbons et al., 1995b; Gibbons et al., 1995a; Picketts et al., 1996). The gene produces two major protein isoforms, a full length 280 kilodalton (kDa) protein (ATRX) encoded by a 10.5 kb messenger RNA (mRNA) (NM_000489.3), and a ~200 kDa truncated protein, ATRXt, encoded by a ~7 kb mRNA transcript truncated at exon 11 by an alternative splicing event that retains this intron and leads to the use of a proximal intronic poly(A) signal (Garrick et al., 2004). The mouse

Atrx gene shows a similar genomic structure to its human homolog, and encodes a protein (mATRX) of similar molecular weight with broad regions of high sequence conservation (Picketts et al., 1998). Both major protein isoforms are highly conserved in human and mouse, suggesting that each likely fulfill important biological functions in both organisms (Garrick et al., 2004). Because of this homology the mouse has been used extensively as a model to study many aspects of the *Atrx* gene and protein, particularly its role in development. *ATRX* transcripts have been detected in all human and mouse tissues examined to date, however the relative transcript abundance varies widely, as does the ratio between the two major transcripts (Gecz et al., 1994; Garrick et al., 2004). An examination of ATRX expression in various human tissues found that, in human fetal tissues *ATRX* mRNA expression is highest in the brain, where the full-length transcript is most abundant. In other fetal tissues where expression levels are lower, each transcript is present in roughly equivalent amounts. In contrast, *ATRX* is poorly expressed in the adult brain, but is most abundant in skeletal muscle, where again the full-length transcript predominates (Garrick et al., 2004). These observations support the hypothesis that the two major isoforms perform independent biological functions, and are subjected to different regulatory mechanisms in a variety of tissues throughout development.

The full-length ATRX protein isoform contains two major conserved domains, (1) a carboxyterminal (C-terminal) helicase/adenosine triphosphatase (ATPase) domain belonging to the Sucrose non-fermenting 2 (Snf2) family of helicase-related chromatin remodeling enzymes, and (2) an N-terminal [ATRX-DNMT3-DNMT3L (ADD)] domain containing a plant homeodomain (PHD)-like zinc finger (Figure 1-1) (Picketts et al., 1996). The major truncated isoform, ATRXt, retains the N-terminal ADD domain but lacks the C-terminal Snf2 domain, likely conferring a unique biological function distinguishing the two isoforms (Garrick et al., 2004). Sequence similarity between ATRX and mATRX are highest within these 2 domains (>90%), suggesting conservation of important functional properties between the two homologs (Picketts et al., 1998).

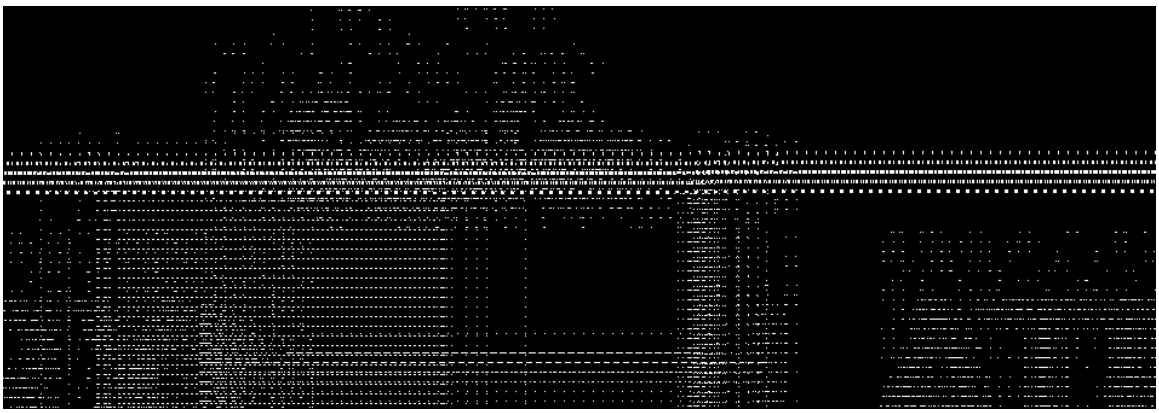

Figure 1-1. Schematic of the ATRX protein domain structure

The full length ATRX, and truncated ATRXt protein are depicted above. Major domains are shown: the PHD zinc finger-like domain (ADD), Snf2 chromatin remodeling domain (Helicase domain), the P box a (P), and glutamine-rich region (Q). Below is a representation of the amino acid similarity between the human and mouse proteins.

Reproduced with permission from: Gibbons et al. (2008) Human Mutation 29(6):796-802

1.2.2 The ATRX Snf2 Domain

The Snf2 protein family belongs to the SF2 superfamily of ATP-hydrolysing DNA and RNA helicases, which are characterized by a conserved stretch of seven short collinear helicase motifs (I, Ia, II, III, IV, V, VI), and have been found in all eukaryotes (Gorbalenya et al., 1988; Singleton et al., 2007). Structurally, this array of motifs is organized into two recA-like domains with an active cleft between them, allowing the transformation of chemical energy from ATP hydrolysis into mechanical motion (Subramanya et al., 1996; Flaus et al., 2006). Members of the large Snf2 protein family are generally believed to utilize the energy of ATP hydrolysis to act as the catalytic molecular motor subunits of larger multi-protein complexes involved in many DNA and chromatin-dependent processes (Knizewski et al., 2008). Snf2 proteins have been identified in many such complexes, including transcription-coupled repair (ERCC6 subfamily), nucleotide excision repair (RAD16), recombination repair (RAD54 subfamily), replication and gene-specific transcriptional activation (SNF2 subfamily), transcriptional repression (MOT1), destabilization of reconstituted nucleosomes (SNF2 and SNF2L subfamilies) and chromosome segregation and mitotic recombination (lodestar) [Reviewed in (Carlson and Laurent, 1994)]. Based on sequence alignment data, ATRX has been classified within the Rad54-like subfamily of Snf2 proteins (Flaus et al., 2006). Despite the presence of the conserved 'helicase'-like motif, no member of the Snf2 family has been shown to possess DNA or RNA helicase (unwinding of double-stranded nucleic acids) activity (Pazin et al., 1997). Rather, most Snf2 family members exhibit ATP-dependent DNA translocation, and likely exert their biological effects through the disruption of DNA-nucleosome interactions, known as chromatin remodeling, as they translocate along a chromatin substrate, thereby altering the accessibility of nucleosomal DNA to functionally specific auxiliary proteins like transcription factors and DNA repair proteins [Reviewed in (Kingston et al., 1996; Mohrmann and Verrijzer, 2005; Clapier and Cairns, 2009)].

Initial *in vitro* studies confirmed that the helicase domain of recombinant ATRX (rATRX) does in fact possess ATPase activity at levels similar to other Snf2 proteins (SNF2H, SNF2L) that was stimulated (2-fold) by the presence of mononucleosomes, but

not by naked DNA (Tang et al., 2004). More recently it was shown that the ATPase activity of rATRX can be stimulated by naked DNA (9-fold) and mononucleosomes (4-fold), consistent with the known enzymatic properties of the Rad54 subfamily of Snf2 proteins to which ATRX belongs (Mitson et al., 2011), however the cause of the disparity between the two studies is unknown. Many Snf2 proteins utilize ATP hydrolysis to fuel DNA translocase activity (Lia et al., 2006; Amitani et al., 2006), which is classically measured by the ability of the enzyme to displace a third strand of DNA wrapped around a DNA double helix, known as a DNA triple helix (Saha et al., 2002; Jaskelioff et al., 2003; Whitehouse et al., 2003; Dürr et al., 2005). Triple-helix displacement activity has been confirmed for rATRX (Xue et al., 2003), and has been shown to depend upon intact ATPase activity (Mitson et al., 2011), confirming that the Snf2 domain of ATRX acts as an ATP-dependent DNA translocase consistent with its conserved sequence similarity to the Snf2 protein family.

1.2.3 The ATRX ADD Domain

The N-terminal ADD domain of ATRX is a cysteine-rich region containing a PHD-like zinc finger, a GATA-like zinc finger, and a flanking C_2C_2 α-helical motif, that assemble into a large globular domain through extensive hydrophobic interactions (Argentaro et al., 2007). This region is highly related to, and unique to, the DNA methyltransferase 3 (DNMT3) family of de-novo DNA methyltransferases (DNMT3A, DNMT3B, and DNMT3L) (Xie et al., 1999; Aapola et al., 2000; Argentaro et al., 2007). Zinc fingers are common in chromatin-associated proteins and generally act to mediate protein-protein interactions that are thought to function primarily as tethers to chromatin via interactions with exposed histone tails (Bienz, 2006). Not surprisingly, the ADD domain of DNMT3A and DNMT3L interact with unmodified histone H3 tails (Ooi et al., 2007; Otani et al., 2009), and ATRX has been found to associate with chromatin through specific histone modifications. The ADD domain of ATRX can bind to histone H3 tails that are trimethylated at lysine 9 (H3K9me3) and unmethylated at lysine 4 (H3K4me0) (Dhayalan et al., 2011), and has recently been proposed to interact with the lysine 4 residue of the histone variant H3.3 in mouse embryonic stem (ES) cells (Wong et al., 2010).

Functionality of PHD domains depends on the coordinated binding of zinc ions within a conserved hydrophobic core that stabilizes protein folding (Frankel et al., 1987; Shi and Berg, 1995). Although not identical in sequence to known PHD and GATA zinc fingers, the structure of the ATRX-ADD domain has been solved and shown to bind zinc ions in a configuration highly similar to those reported for GATA-1 and PHD fingers (Argentaro et al., 2007). The zinc finger of GATA-1 is able to bind directly to target DNA elements, and the domain structure of the ATRX-ADD domain suggests a similar basic patch on α-helix 1 may be used for DNA binding (Argentaro et al., 2007), supported by the observation that the ATRX-ADD domain can bind DNA homopolymers *in vitro* (Cardoso et al., 2000).

Interestingly, the Snf2 and ADD domains are separated by a large unstructured stretch of ~1300 amino acid residues. It has been speculated that this placement of a long, potentially flexible, linker region between these two domains is a functionally important feature of the structure of ATRX (Mitson et al., 2011), as this region is also conserved in chicken and frog.

1.2.4 ATRX Function

In mammalian cells, ATRX is a nuclear protein and >50% of total ATRX is tightly associated with DNA and/or chromatin, consistent with the presence of the conserved domains in ATRX that are commonly found in chromatin associated proteins (McDowell et al., 1999). ATRX is enriched primarily at pericentromeric heterochromatin (PCH), and at promyelocytic nuclear bodies (PML-NBs), and has more recently been localized to telomeric chromatin, and some euchromatic sites. It is believed that ATRX functions primarily as a regulator of gene transcription and of condensed heterochromatin through distinct mechanisms, including direct DNA binding, regulation of genomic imprinting, and deposition of specific histone subunits at a variety of genomic regions.

1.2.5 ATRX Interacts With the Death-Domain Associated Protein DAXX

Because SWI/SNF family proteins are typically found in large nuclear chromatin remodeling complexes, early studies focused on characterizing the potential binding

partners of ATRX, and the nature of the potential complexes to which it belonged. Co-immunoprecipitations (Co-IPs) from human and mouse cells identified a specific interaction between ATRX and the death domain associated protein DAXX (Xue et al., 2003; Tang et al., 2004; Ishov et al., 2004). DAXX is a multifunctional protein found primarily in the nucleus where it localizes to PML-NBs (Ishov et al., 1999; Everett et al., 1999; Torii et al., 1999) and condensed chromatin (Ishov et al., 1999) and interacts with multiple transcription factors, including Pax3, Pax5 and ETS1, and other chromatin associated proteins DNA methyltransferase 1, histone deacetylases, and core histones (Hollenbach et al., 1999; Li et al., 2000; Hollenbach et al., 2002; Lin et al., 2003a). Because of this, DAXX is believed to function primarily as a transcriptional regulator.

Peptide studies revealed that most of the total full length ATRX pool is associated in near equimolar amounts with DAXX in human nuclear extracts (Xue et al., 2003), suggesting that ATRX function might depend primarily on this association. These early studies found that the ATRX-DAXX complex possesses ATP-dependent chromatin remodeling activity, suggesting that together these proteins might influence a range of DNA-dependent processes through the modulation of chromatin structure (Xue et al., 2003; Tang et al., 2004).

1.2.6 The ATRX/DAXX Complex Localizes to PML-NBs and Constitutive Heterochromatin

In both human and mouse cells, ATRX is primarily enriched at PCH throughout the cell cycle (McDowell et al., 1999). Pericentromeric heterochromatin is a constitutively condensed region of heterochromatin flanking the centromeres of eukaryotic chromosomes, and is essential for the normal organization and function of the centromere, kinetochore assembly, and mitotic cell division [reviewed in (Pidoux and Allshire, 2005)]. Distinct mechanisms appear to recruit ATRX to PCH in mammalian cells. The methyl-CpG binding protein 2 (MeCP2) and ATRX interact *in vitro*, and MeCP2 is required for the proper colocalization of ATRX to PCH in cortical neurons from the adult mouse brain (Nan et al., 2007). ATRX also interacts with the heterochromatin binding protein 1 (HP1) family of proteins (Le Douarin et al., 1996; McDowell et al., 1999; Bérubé et al., 2000), and HP1α has been shown to recruit ATRX

to PCH in mESCs (Kourmouli et al., 2005). HP1 proteins are an integral component of condensed chromatin at pericentric regions, and loss of HP1, or the yeast homolog Swi6, leads to loss of heterochromatin, centromeric instability and mitotic defects (Ekwall et al., 1995; Amor et al., 2004). A growing number of chromatin remodeling enzymes have been found to maintain the structural integrity of PCH, with deficiencies leading to mitotic abnormalities (Lejeune et al., 2007; Bourgo et al., 2009). Interestingly, depletion of ATRX in mouse oocytes leads to mitotic spindle and chromosome segregation defects, and centromere dysfunction, including centromere fusions, and centromere containing micronuclei (De La Fuente et al., 2004; Baumann et al., 2010) DAXX colocalizes to PCH with ATRX during S-phase in mouse embryonic fibroblasts (MEFs) (Ishov et al., 2004; Drané et al., 2010), and ATRX is required to recruit DAXX to PCH in mouse oocytes (Baumann et al., 2010). Interestingly, Daxx knockout MEFs are prone to forming bi-nucleated cells, suggesting a defect in cell division in these cells (Ishov et al., 2004).

Within the nucleus, ATRX also co-localizes with DAXX at PML-NBs in human and mouse cells (Xue et al., 2003; Ishov et al., 2004), and the recruitment of ATRX to these sites is mediated by DAXX. PML-NBs are large nuclear protein complexes implicated in nearly every cellular process, making functional classification difficult (Quimby et al., 2006; Shen et al., 2006). It is generally believed that PML-NBs serve two primary functions, (1) as protein depots that sequester abnormal proteins related to pathological conditions, and (2) to act as catalytic surfaces where proteins accumulate to be post-translationally modified (Bernardi and Pandolfi, 2007). More recently it has been proposed that PML-NBs could in fact be active sites for such nuclear functions as transcriptional regulation and chromatin remodeling (Lallemand-Breitenbach and de Thé, 2010).

1.2.7 ATRX and DAXX Deposit H3.3 at Specific Genomic Regions

Recently several independent studies have identified a novel role for the ATRX-DAXX complex in the incorporation of the histone variant H3.3 at specific genomic regions, including telomeres and pericentric heterochromatin (Goldberg et al., 2010; Wong et al., 2010; Drané et al., 2010; Lewis et al., 2010).

Histones can regulate chromatin function through the use of covalent post-translational modification (phosphorylation, methylation, acetylation, ubiquitylation) of amino acid residues on their tail domains, and by the use of non-allelic histone variants [Reviewed in (Kamakaka and Biggins, 2005)]. In mammals, the histone variant H3.3 varies from the canonical H3 (H3.1) at only 5 amino acids, which give H3.3 unique properties, such as targeting to specific chromatin domains. Unlike H3.1, H3.3 can be incorporated into chromatin outside of S-phase, and is typically associated with sites of active DNA transcription. These differences likely reflect the interactions of the histones with different assembly factors, termed histone chaperones. In human cells, H3.1 is found mainly in a complex with the DNA replication dependent chaperone Chromatin Assembly Factor 1 (CAF-1) while H3.3 is found with the DNA replication independent chaperones HIRA or CHD1 (Tagami et al., 2004; Konev et al., 2007).

Surprisingly, ATRX and DAXX were recently identified in purified histone H3.3, but not H3.1 preassembly complexes from HeLa cells (Drané et al., 2010; Lewis et al., 2010). A purified complex of ATRX-DAXX can assemble and mobilize H3.3/H4 containing nucleosomes on a DNA template *in vitro,* indicating that this heterodimer possesses chromatin remodeling activity specific to H3.3-nucleosomes (Lewis et al., 2010).

Depletion of ATRX or DAXX in mouse embryonic fibroblasts (MEFs) using RNAi reduced the amount of H3.3 deposition at pericentromeric heterochromatin, resulting in a downregulation of pericentric repeat transcripts in these cells (Drané et al., 2010). It has recently been shown that pericentric repeats are highly transcribed in mammalian cells, and paradoxically in yeast these transcripts are required for the RNAi mediated heterochromatinization of PCH (Grewal and Elgin, 2007), and disruption of this pathway in yeast leads to loss of PCH and centromeric dysfunction leading to mitotic defects (Verdel and Moazed, 2005).

In addition, ATRX is also enriched at telomeric chromatin in pluripotent mouse ES cells (ESCs) during interphase, when telomeric DNA is undergoing replication and processing (Wong et al., 2010). In *Atrx*-null ESCs, H3.3 is depleted from telomeric regions, and there is an upregulation of telomere specific transcripts (Telomeric repeat containing

RNA, TERRA) in these cells, suggesting loss of a repressive/silent heterochromatic environment (Goldberg et al., 2010). PHD fingers have a marked preference for binding histone H3 lysine 4 (H3K4), and the interaction between ATRX and H3.3 is lost when the K4 residue of H3.3 is mutated, which also prevents the telomeric localization of ATRX (Wong et al., 2010). In contrast, ATRX is not found in the H3.3 complex in $DAXX^{-/-}$ MEFs, indicating that DAXX is also required for the association of ATRX with H3.3 (Lewis et al., 2010).

1.2.8 Mutations in the *ATRX* Gene Cause X-linked Mental Retardation

The human *ATRX* gene (MIM# 300032) was first described in 1995. Mutations in this gene cause ATR-X syndrome (Alpha-Thalassemia mental Retardation, X-linked) syndrome (MIM# 301040), a severe form of X-linked mental retardation (XLMR) that occurs almost exclusively in males (Gibbons et al., 1992; Gibbons et al., 1995b; Gibbons et al., 1995a). Signs of ATR-X syndrome are evident at birth, and constitute a broad but remarkably uniform phenotypic spectrum affecting many bodily organs, most notably the central nervous system. Typically, patients show global developmental delay with moderate to profound learning difficulties associated with severe expressive language disorder, severe to profound mental retardation (95% of cases), and facial dysmorphology (94%). Affected individuals also show postnatal microcephaly (reduced brain and skull size developing after birth, 75%), genital abnormalities (80%), skeletal abnormalities (90%), short statue (65%), seizures (30%), cardiac defects (20%), and renal/urinary abnormalities (15%). One of the characteristic manifestations, commonly used for clinical diagnosis, is a type of anemia called α-thalassemia (86%), caused by the reduction of α-globin gene expression in peripheral red blood cells [summarized in (Gibbons, 2006)]. This α-globin deficiency leads to the consequent aggregation of β-globin peptides into tetrameric β_4 (Haemoglobin H, or HbH), a non-functional form of haemoglobin with very high oxygen affinity and impaired ability to supply oxygen to tissues (Higgs and Weatherall, 2009).

Mutations in *ATRX* have also been identified in a number of other XLMRs with a range of overlapping symptoms, including Juberg-Marsidi (Villard et al., 1996), X-linked

mental retardation with spastic paraplegia (Lossi et al., 1999), Carpenter-Waziri (Abidi et al., 1999), Holmes-Gang (Stevenson et al., 2000), Smith-Fineman-Myers (Villard et al., 2000) and Chudley-Lowry (Abidi et al., 2005) syndromes.

To date over 200 ATR-X cases from 182 families have been identified, carrying a total of 113 different *ATRX* mutations. Despite the steadily growing cohort, no population-based studies have yet been conducted to establish the prevalence of this condition, and the proportion of XLMRs attributable to *ATRX* mutations is currently unknown, but is currently estimated at around 1/1,000,000 (Gibbons et al., 2008).

1.2.9 *ATRX* Disease Mutations Affect Protein Stability and Function

Some pathogenic *ATRX* mutations have been studied biochemically, and all have been found to impair protein function, or reduce steady state protein levels, likely contributing to the disease etiology through protein dysfunction or insufficiency. Nearly all non-truncating ATR-X disease-causing mutations in *ATRX* lie within the conserved ADD (49%) or Snf2 (30%) domains, suggesting their importance for the normal function of ATRX during development (Figure 1-1) (Gibbons et al., 2008). These two regions are separated by a structurally disordered stretch of over 1300 amino acid residues that lack any known pathological mutations. Two theories have been proposed to explain this, (1) it is believed that mutations here may result in neutral polymorphisms, and thus are not detected because they do not result in protein dysfunction or pathology, or (2) mutations here are severely detrimental to normal protein function and act as non-viable null-alleles.

A number of mutations found in the Snf2 domain show impaired DNA stimulated ATPase and DNA translocase activity. Other mutations result in uncoupled DNA binding and ATPase activity, resulting in abnormally high levels of ATPase activity even in the absence of stimulation by DNA, and reduced DNA translocase activity (Mitson et al., 2011). The precise effect of these mutations on ATRX function is unclear, though due to their position within the folded peptide, they are speculated to directly affect ATP

hydrolysis, DNA binding, or the communication of a DNA binding event to the catalytic site.

Structure/function analysis has found that many missense mutations in the ADD domain associated with ATR-X syndrome affect buried residues that are important for protein structural integrity and stability (Argentaro et al., 2007). However other mutations that map to the surface-exposed zinc-binding cysteine residues, or protein binding helical regions, are predicted to directly interfere with DNA or protein interactions (Argentaro et al., 2007). Indeed, some patient mutations in the ADD domain have been found to impair the DNA (Cardoso et al., 2000) or protein (Dhayalan et al., 2011) binding activity of ATRX. Interestingly, mutations in the ADD domain are associated with more severe psychomotor retardation than those found in the Snf2 helicase domain for unknown reasons.

Almost all female carriers of pathogenic *ATRX* mutations show no disease symptoms, however approximately 1 in 4 have signs of mild alpha thalassemia (Gibbons et al., 1992). Most carriers have drastically skewed pattern of X chromosome inactivation with the disease bearing X being preferentially inactivated, preventing pathogenesis. Some exceptions to this paradigm have been documented. Two cases of balanced (random) X inactivation have been documented, one of which presented with mild MR (Wada et al., 2005), however an association with the *ATRX* mutation was not clear. In a unique case, a girl heterozygous for an *ATRX* mutation showed preferential silencing of the wild type X chromosome and presented with characteristics of ATR-X syndrome (Badens et al., 2006).

No known *ATRX* null alleles have been identified, and all clinical mutations assayed to date, including nonsense mutations, retain some basal expression levels of full-length ATRX protein and are thought to primarily disrupt protein function by destabilization or protein mislocalization resulting in hypomorphic alleles (Argentaro et al., 2007; Gibbons et al., 2008; Mitson et al., 2011). The mechanism leading to production of full-length protein from an allele carrying a truncating mutation remains unclear, though it has been speculated that mutational skipping via alternative splicing may be predominantly used to

preserve some full-length protein expression. ATRX dosage also appears to be critical for normal protein function, since all studied disease cases show significantly reduced protein levels (3-55% of normal levels), despite some retaining apparently normal protein function, demonstrated by normal ATPase activity (Argentaro et al., 2007; Mitson et al., 2011). Interestingly, loss of full length ATRX beginning at the morula stage of development results in embryonic lethality by E9.5, likely due to defects in the extraembryonic trophoblast (Garrick et al., 2006), and may explain why no null alleles are observed in humans. Furthermore, depletion of ATRX in the mouse oocyte leads to meiotic abnormalities and aneuploidy in fertilized 1-cell zygotes, and severely reduced fertility (Baumann et al., 2010), suggesting that genomic instability may also contribute to embryonic lethality.

Taken together, the collection of disease causing mutations, and their effects on protein function and stability suggest a critical role of ATRX in development, specifically related to the integrity of the conserved Snf2 and ADD domains.

1.2.10 Loss of DNA Methylation at Repetitive Sequences in ATR-X Patients

In human cells, immunofluorescence staining revealed that ATRX is enriched on the short arms of acrocentric chromosomes where the GC-rich ribosomal DNA (rDNA) arrays are found (McDowell et al., 1999). More recently ATRX was localized to rDNA sequences in human erythroblasts using ChIP (Law et al., 2010). The rDNA genes encode the ribosomal RNAs (rRNA), essential components of the ribosome, and their highly regulated expression is required to meet the demand for protein synthesis in growing cells. Expression of rRNA is regulated by complex patterns of DNA methylation within the promoters and coding sequences, however in general DNA methylation at rDNA genes is associated with transcriptional silencing (Bird et al., 1981).

In peripheral blood cells from normal individuals, approximately 20% of the transcribed rDNA units are methylated within Cytosine-Guanine dinucleotide (CpG) rich regions, likely corresponding to silenced rDNA genes. Surprisingly, in ATR-X patients, most rDNA genes have lost genomic methylation at CpG rich regions, corresponding to the

transcribed 28S, 18S, and 5.8S rDNA genes (Gibbons et al., 2000). A similar loss of rDNA methylation was also observed in mouse ES cells lacking *Atrx* expression (*Atrx*^{null} ES cells) (Garrick et al., 2006), and ATRX deficient mouse brain (Kernohan et al., 2010). The effect of this hypomethylation on rRNA transcription has not yet been assessed, and any relationship to disease pathology is unknown. Furthermore, other repetitive elements from ATR-X patients show disturbed DNA methylation, including a Y chromosome specific repeat element (DYZ2), a subtelomeric/centromeric repeat (TelBam3.4), and loss of pericentromeric DNA methylation (Nan et al., 2007) indicating that ATRX influences DNA methylation at specific regions (Gibbons et al., 2000).

1.2.11 ATRX Regulates Gene Expression

The first evidence that that ATRX regulates the expression of particular genes was the observation that ATR-X patient erythrocytes were severely depleted of α-globin transcripts (leading to α-thalassaemia), despite the presence of a normal α-globin locus, and normal expression from the highly related β-globin locus (Wilkie et al., 1990). The α- and β- globin genes, although related, are found within very distinct genomic environments. The α-globin cluster is found in a GC (Guanine-Cytosine) rich subtelomeric region with a high density of CpG islands and G-rich tandem repeats, suggesting that ATRX might regulate gene expression by targeting specific chromatin environments. Recently it was shown that ATRX is enriched at many GC rich regions of the human and mouse genome, including G-rich telomeric $(TTAGGG)_n$ repeats, subtelomeric TAR1 repeats, and CpG islands (Law et al., 2010). Interestingly, many of these elements are associated with variable nucleotide tandem repeat elements (VNTRs), and are predicted to adopt unusual G-quadruplex (G4) structures under physiological conditions (Lipps and Rhodes, 2009). These non-β G4 DNA conformations are likely to form once the DNA becomes single stranded, such as during DNA replication or transcription, and may consequently interfere with these processes through stochastic inhibition. It was recently shown that ATRX can bind G4 DNA structures *in vitro*, and it has been proposed that under physiological conditions ATRX may associate with, and resolve these structures in different genomic contexts to facilitate gene transcription, DNA replication, and DNA repair (Law et al., 2010). Indeed it is now known that the α-

globin cluster is associated with a VNTR, and that the α-globin downregulation observed in ATR-X patients is proportional to the size of the VNTR associated with the α-globin locus (Law et al., 2010), providing a possible mechanism explaining the variable degrees of α-thalassaemia seen in individuals with identical *ATRX* mutations.

To further examine the role of ATRX in transcriptional regulation of gene expression, microarray studies on ATRX-deficient mouse brain tissue revealed that a number of imprinted genes are upregulated in the absence of ATRX, including the H19 gene (Levy et al., 2008; Kernohan et al., 2010). Imprinted genes are expressed from parental-specific (maternal/paternal) alleles, determined by the differential methylation of regulatory elements (DMRs). The H19/Igf2 imprinted domain contains several DMRs, including one 2 kb upstream of H19 that acts as an imprinting control region (ICR). The *H19* ICR is methylated on the silent paternal allele in many tissues, including the brain (Ferguson-Smith et al., 1993; Bartolomei et al., 1993). It was found that ATRX binds to the maternal *H19* ICR and is required to recruit the proteins MeCP2 and cohesin to this site (Kernohan et al., 2010). Interestingly DNA methylation at the maternal H19/Igf2 ICR was unchanged in the ATRX-deficient cells, but there was increased acetylation of histone H3 and H4 (H3Ac and H4Ac), markers of open chromatin, indicating that ATRX is required for normal epigenetic regulation of specific imprinted loci. Therefor, ATRX can function as a transcriptional regulator of a subset of genes.

1.2.12 ATRX Dosage is Critical for Normal Development of the Mouse Brain

The study of ATRX function in mammalian development has relied exclusively on the mouse model system. To date, conventional zygotic-null *Atrx* mice have proven impossible to obtain, hindering traditional reverse genetic approaches to study global protein function. To circumvent this limitation, conditional models of *Atrx* inactivation have been developed that rely on the Cre recombinase-loxP (Cre-lox) mediated DNA recombination system to induce tissue- and stage-specific *Atrx* null alleles (Bérubé et al., 2005; Garrick et al., 2006; Ritchie et al., 2008; Seah et al., 2008; Levy et al., 2008; Medina et al., 2009; Solomon et al., 2009). The Cre recombinase enzyme is a type I topoisomerase from P1 bacteriophage that catalyzes site-specific DNA recombination,

and has been used extensively in the field of molecular genetics as a tool to modify chromosomal DNA sequences. The enzyme acts on the 34 bp loxP DNA sequence, irreversibly fusing two loxP sites together while excising the intervening DNA.

To apply the Cre-lox system in the study of *Atrx* function during development, an *Atrx* allele with loxP sites flanking exon 18 ($Atrx^{loxP}$) has been generated, and a mouse line has been established using targeted recombination that carries this allele at the endogenous *Atrx* locus (as either heterozygous or homozygous) without any deleterious effects (Bérubé et al., 2005). These $Atrx^{loxP}$ female mice can be mated with male mice carrying the Cre recombinase gene to produce offspring carrying both the $Atrx^{loxP}$ and *Cre* alleles. The expression of Cre in the presence of the $Atrx^{loxP}$ allele leads to the recombination of the loxP sites flanking *Atrx* exon 18 and results in the loss of full length ATRX expression via mRNA truncation and destabilization, yielding no detectable full-length protein, while retaining normal ATRXt expression (Bérubé et al., 2005). Selectivity of the Cre mediated inactivation of ATRX has been achieved by using tissue- or stage-specific promoters to drive Cre expression, either by transgenesis of a full expression cassette or targeted knock-in of the *Cre* coding sequence (CDS) at a specific gene locus (Bérubé et al., 2005; Garrick et al., 2006; Ritchie et al., 2008; Seah et al., 2008; Levy et al., 2008; Medina et al., 2009; Solomon et al., 2009). Using this system, a model of conditional *Atrx* inactivation beginning at the 8-16 cell stage was found to be lethal during embryogenesis due to failure of extraembryonic trophoblast formation (Garrick et al., 2006), indicating a fundamental requirement for ATRX during early placental development.

Since inherited *ATRX* mutations lead to diseases affecting the central nervous system, most molecular genetic approaches have focused on disrupting *Atrx* expression in the developing mouse brain using brain-specific gene promoters from the forkhead box G1 (*Foxg1*) and Nestin genes to drive *Cre* expression (Bérubé et al., 2005; Ritchie et al., 2008; Seah et al., 2008; Levy et al., 2008; Kernohan et al., 2010). In one extensively used model, a targeted knock-in allele of the *Cre* CDS at the *FoxG1* ($Foxg1^{Cre}$) locus results in the expression of *Cre* between E8/E9 wherever Foxg1 is usually expressed, including in the telencephalic neuroepithelium, basal ganglia, olfactory bulbs, and nasal

epithelium (Hébert and McConnell, 2000). When male mice heterozygous for the *Foxg1*^{Cre} allele (*Foxg1*$^{Cre/+}$) are crossed with female mice carrying *Atrx*^{loxP}, the inheritance of both alleles in offspring (*Atrx*^{Foxg1Cre} mice) results in the elimination of full length *Atrx* expression in the tissues where Cre recombinase is expressed, and all tissues derived from them (Bérubé et al., 2005). Importantly, this model eliminates *Atrx* expression in the progenitor cell population of the developing forebrain (the neuronal progenitors of the telencephalic neuroepithelium) prior to the onset of neurogenesis, resulting in the complete loss of *Atrx* expression in nearly all of the cells of the ensuing forebrain. The postnatal *Atrx*^{Foxg1Cre} (also referred to as *Atrx*-null) forebrain is characterized by increased levels of neuronal apoptosis, cortical hypocellularity, and decreased cortical and hippocampal volume at birth (Bérubé et al., 2005). Interestingly, rescue of neuronal cell death using a p53-null background only partially rescues cortical size in the *Atrx*-null mouse, suggesting that additional mechanisms contribute to the hypocellular *Atrx*-null brain outside of strict cell survival (Seah et al., 2008). Furthermore, this model also leads to a reduced birth weight and perinatal lethality in *Atrx*^{Foxg1Cre} offspring, suggesting that *Atrx* expression in the developing brain is important for normal growth and viability.

Another model of Cre mediated *Atrx* inactivation in the developing brain has been characterized that utilizes Cre expression from a randomly integrated *Nestin-Cre* transgene (*Atrx*^{NestinCre} mice) (Bérubé et al., 2005). *Nestin* expression is specific to the neuronal progenitors of the developing forebrain, similar to *Foxg1*, but expression is detected later, resulting in preserved ATRX expression only in the early-born neurons of the marginal zone and subplate of the cortical plate (Bérubé et al., 2005). The cortex of *Atrx*^{NestinCre} mice is hypocellular, however to a lesser extent than *Atrx*^{Foxg1Cre} mice, possibly due to the delayed temporal inactivation of the *Atrx* gene and the retained ATRX expression in a subset of neurons (Bérubé et al., 2005).

To further investigate the role of *Atrx* in neurodevelopment, a transgenic mouse model of *Atrx* overexpression has also been characterized (Bérubé et al., 2002). Global overexpression of human *ATRX* cDNA under the control of a CMV enhancer/chicken β-actin promoter shows growth retardation, neural tube defects, and high incidence of

embryonic death. The embryonic forebrain displays a thickening and disorganization of the neuroepithelium and increased cellularity. Mice that survive into the postnatal period display high rates of perinatal death, seizures, craniofacial defects, and abnormal behaviour (Bérubé et al., 2002).

Taken together, these findings indicate that *ATRX* dosage is essential for normal neuronal proliferation and neuron survival, and is a critical determinant of cortical size, however, the mechanisms linking ATRX deficiency with abnormal neurodevelopment remain largely unknown.

1.3 Mitotic Cell Division

Mitotic cell division (Mitosis) is the process whereby a eukaryotic cell separates its replicated genome, and other cell constituents, into two genetically identical daughter cells. The primary result of mitosis is the propagation and multiplication of a complete genome into a new generation of cells, however in multicellular organisms mitosis also generates the diverse cell types produced during development, and is required for tissue homeostasis in adult organisms, including mammals. Disruption of mitotic cell division can lead to many diseases in humans, including cancer and mental retardation [reviewed in (Thompson et al., 2010) and (Woods et al., 2005)].

1.3.1 The Cell Cycle: Overview

In actively dividing cells, the cell cycle is divided into two major phases, Interphase and the Mitotic (M) phase. Interphase consists of three distinct phases, Gap 1 (G1), Synthesis (S), and Gap 2 (G2), while M-phase consists of both mitosis and cytokinesis. The longest stage of the cell cycle is G1, while the cell undergoes protein and organelle synthesis and growth. Prior to the onset of mitosis, the cellular genome is replicated entirely during S phase of the cell cycle, followed by a second period of growth and protein synthesis during G2 in preparation for cell division.

1.3.2 The Stages of Mitosis

Mitosis is categorized into a sequence of specific phases (Prophase, Prometaphase, Metaphase, Anaphase, and Telophase), each characterized by specific events that occur

within the cell at the microscopic level. Mitotic initiation and progression are tightly regulated by a number of signaling pathways and checkpoints that act to ensure accurate transmission of the cellular genome to the daughter cells, including the G2/M DNA damage checkpoint and spindle assembly checkpoint (SAC).

During prophase, the nuclear envelope is disassembled and the chromatin fibers spread throughout the nucleus are condensed into compacted mitotic chromosomes. Nuclear envelope breakdown (NEBD) allows access of cytosolic factors, including the mitotic spindle and chromosome condensing proteins (the condensin protein complex), to the nuclear chromatin. As prophase proceeds, the mitotic spindle begins to form at the centrosomes and the microtubule fibers elongate in search of the proteinaceous kinetochores assembled on the chromosomal centromeres. Once the mitotic spindle has captured a kinetochore from each sister chromatid, the replicated chromosome begins to move towards the cell equator (or midzone) in preparation for segregation. The process of moving the scattered chromosomes to the midzone is called chromosomes congression. The replicated chromosomes are aligned at the midzone in a bi-orientation, with each kinetochore bound by microtubules from opposing spindle poles. At this point the spindle assembly checkpoint (SAC) prevents sister chromatid separation and segregation by monitoring the kinetochore attachment to spindle microtubules. Once the SAC is satisfied, the protein complex (cohesin) that prevents sister chromatid dissociation is removed, allowing the segregation of one of each sister chromatid towards the opposing spindle poles during anaphase. The polar movement of the sister chromatids is facilitated by the shortening of the spindle microtubules. In addition, microtubules from opposing poles push apart through forces exerted by the motor protein kinesin, and cortical microtubules pull towards each pole through a dynein mediated force. During telophase the chromosomes decondense due to the removal of chromatin bound condensin proteins, and the nuclear lamina reforms around each new diploid complement of chromosomes. The new nuclei, as well as cytosolic components and the plasma membrane are terminally partitioned by a membrane fusion event during cytokinesis, the final stage of M-phase (discussed below).

1.3.3 Centromere Structure and Function

The centromere is the site of kinetochore assembly during mitosis, and is an essential locus on each chromosome that is required for accurate division of genetic material (Pidoux and Allshire, 2000). The kinetochore is a highly proteinaceous structure that interacts with the microtubule fibers of the mitotic spindle, allowing the mechanical motion of the chromosomes during mitosis. Dysfunction of the centromere or kinetochore can cause chromosome missegregation that can lead to aneuploidy or polyploidy, typically rendering the cell inviable or possibly leading to tumorigenesis (Weaver and Cleveland, 2005).

The centromeres of higher eukaryotes form on long stretches of repetitive DNA sequences that typically span many hundreds to many thousands of kilobases (kb) (Gieni et al., 2008). Primate centromeres are comprised of arrays of repetitive alpha satellite DNA, a repeating unit of 171 base pairs (bp), which occur in higher order repeat units of 2-16 alpha-satellite monomers arranged in tandem to form arrays ranging from 200-5,000 kb (Schueler et al., 2001). In the mouse, *Mus musculus domesticus*, centromeric DNA is composed of two distinct repetitive DNA sequences, the minor satellite DNA that is found in the centromere and the major satellite DNA, which is located pericentrically (Choo, 1997). Minor satellite units are 120 bp long and span ~600 kb of genomic DNA, while the major satellite units are 234 bp long and span ~6 megabases (mb). Primate alpha satellite repeat monomers show DNA sequence variation of up to 60% around a common consensus sequence throughout the entire genome, and centromeric DNA sequences between species are highly divergent, suggesting that DNA sequence alone may not specify centromere function (Henikoff et al., 2001). Although the DNA sequences of eukaryotic centromeres vary widely, they are all commonly enriched with nucleosomes containing the histone 3 variant centromeric protein A (CENP-A) (Earnshaw and Migeon, 1985; Palmer et al., 1991; Meluh et al., 1998; Henikoff et al., 2000; Sullivan, 2001; Oegema et al., 2001). The assembly of a functional kinetochore depends on the centromeric enrichment of CENP-A containing nucleosomes, highlighting the importance of chromatin composition in centromere specification. However, CENP-A alone is not sufficient for centromere specification and kinetochore assembly (Van

Hooser et al., 2001). Because of this, it is now believed that epigenetic mechanisms may in fact be the primary means of centromere specification rather than DNA sequence.

1.3.4 Pericentromeric Heterochromatin and Chromatid Cohesion

The centromere is flanked on each side by constitutively condensed regions of chromatin known as pericentromeric heterochromatin (Sullivan, 2001). Rather than being nonfunctional blocks of silent condensed chromatin, these regions are in fact essential for centromere specification and contribute to sister chromatid cohesion and condensation during mitosis (Hendzel et al., 1997; Bernard et al., 2001). Pericentromeric regions are enriched with specific repressive epigenetic marks, including methylation of histone H3 at lysine 9 (H3K9me2 and H3K9me3) and histone H4 at lysine 20 (H4K20me3), and enrichment of heterochromatic factors including Heterochromatin Protein 1 (HP1, the homolog of yeast Swi6). Recruitment of HP1 to pericentromeric chromatin depends on the interaction of its chromodomain with the H3K9me3 modification, which is catalyzed by the histone methyltransferase enzyme Suv39h1 (Lachner et al., 2001). In turn, HP1 recruits the DNA methyltransferase 3b (DNMT3b), which methylates the cytosine (C) residues of cytosine-guanine (G) dinucleotides (CpG), leading to silencing and heterochromatinzation of pericentromeric DNA. These marks serve to maintain the condensed structure of the pericentric chromatin and maintain chromatid cohesion through recruitment of the cohesin protein complex (Nonaka et al., 2002; Amor et al., 2004). HP1 proteins are an integral component of condensed chromatin at pericentric regions, and loss of HP1 or Swi6 leads to loss of heterochromatin, centromeric instability and mitotic defects (Ekwall et al., 1996; Amor et al., 2004). Interestingly, HP1α has been shown to recruit ATRX to PCH in mESCs (Kourmouli et al., 2005), suggesting a specific function for ATRX at this genomic locus. Supporting this hypothesis, a growing number of chromatin remodeling enzymes have been found to maintain the structural integrity of PCH, with deficiencies leading to mitotic abnormalities (Lejeune et al., 2007; Bourgo et al., 2009).

Chromatid cohesion is achieved through the recruitment of the ring-shaped cohesin complex, a protein tetramer that is thought to function by topologically encircling sister chromatids, preventing their dissociation during the early stages of mitosis (Hirano, 2005;

Nasmyth, 2005). The cohesin complex contains four core subunits: two subunits of the structural maintenance of chromosomes (SMC) protein family, Smc1 and Smc3, the kleisin family protein Rad21 and the accessory subunit SA1. At pericentromeric heterochromatin, HP1 recruits the cohesin subunit Rad21. Loss of HP1, and thus PCH integrity, results in abnormal chromosome segregation during mitosis (Taddei et al., 2001), premature loss of sister chromatid cohesion, and aneuploidy (Inoue et al., 2008). Therefore, the proper association of cohesin with pericentromeric regions is essential for normal mitotic cell division.

Recently it was discovered that RNA is an essential component of constitutive pericentromeric heterochromatin (Maison et al., 2002; Muchardt et al., 2002). In the fission yeast *S. pombe*, small double stranded RNA (dsRNA) generated by an RNAi-dependent mechanism is involved in the establishment and maintenance of heterochromatic regions (Reinhart and Bartel, 2002; Volpe et al., 2002; Grewal and Moazed, 2003; Ekwall, 2004; Schramke and Allshire, 2004). Surprisingly, these small dsRNAs are encoded by the repetitive pericentromeric regions that were previously thought to have been transcriptionally silent (Grewal and Elgin, 2007). Mutants for components of the RNAi machinery, Argonaute (Ago1), Dicer (Dcr1) and RNA-dependent RNA polymerase (Rdp1) show loss of pericentric heterochromatin and gene silencing, loss of H3K9me3 and hpSwi6^{hp1} (the *S. pombe* homolog of mammalian HP1) enrichment and mitotic defects (Volpe et al., 2002; Provost et al., 2002; Hall et al., 2003). Because spSwi6^{hp1} contains a chromodomain with RNA binding properties, it is believed that the siRNAs produced by Dicer are used to target Swi6 to pericentric regions to promote heterochromatinization. Transcripts have now been detected from pericentromeric sequences throughout different stages of mammalian development, during cellular differentiation, proliferation, senescence, and adaptation to environmental stress (Jolly et al., 1997; Denegri et al., 2002; Jolly et al., 2004; Eymery et al., 2010), however their role in heterochromatin formation is less clear.

1.3.5 Mitotic Checkpoints

Mitotic entry is ultimately controlled by the G2 DNA-damage checkpoint, which acts as a surveillance mechanism to ensure genomic integrity prior to cell division. Lesions of

DNA damage activate the PI3K (phosphoinositide 3-kinase)-related protein kinases ATM and ATR, which phosphorylate and activate the CHK1/CHK2 effector kinases [reviewed in (Chen et al., 2003)]. Active CHK1/CHK2 phosphorylate and inactivate CDC25C, preventing dephosphorylation and activation of cyclin B1-CDK1. Other signaling pathways are critical for the G2 DNA-damage checkpoint, including the MAPKAPK2 [MAPKAP (MAPK-activated protein) kinase-2] and JNK (c-Jun N-terminal kinase) pathways which act through the phosphorylation and inactivation of CDC25B. Mitosis is initiated by the activation of the M-phase promoting factor (MPF), a heterodimer of cyclin B1-CDK1 (cyclin-dependent kinase 1). Activation of the MPF is achieved by PLK1 (polo-like kinase 1)-mediated phosphorylation of cyclin B1 and CDC25 phosphatase-mediated dephosphorylation of CDK1, which function to retain the MPF in the nucleus, and activate its kinase activity respectively [Reviewed in (Stark and Taylor, 2006)]. The MPF is a Serine/Threonine (Ser/Thr) protein kinase with many substrates involved in mitotic initiation and progression, including nuclear lamins, condensins, microtubule associated proteins, and histones.

The separation of sister chromatids during anaphase is blocked by the spindle assembly checkpoint (SAC), which functions to ensure the accurate segregation of chromosomes during mitosis (Musacchio and Salmon, 2007; Cheeseman and Desai, 2008). To achieve this, the checkpoint blocks chromosome segregation until every kinetochore has been correctly bound by spindle microtubules. The mechanism governing this checkpoint is believed to rely on diffusible signaling emanating from unattached kinetochores that target Cdc20, an essential activator of the anaphase-promoting complex/cyclosome (APC/C). Prior to anaphase, Mad2 (mitotic-arrested deficient), BubR1 (budding uninhibited by benzimidazole), Bub3 and Cdc20 itself are assembled into the mitotic checkpoint complex (MCC) at the kinetochore. The MCC is diffusible throughout the cytoplasm, and binds the anaphase promoting complex/cyclosome (APC/C), preventing APC/C activation by Cdc20. This prevents cells from entering anaphase by inhibiting the ubiquitination and destruction of cyclin B and securin by Cdc20 dependent activation of the APC/C ubiquitin ligase (Musacchio and Salmon, 2007). Securin prevents anaphase onset by binding and sequestering the cysteine protease separase, which, when active, can target and cleave the cohesin subunit Rad21, opening the cohesin ring and allowing sister

chromatid separation (Sun et al., 2009). Defects in the SAC can lead to chromosome non-disjunction and aneuploidy due to premature anaphase onset without chromosome biorientation (Fang and Zhang, 2011).

1.3.6 Cytokinesis

Cytokinesis is the final stage of the mitotic process that culminates in a membrane-fusion event that produces two physically distinct and genetically identical daughter cells, each possessing a diploid (2N) complement of chromosomes. Following the segregation of the replicated sister chromosomes to the opposing poles of the mitotic cell, the two diploid genomes, along with a complement of organelles, cytosolic factors, and plasma membrane components, are physically partitioned into two discrete and fully functional cells.

The first major step in cytokinesis is the accurate placement and ingression of the actomyosin ring, ensuring that the segregated genomes are properly inherited by the two daughter cells. Cleavage furrow ingression involves the contractile activity of the actomyosin ring, made of the actin motor protein non-muscle myosin II and a network of cortical actin filaments. This ring assembles at the equatorial cell cortex on the inner surface of the plasma membrane, and contracts in due to ATP dependent myosin II activity in response to the active form of the small GTPase RhoA, which is enriched in a narrow zone on the cell cortex where the future cleavage furrow will form (Bement et al., 2005). To establish this precise domain of active RhoA the mitotic spindle positions upstream RhoA activators, the GDP-GTP exchange factor (GEF) ECT2/Pebble, and the GTPase-activating protein (GAP) MgcRacGAP/CYK-4/RacGAP50C at the central spindle (Somers and Saint, 2003; Piekny et al., 2005). Active RhoA in turn regulates actin polymerization and myosin II activation, promoting the contractile function of the actomyosin ring. The positional signal for cleavage furrow induction is believed to emanate from the central spindle, which is the region of overlapping microtubules from each spindle pole at the cell equator [Reviewed in (Glotzer, 2004)]. Cleavage furrow ingression continues until the actomyosin contractile ring comes within a close proximity of the central spindle. A number of proteins found at the central spindle are critical regulators of cytokinesis, either through the regulation of microtubule function, or

through discrete signaling pathways. One such signaling protein is the mitotic kinase PLK1. At the midzone, Plk1 phosphorylates a number of substrates, including the kinesin microtubule motor proteins MKLP2 and the dynein component NudC (Zhou et al., 2003; Neef et al., 2003). This phosphorylation is essential for the normal completion of cytokinesis, and overexpression of dominant negative Plk1 leads to cytokinetic failure and multinucleation. Plk1 is also required for cleavage furrow ingression by regulating the localization of RhoA to the cleavage furrow cortex (Petronczki et al., 2007; Brennan et al., 2007). The actomyosin ring however cannot continue ingressing and cleave the cells in two, rather the dense network of microtubules that were the central spindle are condensed into the cytokinetic midbody, an intercellular bridge structure required for the final stages of cytokinesis [Reviewed in (Eggert et al., 2006)]. Proteomic analysis of midbodies has identified over a hundred different proteins, many of which have subsequently been shown to be essential for abscission (Skop et al., 2004).

The final step in cytokinesis is a membrane abscission event that yields two physically independent cells, and involves poorly understood protein degradation pathways and plasma membrane vesicle trafficking. Membrane vesicles accumulate in the cleavage furrow and intercellular bridge, and key membrane trafficking proteins, including SNAREs [SNAP (soluble *N*-ethylmaleimide-sensitive fusion protein-attachment protein) receptors], dynamin, and clathrin, localize to the cleavage furrow and intercellular bridge [Reviewed in (Neto et al., 2011)]. Inhibition of the midbody-localized membrane vesicle transport proteins (the t-SNARE/v-SNARE pair syntaxin 2 and endobrevin/VAMP-8) by dominant-negative overexpression blocks the completion of cytokinesis in mammalian cells, but does not affect earlier events such as cleavage furrow ingression (Low et al., 2003), highlighting the importance of membrane trafficking in the terminal stages of cytokinesis. One view of membrane trafficking in this context may be to ensure delivery of key components to the midbody in the correct temporal sequence. An alternative role for vesicle accumulation in the midbody prior to abscission is to deliver additional membrane area, such that upon fusion with each other and the PM there is a thinning and extension of the intercellular bridge (Neto et al., 2011).

Completion of cytokinesis is also intimately linked with prior events in the mitotic cycle. One well-documented cause of cytokinetic failure is the presence of chromosome bridges spanning the cytoplasmic bridge during cytokinesis (Shi and King, 2005). These bridges are believed to be a consequence of earlier mitotic abnormalities, including chromosome fusions or chromosome misalignment and nondisjunction, which often result in DNA damage, aneuploidy or tetraploidy (Shi and King, 2005). It is thought that the cytokinetic block in these cases is due to genoprotective pathways that detect chromosome missegregation and DNA damage and prevent the completion of cytokinesis by blocking and reversing cleavage furrow ingression (Tutt et al., 1999; Lin et al., 2003b; Daniels et al., 2004; Meng et al., 2007).

1.4 Mammalian Cerebral Cortical Development

1.4.1 The Mammalian Central Nervous System

The mammalian central nervous system (CNS) comprises the brain and spinal cord, and functions to integrate sensory information from the peripheral nervous system (PNS), and coordinate the activity of the body. Mammalian neural development begins with the formation of the neural tube, the precursor to the brain and spinal cord. In the mouse, this process (known as neurulation) begins at embryonic day 8.5 (E8.5) and ends at E11.5 and involves the invagination, folding, and closure of a specialized strip of dorsal ectoderm called the neural plate [Reviewed in (Colas and Schoenwolf, 2001)]. The ensuing neural tube is then regionalized and subdivided, with the brain forming from the anterior-most region. The brain is subdivided along the anterior-posterior axis into the prosencephalon (forebrain) and brain stem (midbrain & hindbrain). The anterior most segment of the forebrain becomes the embryonic telencephalon, which eventually develops into the cerebrum, containing the striatum, hippocampus, and cerebral cortex of the mature brain. The cerebrum is the most complex region of the adult mammalian brain, and is responsible for many higher-order cognitive functions, including motor coordination, conscious thought, learning, memory, emotions, speech and language in humans. Not surprisingly, pathologies affecting the cerebrum are associated with cognitive and behavioural deficits, and intellectual disability (Vaillend et al., 2008).

1.4.2 Cortical Neurogenesis

Neurogenesis is the process of neuron production by neuronal progenitor cells. In the mouse, the neurogenic interval is the period during embryonic development where differentiated cortical neurons are being produced that begins at E11 and terminates at E17 (Takahashi et al., 1995).

The neural tube begins as a single pseudostratified layer of cells known as the neuroepithelium, which composed of neuroepithelial cells, the progenitors of every neuron in the adult CNS. In the dorsal telencephalon, where the cerebral cortex is formed, the neuroepithelium is known as the ventricular zone (VZ). Prior to neurogenesis the neuroepithelial progenitors proliferate through symmetric cell divisions to expand the population of progenitor cells. During the early stages of neurogenesis, the neuroepithelial cells of the VZ begin to divide asymmetrically, producing the earliest born neurons of the cortex, and two other progenitor populations: radial glial cells, and apical progenitors. Radial glial cells are distinguished from neuroepithelial cells by the expression of an array of glial-specific markers, but share many properties, including the undertaking of cell division at the ventricular surface (Kriegstein and Götz, 2003; Huttner and Kosodo, 2005). Radial glial cells in turn give rise to most of the projection neurons of the cerebral cortex, either directly through asymmetric cell division, or indirectly through the generation of another type of progenitor cell, the basal progenitors (BPs). Basal progenitors are distinguished from apical progenitors (neuroepithelial cells and radial glia) because they undergo cell division in the sub-ventricular zone (SVZ) on the basal side of the VZ and typically divide symmetrically, only once, producing two neurons and thus amplifying the neuronal output of the radial glia (Noctor et al., 2004; Haubensak et al., 2004; Miyata et al., 2004). The mature mammalian cerebral cortex is composed of six morphologically distinct cellular layers (I, II, III, IV, V, VI), each populated by neurons that project to specific regions within the cortex, midbrain, and spinal cord. This lamination is achieved through the temporal regulation of neuron production in the two germinal zones, the VZ and SVZ, and their controlled migration of neurons to specific regions depending on the developmental stage. The earliest born post-mitotic neurons migrate to the deepest cortical layers and later-arising neurons

migrate past them to sequentially more superficial layers in a stereotyped 'inside-out' pattern (Sidman and Rakic, 1973; Caviness, 1982).

1.4.3 The Mode of Cell Division Regulates Neurogenesis in the Developing Cerebral Cortex

The apical, but not basal progenitor cells are highly polarized along their apicobasal axis, and this polarity is the basis of their symmetric or asymmetric cell division (Figure 1-2; Figure 1-3) (Götz and Huttner, 2005; Farkas and Huttner, 2008). It has been shown that the angle of progenitor cell division relative to the apical cell surface could largely predict the outcome of the cell division, either proliferative or neurogenic (Kosodo et al., 2004). Because of this, it has been proposed that apical progenitor cell fate is determined primarily by the differential inheritance of specific cellular constituents to the daughter cells (Figure 1-3) (Wodarz and Huttner, 2003; Götz and Huttner, 2005; Huttner and Kosodo, 2005). The apical plasma membrane has been shown to serve such a role: in predicting the cell fate outcome of apical progenitor cell divisions, where inheritance of the apical membrane correlates with the preservation of progenitor cell identity (Kosodo et al., 2004). Although the apical plasma membrane of the apical progenitor cells represents only a tiny fraction of the total cell surface, it is enriched for unique proteins not found on the basolateral membrane. The PAR-3 (partitioning defective 3 homolog) protein is found at the apical membrane, and compromising PAR-3 expression prevents progenitor self-renewal by causing both daughter cells to exit the cycle and become neurogenic (Costa et al., 2008). Another candidate protein is Prominin-1, a transmembrane protein expressed in the apical plasma membrane of many somatic stem cells, including neuroepithelial progenitors and radial glia (Corbeil et al., 2001). The protein interacts with membrane cholesterol, and it has been proposed that apical neuronal progenitor proliferation may involve a poorly understood, cholesterol-dependent mechanism at the apical membrane (Götz and Huttner, 2005). Ultimately, the mechanisms by which these and other potential determinants promote a progenitor-cell fate in neuroepithelial cells are not currently established.

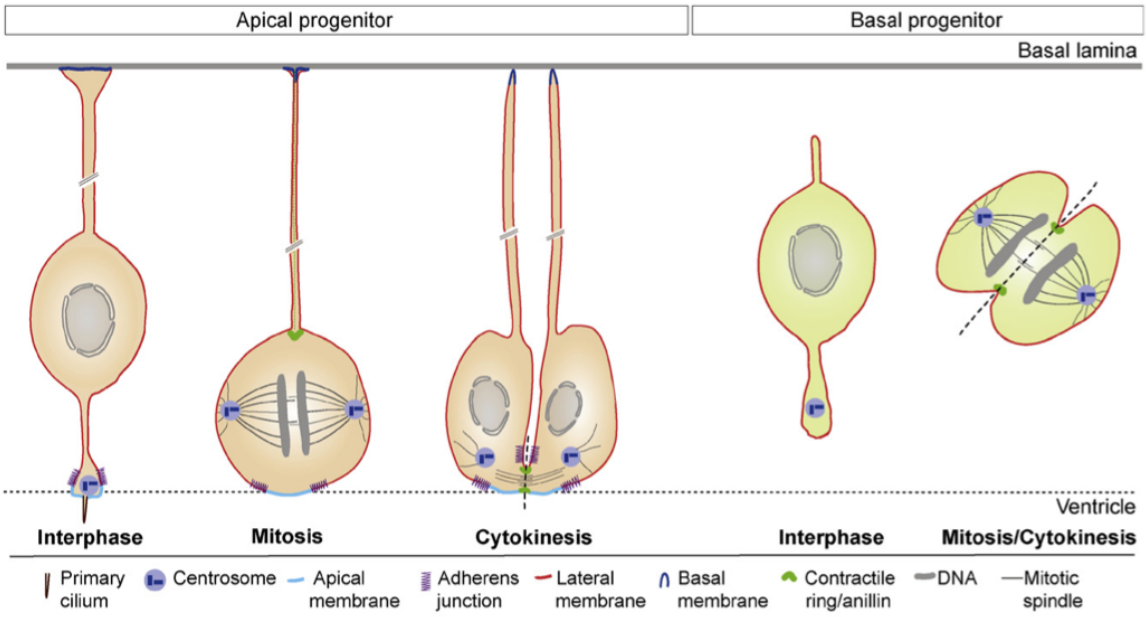

Figure 1-2. The cell biological features of apical and basal progenitors during cell division.

The aspects of apical neuronal progenitor cell polarity compared to basal progenitor cells are illustrated (see legend for details). Importantly, the apical neuronal progenitors are polarized and possess a distinct apical plasma membrane. In contrast, basal neuronal progenitors do not show this type of apical membrane polarization. This difference in membrane organization between these two types of neuronal progenitor cells is thought to influence the symmetry of mitotic cell division and the fate of daughter cells (see Fig 1-3).

Reproduced with permission from Farkas et al. (2008) Curr Opin Cell Biol 20:707-715.

Symmetric self-renewing divisions predominate early during neurogenesis and ultimately expand the progenitor cell population, while asymmetric differentiative divisions become more frequent as neurogenesis proceeds. A disruption in the balance and timing of neurogenic versus proliferative cell divisions can have dramatic results on neuronal output (Caviness et al., 2003). For example, a premature initiation of neurogenic divisions will initially increase the number of early born neurons in the deep cortical layers at the expense of the superficial layers, and result in a smaller cortex. In contrast, a delay in the onset of neurogenesis can lead to the opposite effect (Caviness et al., 2003). A number of centrosomal proteins have been implicated in the regulation of cortical size through control of mitotic spindle angle during apical progenitor cell division. Mutations in the human homologs of a number of these centrosomal proteins are associated with a neurodevelopmental disorder called autosomal recessive primary microcephaly (MCPH) (Woods et al., 2005). Microcephaly is the clinical finding of reduced skull circumference (which closely correlates with reduced brain volume) three standard deviations below the mean (-3SD) for age and gender (Aicardi, 1998), and is often associated with mental retardation, with the severity microcephaly being strongly correlated with the risk and severity of mental retardation (Dolk, 1991). Individuals with MCPH have intellectual disability, and show a reduction of brain growth *in utero*, with the cortex being the most affected, however overall brain structure is normal (Roberts et al., 2002). Primary microcephaly is generally non-progressive and is thought to result from defective neurogenic mitosis during development, leading to a reduction in the number of neurons (Dobyns, 2002; Woods et al., 2005). Conversely, secondary microcephaly, which develops after birth, is believed to be caused by processes such as high rates of pathologic apoptosis, proliferation and patterning abnormalities, migration defects, disturbance of extracellular matrix integrity, and defects of synaptogenesis, and is often a progressive neurodegenerative condition (Woods et al., 2005). Currently, four MCPH related genes have now been identified: autosomal recessive primary microcephaly 1 (*MCPH1*/Microcephalin), abnormal spindle-like microcephaly associated

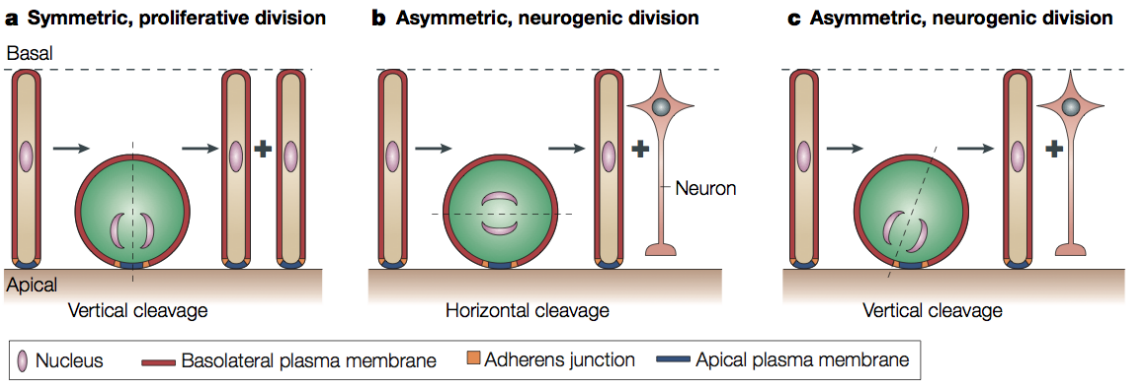

Figure 1-3. A comparison of symmetric and asymmetric cell division of neuroepithelial and radial glial cells.

The relationship between cell polarity and the equal or unequal partitioning of the apical membrane upon (a) symmetric or (b, c) asymmetric cell division, is shown. (a) A vertical cleavage plane results in the partitioning of the apical membrane to both daughter cells and symmetric, self renewing cell division. (b, c) Horizontal cleavage planes result in the asymmetric inheritance of the apical membrane by a single daughter cells and leading to neurogenic differentiation of the other.

Reproduced with permission from Götz and Huttner (2005) Nat Rev Mol Cell Biol (6): 777-788.

(*MCPH5*/*ASPM*), cyclin-dependent kinase 5 regulatory subunit-associated protein 2 (*MCPH3*/*CDK5RAP2*) and centromere protein J (*MCPH6*/*CENPJ*). All four MCPH genes are expressed in the neuroepithelium of the developing brain, three are centrosomal components (ASPM, CENPJ, CDK5RAP2), and one (Microcephalin) is associated with chromatin, which has lead to the hypothesis that MCPH is primarily a result of the disruption of neurogenic mitosis (Jackson et al., 2002; Bond et al., 2003; Bond et al., 2005; Woods et al., 2005). Knockdown of ASPM expression using *in vivo* RNAi electroporation in the developing embryonic mouse forebrain increases the number of asymmetrically oriented mitotic progenitor cells which in turn correlates with an increase of non-progenitor daughter cell fate (Fish et al., 2006). Interestingly, ASPM is naturally downregulated by apical neuronal progenitors undergoing asymmetric neurogenic divisions, suggesting that regulation of ASPM expression is a mechanism used to govern the balance and timing of neurogenetic cell divisions (Fish et al., 2006).

Another MCPH-associated gene, cyclin-dependent kinase 5 regulatory subunits 2 (*CDK5RAP2*), encodes a centrosomal protein with a role in γ-tubulin ring complex (γ-TuRC) recruitment and microtubule nucleation at the centrosome (Fong et al., 2008). The cortex of the CDK5RAP2 null mouse is severely dysmorphic, with cortical hypoplasia, and reduction in brain and hippocampal size (Lizarraga et al., 2010). The cortex is characterized by a loss of later born superficial layer (II/III) neurons and an increase in early born neurons of the deep cortical layer (VI). The apical progenitors show defects in mitotic spindle positioning, with an increase in the proportion of horizontal/asymmetric cell divisions and a premature depletion of the neuronal progenitor cell population.

Cytokinesis has also been found to influence the cellular control of cortical development. Mutations in the citron kinase (*CitK*) gene cause microcephaly in mice and rats, and the mutant cortex is characterized by binucleated cells and massive apoptosis in the proliferative zones of the embryonic cortex (Di Cunto et al., 2000; Sarkisian et al., 2002). Citron kinase is localized to the cytokinetic midzone and cleavage furrow during anaphase and telophase and then translocates to the cytokinetic midbody during

cytokinesis (Di Cunto et al., 1998; Eda et al., 2001). Furthermore, overexpression of truncated mutant isoforms causes erratic cytokinetic behaviour and cytokinesis failure in HeLa cells (Madaule et al., 2000). Taken together, mitotic cell division is clearly a critical regulator of brain size and neurogenesis through the partitioning of cell fate determinants and maintenance of cell viability.

1.5 Thesis Overview

The objective of the work presented in this thesis was to determine whether the chromatin remodeling protein ATRX is required for normal mitotic cell division and whether this requirement is relevant in the proliferating cells of the developing embryonic mouse brain.

1.5.1 Rationale and Hypothesis

Although ATRX is a known transcriptional regulator, many studies have confirmed its enrichment at the highly condensed, gene-poor region of PCH flanking the centromere. In most cells ATRX is recruited to PCH by HP1, an integral component of PCH that is required for the epigenetic maintenance of heterochromatin. I therefore hypothesized that ATRX is an essential component of PCH, and a deficiency in ATRX would lead to mitotic abnormalities and chromosome alignment and segregation errors (Chapter two and three). The mitotic defects observed in ATRX-deficient HeLa cells inspired a second hypothesis, that this mitotic requirement might also exist in the neuroepithelial progenitors of the developing mouse forebrain, and may be relevant to the neurodevelopmental abnormalities in the *Atrx*-null mouse (Chapter four).

1.5.2 Chapter Two: Loss of ATRX Leads to Chromosome Cohesion and Congression Defects

This initial study aimed to determine the possible mitotic requirement for ATRX in mammalian somatic cells. At the time this study was conceived and initiated, a requirement for ATRX in meiotic chromosome alignment had recently been shown in 2004 (De La Fuente et al., 2004), establishing a proof of principle for this study. To achieve this aim, HeLa cells were depleted of ATRX using different RNAi strategies, and

scored for mitotic abnormalities using techniques for both fixed and live-cell imaging. This study showed not only a mitotic disruption, but it revealed that sister chromatids from mitotic ATRX-depleted HeLa cells had greatly reduced centromeric cohesion, identifying a particular mechanism that might underlie the observed mitotic defects. Furthermore I found evidence of mitotic defects in the neuroepithelial progenitors in the developing Atrx-null mouse cortex *in vivo*, suggesting that this mitotic requirement exists in a biologically relevant tissue.

1.5.3 Chapter Three: Cytokinetic Abnormalities and Multinucleation Induced by ATRX Depletion

Chapter three is an extension of the study conducted in chapter two. Although mitotic chromosome congression, alignment, and segregation were disrupted in the ATRX-depleted HeLa cells, live cell imaging revealed that these cells also had dramatically prolonged cytokinesis, which more frequently failed and produced binucleated cells. Assessment of cytokinetic midbody structure in these cells using immunofluorescent staining revealed that ATRX does not influence the formation or integrity of the cytokinetic midbody. This study suggests that a deficiency in ATRX leads to cytokinetic abnormalities and failure through an indirect mechanism, likely related to chromosome nondisjunction.

1.5.4 Chapter Four: ATRX Regulates Cortical Development Through Control of Neuronal Progenitor Cell Division

The final aspect of my studies aimed to identify whether ATRX-dependent mitotic cell division contributed to the neurodevelopmental phenotype of the *Atrx*-null mouse. Using a combination of primary cell culture and histological sectioning, I confirmed that neuronal progenitors from the *Atrx*-null forebrain exhibited mitotic defects identical to those observed in the ATRX-depleted human cells, including chromosome misalignment and missegregation. Furthermore, these cells were more often asymmetrically oriented during cell division *in vivo* and this correlated with a predictably altered neuronal output in the postnatal brain, characterized by a depletion of the late developmental stage neuronal progenitors and late born cortical neurons. The work presented in this thesis

represent the first studies to show a mitotic requirement for the ATRX protein, and the first to link such a requirement to a specific neurogenic role for the *Atrx* gene.

1.6 References

Aapola, U., Kawasaki, K., Scott, H.S., Ollila, J., Vihinen, M., Heino, M., Shintani, A., Kawasaki, K., Minoshima, S., et al. (2000). Isolation and initial characterization of a novel zinc finger gene, DNMT3L, on 21q22.3, related to the cytosine-5-methyltransferase 3 gene family. Genomics *65*, 293-98.

Abidi, F., Schwartz, C.E., Carpenter, N.J., Villard, L., Fontés, M., and Curtis, M. (1999). Carpenter-Waziri syndrome results from a mutation in XNP. Am J Med Genet *85*, 249-251.

Abidi, F.E., Cardoso, C., Lossi, A.M., Lowry, R.B., Depetris, D., Mattéi, M.G., Lubs, H.A., Stevenson, R.E., Fontes, M., et al. (2005). Mutation in the 5' alternatively spliced region of the XNP/ATR-X gene causes Chudley-Lowry syndrome. Eur J Hum Genet *13*, 176-183.

Aicardi, J. (1998). The etiology of developmental delay. Semin Pediatr Neurol *5*, 15-20.

Amitani, I., Baskin, R.J., and Kowalczykowski, S.C. (2006). Visualization of Rad54, a chromatin remodeling protein, translocating on single DNA molecules. Mol Cell *23*, 143-48.

Amor, D.J., Bentley, K., Ryan, J., Perry, J., Wong, L., Slater, H., and Choo, K.H. (2004). Human centromere repositioning "in progress". Proc Natl Acad Sci U S A *101*, 6542-47.

Argentaro, A., Yang, J.C., Chapman, L., Kowalczyk, M.S., Gibbons, R.J., Higgs, D.R., Neuhaus, D., and Rhodes, D. (2007). Structural consequences of disease-causing mutations in the ATRX-DNMT3-DNMT3L (ADD) domain of the chromatin-associated protein ATRX. Proc Natl Acad Sci U S A *104*, 11939-944.

Badens, C., Martini, N., Courrier, S., DesPortes, V., Touraine, R., Levy, N., and Edery, P. (2006). ATRX syndrome in a girl with a heterozygous mutation in the ATRX Zn finger domain and a totally skewed X-inactivation pattern. Am J Med Genet A *140*, 2212-15.

Bartolomei, M.S., Webber, A.L., Brunkow, M.E., and Tilghman, S.M. (1993). Epigenetic mechanisms underlying the imprinting of the mouse H19 gene. Genes Dev *7*, 1663-673.

Baumann, C., Viveiros, M.M., and De La Fuente, R. (2010). Loss of maternal ATRX results in centromere instability and aneuploidy in the mammalian oocyte and pre-implantation embryo. PLoS Genet *6*

*B*ement, W.M., Benink, H.A., and von Dassow, G. (2005). A microtubule-dependent zone of active RhoA during cleavage plane specification. J Cell Biol *170*, 91-101.

Bernard, P., Maure, J.F., Partridge, J.F., Genier, S., Javerzat, J.P., and Allshire, R.C. (2001). Requirement of heterochromatin for cohesion at centromeres. Science *294*, 2539-542.

Bernardi, R., and Pandolfi, P.P. (2007). Structure, dynamics and functions of promyelocytic leukaemia nuclear bodies. Nat Rev Mol Cell Biol *8*, 1006-016.

Bérubé, N.G., Jagla, M., Smeenk, C., De Repentigny, Y., Kothary, R., and Picketts, D.J. (2002). Neurodevelopmental defects resulting from ATRX overexpression in transgenic mice. Hum Mol Genet *11*, 253-261.

Bérubé, N.G., Mangelsdorf, M., Jagla, M., Vanderluit, J., Garrick, D., Gibbons, R.J., Higgs, D.R., Slack, R.S., and Picketts, D.J. (2005). The chromatin-remodeling protein ATRX is critical for neuronal survival during corticogenesis. J Clin Invest *115*, 258-267.

Bérubé, N.G., Smeenk, C.A., and Picketts, D.J. (2000). Cell cycle-dependent phosphorylation of the ATRX protein correlates with changes in nuclear matrix and chromatin association. Hum Mol Genet *9*, 539-547.

Bienz, M. (2006). The PHD finger, a nuclear protein-interaction domain. Trends Biochem Sci *31*, 35-40.

Bird, A.P., Taggart, M.H., and Gehring, C.A. (1981). Methylated and unmethylated ribosomal RNA genes in the mouse. J Mol Biol *152*, 1-17.

Bond, J., Roberts, E., Springell, K., Lizarraga, S.B., Lizarraga, S., Scott, S., Higgins, J., Hampshire, D.J., Morrison, E.E., et al. (2005). A centrosomal mechanism involving CDK5RAP2 and CENPJ controls brain size. Nat Genet *37*, 353-55.

Bond, J., Scott, S., Hampshire, D.J., Springell, K., Corry, P., Abramowicz, M.J., Mochida, G.H., Hennekam, R.C., Maher, E.R., et al. (2003). Protein-truncating mutations in ASPM cause variable reduction in brain size. Am J Hum Genet *73*, 1170-77.

Bourgo, R.J., Siddiqui, H., Fox, S., Solomon, D., Sansam, C.G., Yaniv, M., Muchardt, C., Metzger, D., Chambon, P., et al. (2009). SWI/SNF deficiency results in aberrant chromatin organization, mitotic failure, and diminished proliferative capacity. Mol Biol Cell *20*, 3192-99.

Brennan, I.M., Peters, U., Kapoor, T.M., and Straight, A.F. (2007). Polo-like kinase controls vertebrate spindle elongation and cytokinesis. PLoS One *2*, e409.

Cardoso, C., Lutz, Y., Mignon, C., Compe, E., Depetris, D., Mattei, M.G., Fontes, M., and Colleaux, L. (2000). ATR-X mutations cause impaired nuclear location and altered DNA binding properties of the XNP/ATR-X protein. J Med Genet *37*, 746-751.

Carlson, M., and Laurent, B.C. (1994). The SNF/SWI family of global transcriptional activators. Curr Opin Cell Biol *6*, 396-402.

Caviness, V.S. (1982). Neocortical histogenesis in normal and reeler mice: a developmental study based upon [3H]thymidine autoradiography. Brain Res *256*, 293-302.

Caviness, V.S., Goto, T., Tarui, T., Takahashi, T., Bhide, P.G., and Nowakowski, R.S. (2003). Cell output, cell cycle duration and neuronal specification: a model of integrated mechanisms of the neocortical proliferative process. Cereb Cortex *13*, 592-98.

Caviness, V.S., Takahashi, T., and Nowakowski, R.S. (2000). Neuronogenesis and the early events of neocortical histogenesis. Results Probl Cell Differ *30*, 107-143.

Cheeseman, I.M., and Desai, A. (2008). Molecular architecture of the kinetochore-microtubule interface. Nat Rev Mol Cell Biol *9*, 33-46.

Chen, Z., Xiao, Z., Chen, J., Ng, S.C., Sowin, T., Sham, H., Rosenberg, S., Fesik, S., and Zhang, H. (2003). Human Chk1 expression is dispensable for somatic cell death and critical for sustaining G2 DNA damage checkpoint. Mol Cancer Ther *2*, 543-48.

Choo, K.H. (1997). Centromere DNA dynamics: latent centromeres and neocentromere formation. Am J Hum Genet *61*, 1225-233.

Clapier, C.R., and Cairns, B.R. (2009). The biology of chromatin remodeling complexes. Annu Rev Biochem *78*, 273-304.

Colas, J.F., and Schoenwolf, G.C. (2001). Towards a cellular and molecular understanding of neurulation. Dev Dyn *221*, 117-145.

Corbeil, D., Röper, K., Fargeas, C.A., Joester, A., and Huttner, W.B. (2001). Prominin: a story of cholesterol, plasma membrane protrusions and human pathology. Traffic *2*, 82-91.

Costa, M.R., Wen, G., Lepier, A., Schroeder, T., and Götz, M. (2008). Par-complex proteins promote proliferative progenitor divisions in the developing mouse cerebral cortex. Development *135*, 11-22.

Daniels, M.J., Wang, Y., Lee, M., and Venkitaraman, A.R. (2004). Abnormal cytokinesis in cells deficient in the breast cancer susceptibility protein BRCA2. Science *306*, 876-79.

Denegri, M., Moralli, D., Rocchi, M., Biggiogera, M., Raimondi, E., Cobianchi, F., De Carli, L., Riva, S., and Biamonti, G. (2002). Human chromosomes 9, 12, and 15 contain the nucleation sites of stress-induced nuclear bodies. Mol Biol Cell *13*, 2069-079.

Dhayalan, A., Tamas, R., Bock, I., Tattermusch, A., Dimitrova, E., Kudithipudi, S., Ragozin, S., and Jeltsch, A. (2011). The ATRX-ADD domain binds to H3 tail peptides and reads the combined methylation state of K4 and K9. Hum Mol Genet *20*, 2195-2203.

Di Cunto, F., Calautti, E., Hsiao, J., Ong, L., Topley, G., Turco, E., and Dotto, G.P. (1998). Citron rho-interacting kinase, a novel tissue-specific ser/thr kinase encompassing the Rho-Rac-binding protein Citron. J Biol Chem *273*, 29706-711.

Di Cunto, F., Imarisio, S., Hirsch, E., Broccoli, V., Bulfone, A., Migheli, A., Atzori, C., Turco, E., Triolo, R., et al. (2000). Defective neurogenesis in citron kinase knockout mice by altered cytokinesis and massive apoptosis. Neuron *28*, 115-127.

Dobyns, W.B. (2002). Primary microcephaly: new approaches for an old disorder. Am J Med Genet *112*, 315-17.

Dolk, H. (1991). The predictive value of microcephaly during the first year of life for mental retardation at seven years. Dev Med Child Neurol *33*, 974-983.

Drané, P., Ouararhni, K., Depaux, A., Shuaib, M., and Hamiche, A. (2010). The death-associated protein DAXX is a novel histone chaperone involved in the replication-independent deposition of H3.3. Genes Dev *24*, 1253-265.

Dürr, H., Körner, C., Müller, M., Hickmann, V., and Hopfner, K.P. (2005). X-ray structures of the Sulfolobus solfataricus SWI2/SNF2 ATPase core and its complex with DNA. Cell *121*, 363-373.

Earnshaw, W.C., and Migeon, B.R. (1985). Three related centromere proteins are absent from the inactive centromere of a stable isodicentric chromosome. Chromosoma *92*, 290-96.

Eda, M., Yonemura, S., Kato, T., Watanabe, N., Ishizaki, T., Madaule, P., and Narumiya, S. (2001). Rho-dependent transfer of Citron-kinase to the cleavage furrow of dividing cells. J Cell Sci *114*, 3273-284.

Eggert, U.S., Mitchison, T.J., and Field, C.M. (2006). Animal cytokinesis: from parts list to mechanisms. Annu Rev Biochem *75*, 543-566.

Ekwall, K. (2004). The RITS complex-A direct link between small RNA and heterochromatin. Mol Cell *13*, 304-05.

Ekwall, K., Javerzat, J.P., Lorentz, A., Schmidt, H., Cranston, G., and Allshire, R. (1995). The chromodomain protein Swi6: a key component at fission yeast centromeres. Science *269*, 1429-431.

Ekwall, K., Nimmo, E.R., Javerzat, J.P., Borgstrøm, B., Egel, R., Cranston, G., and Allshire, R. (1996). Mutations in the fission yeast silencing factors clr4+ and rik1+ disrupt the localisation of the chromo domain protein Swi6p and impair centromere function. J Cell Sci *109 (Pt 11)*, 2637-648.

Everett, R.D., Earnshaw, W.C., Pluta, A.F., Sternsdorf, T., Ainsztein, A.M., Carmena, M., Ruchaud, S., Hsu, W.L., and Orr, A. (1999). A dynamic connection between centromeres and ND10 proteins. J Cell Sci *112 (Pt 20)*, 3443-454.

Eymery, A., Souchier, C., Vourc'h, C., and Jolly, C. (2010). Heat shock factor 1 binds to and transcribes satellite II and III sequences at several pericentromeric regions in heat-shocked cells. Exp Cell Res *316*, 1845-855.

Fang, X., and Zhang, P. (2011). Aneuploidy and tumorigenesis. Semin Cell Dev Biol

Farkas, L.M., and Huttner, W.B. (2008). The cell biology of neural stem and progenitor cells and its significance for their proliferation versus differentiation during mammalian brain development. Curr Opin Cell Biol *20*, 707-715.

Ferguson-Smith, A.C., Sasaki, H., Cattanach, B.M., and Surani, M.A. (1993). Parental-origin-specific epigenetic modification of the mouse H19 gene. Nature *362*, 751-55.

Fish, J.L., Kosodo, Y., Enard, W., Pääbo, S., and Huttner, W.B. (2006). Aspm specifically maintains symmetric proliferative divisions of neuroepithelial cells. Proc Natl Acad Sci U S A *103*, 10438-443.

Flaus, A., Martin, D.M., Barton, G.J., and Owen-Hughes, T. (2006). Identification of multiple distinct Snf2 subfamilies with conserved structural motifs. Nucleic Acids Res *34*, 2887-2905.

Fong, K.W., Choi, Y.K., Rattner, J.B., and Qi, R.Z. (2008). CDK5RAP2 is a pericentriolar protein that functions in centrosomal attachment of the gamma-tubulin ring complex. Mol Biol Cell *19*, 115-125.

Frankel, A.D., Berg, J.M., and Pabo, C.O. (1987). Metal-dependent folding of a single zinc finger from transcription factor IIIA. Proc Natl Acad Sci U S A *84*, 4841-45.

Garrick, D., Samara, V., McDowell, T.L., Smith, A.J., Dobbie, L., Higgs, D.R., and Gibbons, R.J. (2004). A conserved truncated isoform of the ATR-X syndrome protein lacking the SWI/SNF-homology domain. Gene *326*, 23-34.

Garrick, D., Sharpe, J.A., Arkell, R., Dobbie, L., Smith, A.J., Wood, W.G., Higgs, D.R., and Gibbons, R.J. (2006). Loss of Atrx affects trophoblast development and the pattern of X-inactivation in extraembryonic tissues. PLoS Genet *2*, e58.

Gecz, J., Pollard, H., Consalez, G., Villard, L., Stayton, C., Millasseau, P., Khrestchatisky, M., and Fontes, M. (1994). Cloning and expression of the murine homologue of a putative human X-linked nuclear protein gene closely linked to PGK1 in Xq13.3. Hum Mol Genet *3*, 39-44.

Gibbons, R. (2006). Alpha thalassaemia-mental retardation, X linked. Orphanet J Rare Dis *1*, 15.

Gibbons, R.J., McDowell, T.L., Raman, S., O'Rourke, D.M., Garrick, D., Ayyub, H., and Higgs, D.R. (2000). Mutations in ATRX, encoding a SWI/SNF-like protein, cause diverse changes in the pattern of DNA methylation. Nat Genet *24*, 368-371.

Gibbons, R.J., Picketts, D.J., and Higgs, D.R. (1995a). Syndromal mental retardation due to mutations in a regulator of gene expression. Hum Mol Genet *4 Spec No*, 1705-09.

Gibbons, R.J., Picketts, D.J., Villard, L., and Higgs, D.R. (1995b). Mutations in a putative global transcriptional regulator cause X-linked mental retardation with alpha-thalassemia (ATR-X syndrome). Cell *80*, 837-845.

Gibbons, R.J., Suthers, G.K., Wilkie, A.O., Buckle, V.J., and Higgs, D.R. (1992). X-linked alpha-thalassemia/mental retardation (ATR-X) syndrome: localization to Xq12-q21.31 by X inactivation and linkage analysis. Am J Hum Genet *51*, 1136-149.

Gibbons, R.J., Wada, T., Fisher, C.A., Malik, N., Mitson, M.J., Steensma, D.P., Fryer, A., Goudie, D.R., Krantz, I.D., and Traeger-Synodinos, J. (2008). Mutations in the chromatin-associated protein ATRX. Hum Mutat *29*, 796-802.

Gieni, R.S., Chan, G.K., and Hendzel, M.J. (2008). Epigenetics regulate centromere formation and kinetochore function. J Cell Biochem *104*, 2027-039.

Glotzer, M. (2004). Cleavage furrow positioning. J Cell Biol *164*, 347-351.

Goldberg, A.D., Banaszynski, L.A., Noh, K.M., Lewis, P.W., Elsaesser, S.J., Stadler, S., Dewell, S., Law, M., Guo, X., et al. (2010). Distinct factors control histone variant H3.3 localization at specific genomic regions. Cell *140*, 678-691.

Gorbalenya, A.E., Koonin, E.V., Donchenko, A.P., and Blinov, V.M. (1988). A novel superfamily of nucleoside triphosphate-binding motif containing proteins which are probably involved in duplex unwinding in DNA and RNA replication and recombination. FEBS Lett *235*, 16-24.

Götz, M., and Huttner, W.B. (2005). The cell biology of neurogenesis. Nat Rev Mol Cell Biol *6*, 777-788.

Grewal, S.I., and Elgin, S.C. (2007). Transcription and RNA interference in the formation of heterochromatin. Nature *447*, 399-406.

Grewal, S.I., and Moazed, D. (2003). Heterochromatin and epigenetic control of gene expression. Science *301*, 798-802.

Hall, I.M., Noma, K., and Grewal, S.I. (2003). RNA interference machinery regulates chromosome dynamics during mitosis and meiosis in fission yeast. Proc Natl Acad Sci U S A *100*, 193-98.

Haubensak, W., Attardo, A., Denk, W., and Huttner, W.B. (2004). Neurons arise in the basal neuroepithelium of the early mammalian telencephalon: a major site of neurogenesis. Proc Natl Acad Sci U S A *101*, 3196-3201.

Hendzel, M.J., Wei, Y., Mancini, M.A., Van Hooser, A., Ranalli, T., Brinkley, B.R., Bazett-Jones, D.P., and Allis, C.D. (1997). Mitosis-specific phosphorylation of histone H3 initiates primarily within pericentromeric heterochromatin during G2 and spreads in an ordered fashion coincident with mitotic chromosome condensation. Chromosoma *106*, 348-360.

Henikoff, S., Ahmad, K., and Malik, H.S. (2001). The centromere paradox: stable inheritance with rapidly evolving DNA. Science *293*, 1098-1102.

Henikoff, S., Ahmad, K., Platero, J.S., and van Steensel, B. (2000). Heterochromatic deposition of centromeric histone H3-like proteins. Proc Natl Acad Sci U S A *97*, 716-721.

Hébert, J.M., and McConnell, S.K. (2000). Targeting of cre to the Foxg1 (BF-1) locus mediates loxP recombination in the telencephalon and other developing head structures. Dev Biol *222*, 296-306.

Higgs, D.R., and Weatherall, D.J. (2009). The alpha thalassaemias. Cell Mol Life Sci *66*, 1154-162.

Hirano, T. (2005). SMC proteins and chromosome mechanics: from bacteria to humans. Philos Trans R Soc Lond B Biol Sci *360*, 507-514.

Hollenbach, A.D., McPherson, C.J., Mientjes, E.J., Iyengar, R., and Grosveld, G. (2002). Daxx and histone deacetylase II associate with chromatin through an interaction with core histones and the chromatin-associated protein Dek. J Cell Sci *115*, 3319-330.

Hollenbach, A.D., Sublett, J.E., McPherson, C.J., and Grosveld, G. (1999). The Pax3-FKHR oncoprotein is unresponsive to the Pax3-associated repressor hDaxx. EMBO J *18*, 3702-711.

Horvitz, H.R., and Herskowitz, I. (1992). Mechanisms of asymmetric cell division: two Bs or not two Bs, that is the question. Cell *68*, 237-255.

Huttner, W.B., and Kosodo, Y. (2005). Symmetric versus asymmetric cell division during neurogenesis in the developing vertebrate central nervous system. Curr Opin Cell Biol *17*, 648-657.

Inoue, A., Hyle, J., Lechner, M.S., and Lahti, J.M. (2008). Perturbation of HP1 localization and chromatin binding ability causes defects in sister-chromatid cohesion. Mutat Res *657*, 48-55.

Ishov, A.M., Sotnikov, A.G., Negorev, D., Vladimirova, O.V., Neff, N., Kamitani, T., Yeh, E.T., Strauss, J.F., and Maul, G.G. (1999). PML is critical for ND10 formation and recruits the PML-interacting protein daxx to this nuclear structure when modified by SUMO-1. J Cell Biol *147*, 221-234.

Ishov, A.M., Vladimirova, O.V., and Maul, G.G. (2004). Heterochromatin and ND10 are cell-cycle regulated and phosphorylation-dependent alternate nuclear sites of the transcription repressor Daxx and SWI/SNF protein ATRX. J Cell Sci *117*, 3807-820.

Jackson, A.P., Eastwood, H., Bell, S.M., Adu, J., Toomes, C., Carr, I.M., Roberts, E., Hampshire, D.J., Crow, Y.J., et al. (2002). Identification of microcephalin, a protein implicated in determining the size of the human brain. Am J Hum Genet *71*, 136-142.

Jaskelioff, M., Van Komen, S., Krebs, J.E., Sung, P., and Peterson, C.L. (2003). Rad54p is a chromatin remodeling enzyme required for heteroduplex DNA joint formation with chromatin. J Biol Chem *278*, 9212-18.

Jolly, C., Metz, A., Govin, J., Vigneron, M., Turner, B.M., Khochbin, S., and Vourc'h, C. (2004). Stress-induced transcription of satellite III repeats. J Cell Biol *164*, 25-33.

Jolly, C., Mongelard, F., Robert-Nicoud, M., and Vourc'h, C. (1997). Optimization of nuclear transcript detection by FISH and combination with fluorescence immunocytochemical detection of transcription factors. J Histochem Cytochem *45*, 1585-592.

Kaindl, A.M., Passemard, S., and Gressens, P. (2009). Autosomal recessive primary microcephalies (MCPH). Eur J Paediatr Neurol *13*, 458.

Kamakaka, R.T., and Biggins, S. (2005). Histone variants: deviants? Genes Dev *19*, 295-310.

Kernohan, K.D., Jiang, Y., Tremblay, D.C., Bonvissuto, A.C., Eubanks, J.H., Mann, M.R., and Bérubé, N.G. (2010). ATRX partners with cohesin and MeCP2 and contributes to developmental silencing of imprinted genes in the brain. Dev Cell *18*, 191-202.

Kingston, R.E., Bunker, C.A., and Imbalzano, A.N. (1996). Repression and activation by multiprotein complexes that alter chromatin structure. Genes Dev *10*, 905-920.

Knizewski, L., Ginalski, K., and Jerzmanowski, A. (2008). Snf2 proteins in plants: gene silencing and beyond. Trends Plant Sci *13*, 557-565.

Konev, A.Y., Tribus, M., Park, S.Y., Podhraski, V., Lim, C.Y., Emelyanov, A.V., Vershilova, E., Pirrotta, V., Kadonaga, J.T., et al. (2007). CHD1 motor protein is required for deposition of histone variant H3.3 into chromatin in vivo. Science *317*, 1087-090.

Kosodo, Y., Röper, K., Haubensak, W., Marzesco, A.M., Corbeil, D., and Huttner, W.B. (2004). Asymmetric distribution of the apical plasma membrane during neurogenic divisions of mammalian neuroepithelial cells. EMBO J *23*, 2314-324.

Kourmouli, N., Sun, Y.M., van der Sar, S., Singh, P.B., and Brown, J.P. (2005). Epigenetic regulation of mammalian pericentric heterochromatin in vivo by HP1. Biochem Biophys Res Commun *337*, 901-07.

Kriegstein, A.R., and Götz, M. (2003). Radial glia diversity: a matter of cell fate. Glia *43*, 37-43.

Lachner, M., O'Carroll, D., Rea, S., Mechtler, K., and Jenuwein, T. (2001). Methylation of histone H3 lysine 9 creates a binding site for HP1 proteins. Nature *410*, 116-120.

De La Fuente, R., Viveiros, M.M., Wigglesworth, K., and Eppig, J.J. (2004). ATRX, a member of the SNF2 family of helicase/ATPases, is required for chromosome alignment and meiotic spindle organization in metaphase II stage mouse oocytes. Dev Biol *272*, 1-14.

Lallemand-Breitenbach, V., and de Thé, H. (2010). PML nuclear bodies. Cold Spring Harb Perspect Biol *2*, a000661.

Law, M.J., Lower, K.M., Voon, H.P., Hughes, J.R., Garrick, D., Viprakasit, V., Mitson, M., De Gobbi, M., Marra, M., et al. (2010). ATR-X syndrome protein targets tandem repeats and influences allele-specific expression in a size-dependent manner. Cell *143*, 367-378.

Le Douarin, B., Nielsen, A.L., Garnier, J.M., Ichinose, H., Jeanmougin, F., Losson, R., and Chambon, P. (1996). A possible involvement of TIF1 alpha and TIF1 beta in the epigenetic control of transcription by nuclear receptors. EMBO J *15*, 6701-715.

Lejeune, E., Bortfeld, M., White, S.A., Pidoux, A.L., Ekwall, K., Allshire, R.C., and Ladurner, A.G. (2007). The chromatin-remodeling factor FACT contributes to centromeric heterochromatin independently of RNAi. Curr Biol *17*, 1219-224.

Levy, M.A., Fernandes, A.D., Tremblay, D.C., Seah, C., and Bérubé, N.G. (2008). The SWI/SNF protein ATRX co-regulates pseudoautosomal genes that have translocated to autosomes in the mouse genome. BMC Genomics *9*, 468.

Lewis, P.W., Elsaesser, S.J., Noh, K.M., Stadler, S.C., and Allis, C.D. (2010). Daxx is an H3.3-specific histone chaperone and cooperates with ATRX in replication-independent chromatin assembly at telomeres. Proc Natl Acad Sci U S A *107*, 14075-080.

Li, R., Pei, H., Watson, D.K., and Papas, T.S. (2000). EAP1/Daxx interacts with ETS1 and represses transcriptional activation of ETS1 target genes. Oncogene *19*, 745-753.

Lia, G., Praly, E., Ferreira, H., Stockdale, C., Tse-Dinh, Y.C., Dunlap, D., Croquette, V., Bensimon, D., and Owen-Hughes, T. (2006). Direct observation of DNA distortion by the RSC complex. Mol Cell *21*, 417-425.

Lin, D.Y., Lai, M.Z., Ann, D.K., and Shih, H.M. (2003a). Promyelocytic leukemia protein (PML) functions as a glucocorticoid receptor co-activator by sequestering Daxx to the PML oncogenic domains (PODs) to enhance its transactivation potential. J Biol Chem *278*, 15958-965.

Lin, J.K., Chang, S.C., Yang, Y.C., and Li, A.F. (2003b). Loss of heterozygosity and DNA aneuploidy in colorectal adenocarcinoma. Ann Surg Oncol *10*, 1086-094.

Lipps, H.J., and Rhodes, D. (2009). G-quadruplex structures: in vivo evidence and function. Trends Cell Biol *19*, 414-422.

Lizarraga, S.B., Margossian, S.P., Harris, M.H., Campagna, D.R., Han, A.P., Blevins, S., Mudbhary, R., Barker, J.E., Walsh, C.A., and Fleming, M.D. (2010). Cdk5rap2 regulates centrosome function and chromosome segregation in neuronal progenitors. Development *137*, 1907-917.

Lossi, A.M., Millán, J.M., Villard, L., Orellana, C., Cardoso, C., Prieto, F., Fontés, M., and Martínez, F. (1999). Mutation of the XNP/ATR-X gene in a family with severe mental retardation, spastic paraplegia and skewed pattern of X inactivation: demonstration that the mutation is involved in the inactivation bias. Am J Hum Genet *65*, 558-562.

Low, S.H., Li, X., Miura, M., Kudo, N., Quiñones, B., and Weimbs, T. (2003). Syntaxin 2 and endobrevin are required for the terminal step of cytokinesis in mammalian cells. Dev Cell *4*, 753-59.

Madaule, P., Furuyashiki, T., Eda, M., Bito, H., Ishizaki, T., and Narumiya, S. (2000). Citron, a Rho target that affects contractility during cytokinesis. Microsc Res Tech *49*, 123-26.

Maison, C., Bailly, D., Peters, A.H., Quivy, J.P., Roche, D., Taddei, A., Lachner, M., Jenuwein, T., and Almouzni, G. (2002). Higher-order structure in pericentric heterochromatin involves a distinct pattern of histone modification and an RNA component. Nat Genet *30*, 329-334.

McDowell, T.L., Gibbons, R.J., Sutherland, H., O'Rourke, D.M., Bickmore, W.A., Pombo, A., Turley, H., Gatter, K., Picketts, D.J., et al. (1999). Localization of a putative transcriptional regulator (ATRX) at pericentromeric heterochromatin and the short arms of acrocentric chromosomes. Proc Natl Acad Sci U S A *96*, 13983-88.

Medina, C.F., Mazerolle, C., Wang, Y., Bérubé, N.G., Coupland, S., Gibbons, R.J., Wallace, V.A., and Picketts, D.J. (2009). Altered visual function and interneuron survival in Atrx knockout mice: inference for the human syndrome. Hum Mol Genet *18*, 966-977.

Meluh, P.B., Yang, P., Glowczewski, L., Koshland, D., and Smith, M.M. (1998). Cse4p is a component of the core centromere of Saccharomyces cerevisiae. Cell *94*, 607-613.

Meng, X., Fan, J., and Shen, Z. (2007). Roles of BCCIP in chromosome stability and cytokinesis. Oncogene *26*, 6253-260.

Mitson, M., Kelley, L.A., Sternberg, M.J., Higgs, D.R., and Gibbons, R.J. (2011). Functional significance of mutations in the Snf2 domain of ATRX. Hum Mol Genet

Miyata, T., Kawaguchi, A., Saito, K., Kawano, M., Muto, T., and Ogawa, M. (2004). Asymmetric production of surface-dividing and non-surface-dividing cortical progenitor cells. Development *131*, 3133-145.

Mohrmann, L., and Verrijzer, C.P. (2005). Composition and functional specificity of SWI2/SNF2 class chromatin remodeling complexes. Biochim Biophys Acta *1681*, 59-73.

Muchardt, C., Guilleme, M., Seeler, J.S., Trouche, D., Dejean, A., and Yaniv, M. (2002). Coordinated methyl and RNA binding is required for heterochromatin localization of mammalian HP1alpha. EMBO Rep *3*, 975-981.

Musacchio, A., and Salmon, E.D. (2007). The spindle-assembly checkpoint in space and time. Nat Rev Mol Cell Biol *8*, 379-393.

Nan, X., Hou, J., Maclean, A., Nasir, J., Lafuente, M.J., Shu, X., Kriaucionis, S., and Bird, A. (2007). Interaction between chromatin proteins MECP2 and ATRX is disrupted by mutations that cause inherited mental retardation. Proc Natl Acad Sci U S A *104*, 2709-714.

Nasmyth, K. (2005). How might cohesin hold sister chromatids together? Philos Trans R Soc Lond B Biol Sci *360*, 483-496.

Neef, R., Preisinger, C., Sutcliffe, J., Kopajtich, R., Nigg, E.A., Mayer, T.U., and Barr, F.A. (2003). Phosphorylation of mitotic kinesin-like protein 2 by polo-like kinase 1 is required for cytokinesis. J Cell Biol *162*, 863-875.

Neto, H., Collins, L.L., and Gould, G.W. (2011). Vesicle trafficking and membrane remodelling in cytokinesis. Biochem J *437*, 13-24.

Noctor, S.C., Martínez-Cerdeño, V., Ivic, L., and Kriegstein, A.R. (2004). Cortical neurons arise in symmetric and asymmetric division zones and migrate through specific phases. Nat Neurosci *7*, 136-144.

Nonaka, N., Kitajima, T., Yokobayashi, S., Xiao, G., Yamamoto, M., Grewal, S.I., and Watanabe, Y. (2002). Recruitment of cohesin to heterochromatic regions by Swi6/HP1 in fission yeast. Nat Cell Biol *4*, 89-93.

Oegema, K., Desai, A., Rybina, S., Kirkham, M., and Hyman, A.A. (2001). Functional analysis of kinetochore assembly in Caenorhabditis elegans. J Cell Biol *153*, 1209-226.

Ooi, S.K., Qiu, C., Bernstein, E., Li, K., Jia, D., Yang, Z., Erdjument-Bromage, H., Tempst, P., Lin, S.P., et al. (2007). DNMT3L connects unmethylated lysine 4 of histone H3 to de novo methylation of DNA. Nature *448*, 714-17.

Otani, J., Nankumo, T., Arita, K., Inamoto, S., Ariyoshi, M., and Shirakawa, M. (2009). Structural basis for recognition of H3K4 methylation status by the DNA methyltransferase 3A ATRX-DNMT3-DNMT3L domain. EMBO Rep *10*, 1235-241.

Palmer, D.K., O'Day, K., Trong, H.L., Charbonneau, H., and Margolis, R.L. (1991). Purification of the centromere-specific protein CENP-A and demonstration that it is a distinctive histone. Proc Natl Acad Sci U S A *88*, 3734-38.

Pazin, M.J., Bhargava, P., Geiduschek, E.P., and Kadonaga, J.T. (1997). Nucleosome mobility and the maintenance of nucleosome positioning. Science *276*, 809-812.

Petronczki, M., Glotzer, M., Kraut, N., and Peters, J.M. (2007). Polo-like kinase 1 triggers the initiation of cytokinesis in human cells by promoting recruitment of the RhoGEF Ect2 to the central spindle. Dev Cell *12*, 713-725.

Picketts, D.J., Higgs, D.R., Bachoo, S., Blake, D.J., Quarrell, O.W., and Gibbons, R.J. (1996). ATRX encodes a novel member of the SNF2 family of proteins: mutations point to a common mechanism underlying the ATR-X syndrome. Hum Mol Genet *5*, 1899-1907.

Picketts, D.J., Tastan, A.O., Higgs, D.R., and Gibbons, R.J. (1998). Comparison of the human and murine ATRX gene identifies highly conserved, functionally important domains. Mamm Genome *9*, 400-03.

Pidoux, A.L., and Allshire, R.C. (2000). Centromeres: getting a grip of chromosomes. Curr Opin Cell Biol *12*, 308-319.

Pidoux, A.L., and Allshire, R.C. (2005). The role of heterochromatin in centromere function. Philos Trans R Soc Lond B Biol Sci *360*, 569-579.

Piekny, A., Werner, M., and Glotzer, M. (2005). Cytokinesis: welcome to the Rho zone. Trends Cell Biol *15*, 651-58.

Provost, P., Silverstein, R.A., Dishart, D., Walfridsson, J., Djupedal, I., Kniola, B., Wright, A., Samuelsson, B., Radmark, O., and Ekwall, K. (2002). Dicer is required for

chromosome segregation and gene silencing in fission yeast cells. Proc Natl Acad Sci U S A *99*, 16648-653.

Quimby, B.B., Yong-Gonzalez, V., Anan, T., Strunnikov, A.V., and Dasso, M. (2006). The promyelocytic leukemia protein stimulates SUMO conjugation in yeast. Oncogene *25*, 2999-3005.

Reinhart, B.J., and Bartel, D.P. (2002). Small RNAs correspond to centromere heterochromatic repeats. Science *297*, 1831.

Ritchie, K., Seah, C., Moulin, J., Isaac, C., Dick, F., and Bérubé, N.G. (2008). Loss of ATRX leads to chromosome cohesion and congression defects. J Cell Biol *180*, 315-324.

Roberts, E., Hampshire, D.J., Pattison, L., Springell, K., Jafri, H., Corry, P., Mannon, J., Rashid, Y., Crow, Y., et al. (2002). Autosomal recessive primary microcephaly: an analysis of locus heterogeneity and phenotypic variation. J Med Genet *39*, 718-721.

Saha, A., Wittmeyer, J., and Cairns, B.R. (2002). Chromatin remodeling by RSC involves ATP-dependent DNA translocation. Genes Dev *16*, 2120-134.

Sarkisian, M.R., Li, W., Di Cunto, F., D'Mello, S.R., and LoTurco, J.J. (2002). Citron-kinase, a protein essential to cytokinesis in neuronal progenitors, is deleted in the flathead mutant rat. J Neurosci *22*, RC217.

Schramke, V., and Allshire, R. (2004). Those interfering little RNAs! Silencing and eliminating chromatin. Curr Opin Genet Dev *14*, 174-180.

Schueler, M.G., Higgins, A.W., Rudd, M.K., Gustashaw, K., and Willard, H.F. (2001). Genomic and genetic definition of a functional human centromere. Science *294*, 109-115.

Seah, C., Levy, M.A., Jiang, Y., Mokhtarzada, S., Higgs, D.R., Gibbons, R.J., and Bérubé, N.G. (2008). Neuronal death resulting from targeted disruption of the Snf2 protein ATRX is mediated by p53. J Neurosci *28*, 12570-580.

Shen, T.H., Lin, H.K., Scaglioni, P.P., Yung, T.M., and Pandolfi, P.P. (2006). The mechanisms of PML-nuclear body formation. Mol Cell *24*, 331-39.

Shi, Q., and King, R.W. (2005). Chromosome nondisjunction yields tetraploid rather than aneuploid cells in human cell lines. Nature *437*, 1038-042.

Shi, Y., and Berg, J.M. (1995). A direct comparison of the properties of natural and designed zinc-finger proteins. Chem Biol *2*, 83-89.

Sidman, R.L., and Rakic, P. (1973). Neuronal migration, with special reference to developing human brain: a review. Brain Res *62*, 1-35.

Singleton, M.R., Dillingham, M.S., and Wigley, D.B. (2007). Structure and mechanism of helicases and nucleic acid translocases. Annu Rev Biochem *76*, 23-50.

Skop, A.R., Liu, H., Yates, J., Meyer, B.J., and Heald, R. (2004). Dissection of the mammalian midbody proteome reveals conserved cytokinesis mechanisms. Science *305*, 61-66.

Solomon, L.A., Li, J.R., Bérubé, N.G., and Beier, F. (2009). Loss of ATRX in chondrocytes has minimal effects on skeletal development. PLoS One *4*, e7106.

Somers, W.G., and Saint, R. (2003). A RhoGEF and Rho family GTPase-activating protein complex links the contractile ring to cortical microtubules at the onset of cytokinesis. Dev Cell *4*, 29-39.

Stark, G.R., and Taylor, W.R. (2006). Control of the G2/M transition. Mol Biotechnol *32*, 227-248.

Stevenson, R.E., Abidi, F., Schwartz, C.E., Lubs, H.A., and Holmes, L.B. (2000). Holmes-Gang syndrome is allelic with XLMR-hypotonic face syndrome. Am J Med Genet *94*, 383-85.

Subramanya, H.S., Bird, L.E., Brannigan, J.A., and Wigley, D.B. (1996). Crystal structure of a DExx box DNA helicase. Nature *384*, 379-383.

Sullivan, K.F. (2001). A solid foundation: functional specialization of centromeric chromatin. Curr Opin Genet Dev *11*, 182-88.

Sun, Y., Kucej, M., Fan, H.Y., Yu, H., Sun, Q.Y., and Zou, H. (2009). Separase is recruited to mitotic chromosomes to dissolve sister chromatid cohesion in a DNA-dependent manner. Cell *137*, 123-132.

Taddei, A., Maison, C., Roche, D., and Almouzni, G. (2001). Reversible disruption of pericentric heterochromatin and centromere function by inhibiting deacetylases. Nat Cell Biol *3*, 114-120.

Tagami, H., Ray-Gallet, D., Almouzni, G., and Nakatani, Y. (2004). Histone H3.1 and H3.3 complexes mediate nucleosome assembly pathways dependent or independent of DNA synthesis. Cell *116*, 51-61.

Takahashi, T., Nowakowski, R.S., and Caviness, V.S. (1995). Early ontogeny of the secondary proliferative population of the embryonic murine cerebral wall. J Neurosci *15*, 6058-068.

Tang, J., Wu, S., Liu, H., Stratt, R., Barak, O.G., Shiekhattar, R., Picketts, D.J., and Yang, X. (2004). A novel transcription regulatory complex containing death domain-associated protein and the ATR-X syndrome protein. J Biol Chem *279*, 20369-377.

Thompson, S.L., Bakhoum, S.F., and Compton, D.A. (2010). Mechanisms of chromosomal instability. Curr Biol *20*, R285-295.

Torii, S., Egan, D.A., Evans, R.A., and Reed, J.C. (1999). Human Daxx regulates Fas-induced apoptosis from nuclear PML oncogenic domains (PODs). EMBO J *18*, 6037-049.

Tutt, A., Gabriel, A., Bertwistle, D., Connor, F., Paterson, H., Peacock, J., Ross, G., and Ashworth, A. (1999). Absence of Brca2 causes genome instability by chromosome breakage and loss associated with centrosome amplification. Curr Biol *9*, 1107-110.

Vaillend, C., Poirier, R., and Laroche, S. (2008). Genes, plasticity and mental retardation. Behav Brain Res *192*, 88-105.

Van Hooser, A.A., Ouspenski, I.I., Gregson, H.C., Starr, D.A., Yen, T.J., Goldberg, M.L., Yokomori, K., Earnshaw, W.C., Sullivan, K.F., and Brinkley, B.R. (2001). Specification of kinetochore-forming chromatin by the histone H3 variant CENP-A. J Cell Sci *114*, 3529-542.

Verdel, A., and Moazed, D. (2005). RNAi-directed assembly of heterochromatin in fission yeast. FEBS Lett *579*, 5872-78.

Villard, L., Fontès, M., Adès, L.C., and Gecz, J. (2000). Identification of a mutation in the XNP/ATR-X gene in a family reported as Smith-Fineman-Myers syndrome. Am J Med Genet *91*, 83-85.

Villard, L., Gecz, J., Mattéi, J.F., Fontés, M., Saugier-Veber, P., Munnich, A., and Lyonnet, S. (1996). XNP mutation in a large family with Juberg-Marsidi syndrome. Nat Genet *12*, 359-360.

Volpe, T.A., Kidner, C., Hall, I.M., Teng, G., Grewal, S.I., and Martienssen, R.A. (2002). Regulation of heterochromatic silencing and histone H3 lysine-9 methylation by RNAi. Science *297*, 1833-37.

Wada, T., Sugie, H., Fukushima, Y., and Saitoh, S. (2005). Non-skewed X-inactivation may cause mental retardation in a female carrier of X-linked alpha-thalassemia/mental retardation syndrome (ATR-X): X-inactivation study of nine female carriers of ATR-X. Am J Med Genet A *138*, 18-20.

Weaver, B.A., and Cleveland, D.W. (2005). Decoding the links between mitosis, cancer, and chemotherapy: The mitotic checkpoint, adaptation, and cell death. Cancer Cell *8*, 7-12.

Whitehouse, I., Stockdale, C., Flaus, A., Szczelkun, M.D., and Owen-Hughes, T. (2003). Evidence for DNA translocation by the ISWI chromatin-remodeling enzyme. Mol Cell Biol *23*, 1935-945.

Wilkie, A.O., Zeitlin, H.C., Lindenbaum, R.H., Buckle, V.J., Fischel-Ghodsian, N., Chui, D.H., Gardner-Medwin, D., MacGillivray, M.H., Weatherall, D.J., and Higgs, D.R. (1990). Clinical features and molecular analysis of the alpha thalassemia/mental retardation syndromes. II. Cases without detectable abnormality of the alpha globin complex. Am J Hum Genet *46*, 1127-140.

Wodarz, A., and Huttner, W.B. (2003). Asymmetric cell division during neurogenesis in Drosophila and vertebrates. Mech Dev *120*, 1297-1309.

Wong, L.H., McGhie, J.D., Sim, M., Anderson, M.A., Ahn, S., Hannan, R.D., George, A.J., Morgan, K.A., Mann, J.R., and Choo, K.H. (2010). ATRX interacts with H3.3 in maintaining telomere structural integrity in pluripotent embryonic stem cells. Genome Res *20*, 351-360.

Woods, C.G., Bond, J., and Enard, W. (2005). Autosomal recessive primary microcephaly (MCPH): a review of clinical, molecular, and evolutionary findings. Am J Hum Genet *76*, 717-728.

Xie, S., Wang, Z., Okano, M., Nogami, M., Li, Y., He, W.W., Okumura, K., and Li, E. (1999). Cloning, expression and chromosome locations of the human DNMT3 gene family. Gene *236*, 87-95.

Xue, Y., Gibbons, R., Yan, Z., Yang, D., McDowell, T.L., Sechi, S., Qin, J., Zhou, S., Higgs, D., and Wang, W. (2003). The ATRX syndrome protein forms a chromatin-remodeling complex with Daxx and localizes in promyelocytic leukemia nuclear bodies. Proc Natl Acad Sci U S A *100*, 10635-640.

Zhou, T., Aumais, J.P., Liu, X., Yu-Lee, L.Y., and Erikson, R.L. (2003). A role for Plk1 phosphorylation of NudC in cytokinesis. Dev Cell *5*, 127-138.

Chapter 2

2 Loss of ATRX Leads to Chromosome Cohesion and Congression Defects

In 2005, prior to undertaking the research presented in this chapter, the ATRX protein had been studied almost exclusively in the context of gene regulation. However in 1999 it was surprisingly reported that ATRX is highly enriched at PCH in mouse and human somatic cells (McDowell et al., 1999), and in mouse oocytes in 2004 (De La Fuente et al., 2004). The highly condensed domains of PCH on each chromosome are devoid of traditional mRNA producing genes, but are required structurally to ensure the proper interaction of the centromere with the mitotic spindle. Subsequently it was reported that ATRX was required for normal chromosome alignment on the metaphase II (MII) meiotic spindle (De La Fuente et al., 2004), however a similar requirement in somatic cells had not yet been reported. In this chapter I sought to investigate whether ATRX was required for normal chromosome alignment during mitotic cell division in human and mouse somatic cells.

This chapter was previously published as (Ritchie et al., 2008). Permissions for reproduction are found in Appendix 1.

2.1 Introduction

ATRX is a chromatin-remodeling enzyme implicated in early development of several organs, particularly the central nervous system (CNS). The ATRX protein contains conserved domains suggestive of a role in the epigenetic regulation of chromatin structure and function, including a plant homeodomain-like zinc finger domain shared with *de novo* methyltransferases (DNMT3A/B, 3L) and a SWI/SNF family ATPase domain. ATRX has the ability to remodel chromatin and displays ATP-dependent translocase activity (Xue et al., 2003). It is highly enriched at pericentromeric heterochromatin (PCH) in mouse and human cells (McDowell et al., 1999) and associates directly with the chromoshadow domain of heterochromatin protein 1α (HP1α) (Lechner et al., 2005). It is also targeted to promyelocytic leukemia nuclear bodies (PML-NBs) by

the C-terminal portion of the protein (Bérubé et al., 2008). *Atrx* loss of function in the mouse starting at the 8 to 16 cell stage is embryonic lethal (Garrick et al., 2006), and conditional ablation of the full-length ATRX isoform in the mouse forebrain results in decreased cortical size at birth (Bérubé et al., 2005). Although ATRX has been proposed to regulate gene transcription, the protein appears to be hyperphosphorylated and highly enriched at condensed chromosomes during mitosis in human cells, suggesting an additional function during this stage of the cell cycle (Bérubé et al., 2000).

The faithful segregation of chromosomes during mitosis requires the physical linkage of sister chromatids from S-phase until the onset of anaphase. The ring-shaped cohesin multiprotein complex is required for the maintenance of sister chromatid cohesion, and plays a role in the proper separation and segregation of sisters during anaphase (Hirano, 2005). Cohesin at the chromosomal arms is released during prophase by the Polo and Aurora B kinases and the chromatin protein wings apart-like (Wapl) (Sumara et al., 2002; Kueng et al., 2006; Gandhi et al., 2006). Cohesion at pericentromeric heterochromatin is protected by the Shugoshin (Sgo) family of proteins and prohibitin 2 (PHB2) and consequently persists until all the chromosomes are bi-oriented at the metaphase plate (McGuinness et al., 2005; Kitajima et al., 2006; Takata et al., 2007). Only then is the spindle checkpoint satisfied, resulting in the activation of the anaphase-promoting complex/cyclosome (APC/C) and subsequent cohesin cleavage by the thiol protease separase.

Stable loading of cohesin onto chromatin before DNA replication is mediated by the Scc2-Scc4 heterodimer in yeast (Ciosk et al., 2000; Watrin et al., 2006). Human Scc2, known as *NIPBL* (Delangin), mediates cohesin transfer onto chromatin during S phase and, like ATRX, associates with the chromoshadow domain of HP1α (Lechner et al., 2005). Chromatin remodeling proteins have been implicated in chromosome cohesion. The Sth1 subunit of the yeast RSC chromatin remodeling complex has been shown to participate in cohesin loading on chromosomal arms, but not at the centromere (Baetz et al., 2004; Huang et al., 2004). In human cells, the SNF2h/ISWI chromatin remodeling protein, a component of several remodeling complexes, was shown to participate in cohesin recruitment to specific sites on chromosome arms (Hakimi et al., 2002).

ATRX mutations in humans cause mental retardation and microcephaly (Gibbons et al., 1995; Picketts et al., 1996). Given that *Atrx* loss of function in the mouse forebrain results in reduced cortical mass (Bérubé et al., 2005) and that the protein becomes hyperphosphorylated at the onset of mitosis (Bérubé et al., 2000), we postulated that ATRX could have specific functions during mitosis. We now provide evidence that the SWI/SNF-like chromatin remodeling protein ATRX is required for normal chromosome congression, cohesion and segregation in human cultured cells. Loss of ATRX in neuronal progenitors by Cre/loxP recombination *in vivo* also resulted in abnormal chromosome segregation, as evidenced by the high incidence of micronuclei and dispersed chromosomes. Mitotic dysfunction could induce cell death in the developing brain and/or cause a reduction in symmetric cell divisions, therefore reducing the progenitor pool. Either of these scenarios or a combination thereof would be predicted to reduce cortical size at birth.

2.2 Materials and Methods

2.2.1 Cell Culture and Transfection

HeLa cells (ATCC) and HeLa-H2B-GFP cells (GM Wahl, The Salk Institute, La Jolla, CA 92037) were grown at 37^{o}C with 5% CO_2 in Dulbecco's Modified Eagle's Medium supplemented with 10% fetal bovine serum (Sigma-Aldrich, St. Louis, MO). HeLa-H2B-GFP growth media was supplemented with 2μg/ml Blasticidin S HCl (Invitrogen, Carlsbad, CA) to maintain transgene expression. For siRNA transfection, cells were seeded 24 hours prior to transfection using Lipofectamine 2000 following the manufacturer's instructions (Invitrogen). The final siRNA concentration used in all experiments was 8nM. In HeLa cells, the transfection efficiency was approximately 90-95% based on immunofluorescence detection of the ATRX protein isoforms. For population synchronization at G1/S, transfected cells were incubated with hydroxyurea (10μM) and released after 16 hours by removal of the drug.

2.2.2 RNA Interference

The synthetic oligonucleotides siATRX1 (5'-GAGGAAACCUUCAAUUGUAUU-3'), siATRX2 (5'- GCAGAGAAAUUCCUAAAGAUU-3') and siATRX1 Scrambled (5'-

GAUUGAAGACUGAUAUCACUU-3') were obtained from Dharmacon (Lafayette, CO). Control (non-targeting) siRNA duplex was obtained from Sigma. siRNA duplexes were transfected with Lipofectamine 2000 (Invitrogen) according to the manufacturer's instructions. Mock-transfected samples were treated similarly but without addition of siRNA.

2.2.3 Western Blot Analysis

Cells were lysed with RIPA buffer [150 mM NaCl, 1 % NP-40, 50 mM Tris pH 8.0, 0.5 % deoxycholic acid, 0.1 % SDS, 0.2 mM phenylmethylsulfonyl fluoride (PMSF), 0.5 mM NaF, 0.1 mM Na_3VO_4, 1 protease inhibitor cocktail tablet (Complete Mini, EDTA-free, Roche Diagnostics GmbH, Mannheim, Germany)] for 5 min on ice. Extracts were sonicated and quantified using the DC Protein Assay (Bio-Rad, Hercules, CA). Protein (20 μg) was resolved on 6 % or 12 % SDS-PAGE and transferred onto nitrocellulose membranes (Bio-Rad). The membranes were probed with rabbit α-ATRX H300 (Santa Cruz Biotechnology, Santa Cruz, CA), mouse α-ATRX 39f (gift of D.J. Picketts and D. Higgs, Institute of Molecular Medicine, John Radcliffe Hospital, Headington, Oxford, UK), followed by appropriate horseradish peroxidase-conjugated secondary antibody (Amersham Biosciences, Quebec, 1:5000). After washing, the membrane was incubated in ECL before exposure to X-ray film. The membrane was re-probed with mouse α-anti-tubulin (Sigma; 1:40,000) as a loading control.

2.2.4 Quantitative Reverse-Transcriptase Polymerase Chain Reaction (Q-RT-PCR) Analysis

Total RNA was isolated using the RNeasy Mini kit (QIAGEN, Valencia, CA). First-strand cDNA was synthesized from 3 μg of total RNA using random primers and a reverse transcriptase (RT) cocktail containing 5X first strand buffer, 100 mM DTT, 25 mM dNTPs, RNA guard and Superscript RT. PCR reactions were performed on a Chromo4 Continuous Fluorescence Detector (MJ Research) in the presence of iQ^{TM} SYBR Green supermix (Bio-Rad) and analyzed with Opticon Monitor 3 and GeneX software (Bio-Rad) using the standard curve Ct method of quantification. Samples were amplified as follows: 95 ^{o}C for 30 sec, 55 ^{o}C for 30 sec, 72 ^{o}C for 30 sec. After 30 cycles,

a melting curve was generated to visualize amplicon purity. Standard curves were generated for each primer pair using fivefold serial dilutions of control cDNA. Primer efficiency was calculated as $\%E = [(10^{-1/slope}) - 1]x100$, where a desirable slope is –3.32 and $r^2>0.99$. All data was normalized GAPDH expression levels. The primers used for Q-RT-PCR were as follows: ATRX-F: 5'-TCCTTGCACACTCATCAGAAGAATC-3' ATRX-R: 5'-CGTGACGATCCTGAAGACTTGG-3' GAPDH-F: 5'-GAGTCAACGG ATTTGGTCGT-3' GAPDH-R: 5'-GACAAGCTTCCCGTTCTCAG-3'.

2.2.5 Flow Cytometry

Exponentially growing cells were harvested, washed with CMF PBS (NaCl 137mM, KCl 2.7mM, Potassium Phosphate Monobasic 1.5mM, Sodium Phosphate Dibasic 12mM) three times and $1.5x10^6$ cells fixed drop wise with 90% ethanol and stored at 4ºC for at least 12 hours. To detect DNA content, cells were washed and stained with propidium iodide/RNase staining solution (10μg/ml PI), 250μg/ml RNase A (Sigma) 2% BSA in CMF PBS for 30 min at room temperature, followed by overnight incubation at 4°C. Cell populations were analyzed by flow cytometry on a Beckman-Coulter EPICS XL-MCL instrument. Data analysis to determine the proportion of cells in each phase of the cell cycle was carried out using the Expo 32 software package (Beckman Coulter).

2.2.6 Indirect Immunofluorescence Microscopy

For immunofluorescence detection, cells were fixed with EtOH:MeOH (3:1) up to four days following siRNA transfection and incubated with the following primary antibodies: α-ATRX H300 antibody (Santa Cruz, 1:200), α-ATRX 39f antibody (D.J. Picketts, Ottawa Health Research Institute, Ottawa, Canada; 1:20) α-alpha tubulin (Sigma, 1:1500), α-phosphohistone H3(S10) (Upstate, Billerica, MA; 1:200) human α-CREST (W. Brinkley, Baylor College of Medicine, Houston, TX; 1:10000) α-BubR1 (BD Transduction Labs, 1:200), α-Bub1 (a gift from S. Taylor, University of Manchester, Manchester, UK, M13 9PT; 1:1000), α-CENP-E (Santa Cruz; 1:400), α-CENP-F (S. Taylor 1:100), α-HP1α (Upstate, 1:200), α-HP1β (Upstate, 1:200). Secondary antibodies included goat α-rabbit Alexa 594 (1:1500), donkey α-rabbit Alexa 488 (1:1500) goat α-mouse Alexa 488 (1:1500), goat α-mouse Alexa 594 (1:1500), and goat α-human Alexa

647 (1:1500) (Invitrogen). Coverslips were mounted with Vectashield H-1000 (Vector Laboratories).

2.2.7 Generation of ATRX-depleted Stable Clones

Pairs of sense 60-mer oligonucleotides corresponding to the 19-mer siATRX1 and siATRX2 siRNA target sequences and their reverse complement (underlined sequences) were designed that contained 5' BglII and 3' HindIII restriction sites to facilitate cloning (Integrated DNA Technologies, Inc): shATRX1 (sense) 5'-GATCCCCGAGGAAACCTTCAATTGTATTCAAGAGATACAATTGAAGGTTTCCTCTTTTTA-3' and shATRX2 (sense) 5'-GATCCCCGCAGAGAAATTCCTAAAGATTCAAGAGATCTTTAGGAATTTCTCTGCTTTTTA-3'. The oligonucleotides were annealed to complimentary anti-sense 60-mer oligonucleotides in buffer containing 10mM Tris pH 7.5, 50 mM NaCl, and 1 mM EDTA at 90ºC for 4 min, followed by 70ºC for 10 min, then step cooled to 37ºC for 20 min using a thermocycler (MJ research) and cloned into the pSuper.retro.neo plasmid (Oligoengine Inc.) using the Quick Ligation Kit according to manufacturer's instructions (New England Biolabs). The resulting vectors, designated pSUPER-shATRX1 and pSUPER-shATRX2, were subsequently sequenced to confirm sequence identity. Exponentially growing HeLa-H2B-GFP were transfected with empty pSuper vector or with pSuper-shATRX1 and pSuper-shATRX2 vectors (1μg/ml) using Lipofectamine 2000 (Invitrogen). Two days after transfection, cells were replated at low density and selection was applied 24 hours later (800μg/ml Geneticin, GIBCO). Drug-resistant colonies were picked and expanded in selection media (400μg/ml Geneticin).

2.2.8 Time-Lapse and Live-Cell Microscopy

HeLa-HG, HG-pSuper, HG-shATRX1, or HG-shATRX2 cells were plated on 35mm glass bottom tissue culture dishes (Mattek) in DMEM 10% FBS. After 24h, the media was replaced with CO_2-independent media (Gibco) supplemented with 10% FBS and 4mM L-glutamine (Sigma). For transient experiments, cells were plated and transfected and scored 48-72h following transfection. Cells were imaged using a Leica DMI 6000b automated inverted microscope equipped with a live cell stage-mounted environment chamber (Neue Biosciences) to maintain the cells at 37°C during imaging. Phase

contrast and fluorescence (GFP) images were captured every 3 min for 10 hours using Openlab Software automation (v5.0, Improvision). To measure mitotic duration, cells that initiated mitosis (determined by nuclear envelope breakdown) and re-entered G1 (nuclear decondensation) within the time frame of the experiment (10 hours) were analyzed (n>50). This analysis did not include cells that were arrested at pro-metaphase or that died during the timeframe of the experiment. To measure the frequency of unaligned chromosomes at metaphase, cells were seeded in 35mm culture wells (BD Bioscience) in DMEM 10% FBS, and at least 500 metaphase cells were scored per sample. For mitotic spindle checkpoint arrest, HeLa-HG or HG-shATRX1 cells were treated with 100ng/ml nocodazole for 16 hours. Rounded mitotic cells and adherent interphase cells were quantified using live cell microscopy (n>1000).

2.2.9 Fixed Chromosome Spreads

HeLa cells were transiently transfected with no siRNA duplex (mock), siATRX1 Scrambled (non-specific control), siATRX1, or siATRX2. Mitotically arrested cells were removed by shake-off 70 hours following transfection and adherent cells were treated with 100 ng/ml Karyomax Colcemid (Invitrogen) for 2 hours. Mitotic cells were then isolated and incubated in hypotonic solution (75mM KCl) for 20 minutes, followed by fixation in Carnoy's Fix (3:1 MeOH:AcOH) and stored at -20°C. Fixed cells were dropped onto Fisher Superfrost Plus glass microscope slides and air dried, DNA was counterstained with DAPI (100ng/ml) and mounted in Vectashield H-1000 (Vector Labs). For Z-stack imaging, 0.4 μm interval Z-stacks were captured and deconvolved using iterative restoration with Volocity imaging software (v4.0 Improvision).

2.2.10 Measure of Interkinetochore Distances

To measure interkinetochore distance, mitotic HeLa-HG, HG-pSuper, HG-shATRX1 and HG-shATRX2 stable cells were fixed in 3:1 EtOH:MeOH, the kinetochores were stained using the human CREST antibody (1:10,000), and imaged using a 63x 1.4na oil-immersion objective. Z-stacks were captured at 0.4μm z-intervals spanning 20μm. Kinetochore pairs were connected from the outer edges of the CREST signal and the distance measured using Volocity software (v4.0, Improvision). Only kinetochore pairs

in single optical sections that were aligned at the metaphase plate were used to measure interkinetochore distances (n≥100). Statistical differences were assessed by analysis of variance (ANOVA). Significant differences in mean interkinetochore distance were assessed by Analysis of Variance (ANOVA) and a Tukey's multiple comparison post hoc test. Differences were considered significant when $p<0.05$. Statistical analysis was performed using Graph Pad Prism (v4.02).

2.2.11 Kinetochore Microtubule Assay

HeLa-HG, HG-pSuper, HG-shATRX1, or HG-shATRX2 cells were seeded in 35mm dishes (Corning) in 2ml DMEM 10% FBS on 22mm^2 glass coverslips (VWR scientific). After 48h, the growth media was replaced with ice-cold growth media and the cells were incubated on ice for 10 minutes. The cells were rinsed twice with ice cold PHEM buffer (60mM piperazine ethanesulfonic acid, 45mM HEPES, 10mM EGTA, 2mM $MgCl_2$, pH 6.9), permeabilized with cold 0.5% TritonX-100 in PHEM buffer for 3 minutes, and then fixed in cold 3.5% paraformaldehyde in PHEM for 15 minutes. The coverslips were rinsed with PHEM and processed for immunofluorescence staining and microscopy.

2.2.12 Analysis of Mitotic Cells in the Developing Telencephalon

The generation of *Atrx*^{loxP} mice was described previously (Bérubé et al., 2005; Garrick et al., 2006) and were obtained from D. Higgs and R. Gibbons (University of Oxford, Oxford, UK, OX3 9DS). Male embryos conditionally deficient for *Atrx* were obtained by crossing homozygous *Atrx*^{loxP} females to heterozygous Foxg1Cre knock-in male mice and embryonic yolk sac DNA from E13.5 embryos were genotyped by PCR as previously described (Bérubé et al., 2005). Midday of the day of vaginal plug discovery was considered as embryonic day 0.5. At scheduled times, pregnant females were anesthetized by CO_2 and sacrificed by cervical dislocation. Embryos and postnatal brains were fixed in 4% paraformaldehyde/phosphate buffered saline (PBS) overnight at 4^{o}C, sunk in 30% sucrose in PBS and embedded in 15% sucrose and 50% OCT (Sakura Finetek USA Inc.). Tissue sections were cut at 10 μm thickness and mounted on Fisher SuperFrost Plus slides, air dried at room temperature and stored at –80^{o}C. For immunofluorescence staining, sections were thawed, rehydrated in PBS for 10 min,

counterstained with DAPI and mounted in Vectashield (Vector Laboratories). Micronuclei and misaligned chromosomes from the mitotic layer lining the lateral ventricle were scored from both hemispheres of brain sections (n=3) in four litter matched control (Foxg1Cre) and ATRX-null embryos using fluorescence microscopy. Analysis was restricted to the mitotic layer that lines the hippocampal hem, hippocampal primordium and the dorsal cortical neuroepithelium (indicated by the area between 1 and 2 in Figure 5C).

2.2.13 Details of Image Acquisition and Processing

All samples processed for microscopy were imaged using a Leica DMI 6000b automated inverted microscope. Images were captured using a 63x 1.4NA and 40x NA 1.25 oil immersion lens (Leica), or a 5x dry objective (Leica). For oil immersion microscopy, we used Leica immersion oil with a refractive index of 1.518. All images were captured at ambient temperature, except for image capture of live cells and time-lapse experiments, which were performed at 37°C. Experiments used different combinations of DAPI, Goat anti-rabbit Alexa 594, Goat anti-mouse Alexa 594, Donkey anti- rabbit Alexa 488, Goat anti-mouse Alexa 488, and Goat anti-human 594 secondary antibodies. Digital microscopy images were captured with a Hammamatsu ORCA-ER digital camera. Openlab (v5.0, Improvision) imaging software was used for manual and automated image capture, and processing was performed using Volocity (v4.0, Improvision). All deconvolution was performed using iterative restoration set with a confidence limit of 95%.

2.3 Results

2.3.1 ATRX-depleted HeLa Cells Exhibit Unusual Nuclear Morphology and DNA Bridging

The *ATRX* gene yields two major protein isoforms: a full-length 280kDa protein and a truncated form, ATRXt, of 180kDa (Garrick et al., 2004). Both ATRX protein isoforms exhibit an exclusive nuclear localization and are highly enriched at pericentromeric heterochromatin (Figures 2-1A and 2-1C). We induced transient ATRX depletion in HeLa cells by transfecting small interfering (si)RNAs. Cells were treated with two

siRNA duplexes, siATRX1 and siATRX2, each designed to simultaneously silence the full length and truncated ATRX proteins. Both duplexes caused substantial silencing of ATRX isoforms as assessed by immunostaining (Supplementary Figure 2-1A), and this was confirmed by quantitative reverse-transcriptase-PCR (Q-RT-PCR; Supplementary Figure 2-1B) and Western blot analysis (Figure 2-1B). Co-immunofluorescence staining of centromeres using the CREST antibody demonstrated that only minimal amounts of ATRX protein are detectable at pericentromeric heterochromatin in siRNA-treated cells (Figure 2-1C). We observed that the nuclei of depleted cells appeared lobulated and the cells showed evidence of intranuclear DNA bridges and poorly resolved chromatin masses during interphase (Figure 2-1D). We scored the number of abnormal nuclei at 48, 72 and 96 hours post-transfection and found an increased incidence of lobulated nuclei and of intranuclear bridges (Figure 2-1E). Such abnormalities can be indicative of mitotic defects and prompted us to further investigate the function of ATRX in mitosis.

2.3.2 Prolonged Prometaphase to Metaphase Transition upon Downregulation of ATRX

To investigate the kinetics of mitotic progression, we assessed the outcome of both transient and stable depletion of ATRX in HeLa cells that express histone H2B fused to the green fluorescent protein, HeLa-H2B-GFP (HG). Stable clones were difficult to expand, suggesting that reduced ATRX expression imparts negative effects on cell division, proliferation, or viability. A negative impact on cell division was previously reported upon conditional ablation of the full-length ATRX protein in embryonic stem (ES), although the cause was not determined (Garrick et al., 2006) We chose two stable cell lines for our analysis, designated shATRX1 and shATRX2, each expressing a shRNA that targets a distinct sequence within the *ATRX* transcript. Both stable clones expressed substantially reduced levels of *ATRX* RNA and protein as determined by Q-RT-PCR and Western blot analysis (Figure 2-2A).

Time-lapse videomicroscopy was used to evaluate the outcome of both transient and stable ATRX silencing. We generated videos of live cells (10 hours) and from these, measured the time required to complete each stage of mitosis (stable clone n=50; transient depletion n≥120). This analysis revealed that ATRX-depleted cells took longer

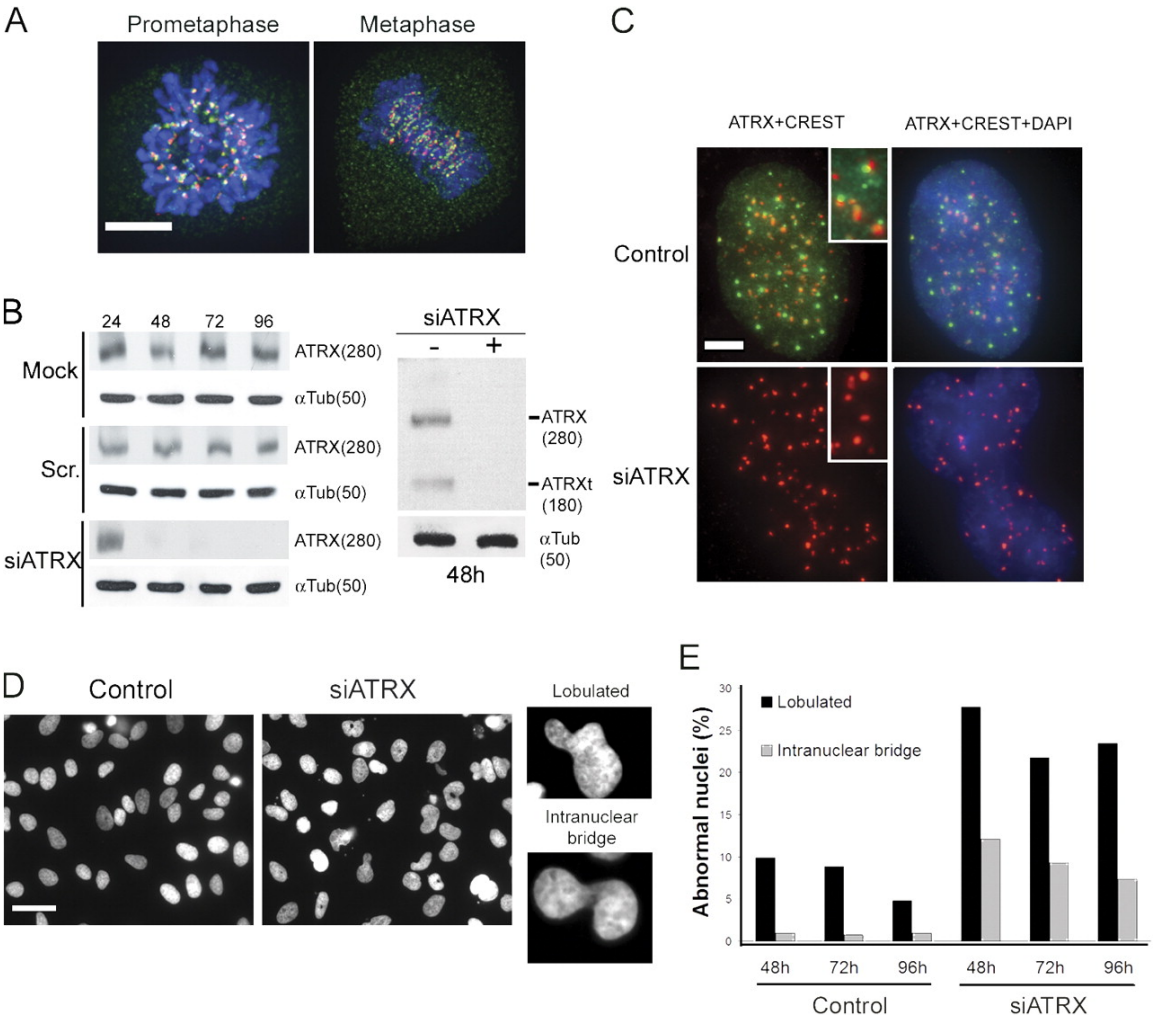

Figure 2-1. Transient ATRX depletion in HeLa cells induces abnormal nuclear morphology.

(A) Immunofluorescence detection of ATRX (green) and the kinetochore marker CREST (red) on prometaphase and metaphase chromosomes. (B) Western blot analysis of HeLa cells transiently transfected with siATRX 19-mer duplexes demonstrate ATRX protein depletion starting at 48 h and up to 96 h after transfection. ATRX protein levels remained constant upon mock transfection and in cells transfected with a control siATRX scrambled sequence duplex (left). Both ATRX isoforms were effectively silenced by 48 h after transfection (right). α-Tubulin protein expression (αTub) was used as a control in all experiments. Numbers on top of the blot indicate hours after transfection and numbers in parenthesis indicate the molecular mass in kDa. (C) Co-staining of kinetochores and ATRX with the CREST and 39f antibodies, respectively, reveals loss of ATRX protein at PCH in siRNA-treated cells. (D) Cells stained with DAPI show abnormal nuclear morphology in ATRX-depleted cells compared with control (scrambled siRNA) treated cells. Common defects include lobulated nuclei and intranuclear DNA bridges (right). (E) The number of nuclei displaying abnormalities was quantified at 48, 72, and 96 h after siRNA treatment (n > 1,000 nuclei at each time point). Bars: (A and C) 5 μm; (D) 20 μm.

than control siRNA transfected cells to undergo mitosis (Supplementary Figure 2-2) due to an extended transition from prometaphase to a fully aligned metaphase (Figure 2B, $p<0.001$). The delays in prometaphase were underestimated since a subset of mitotic cells that were arrested at prometaphase or metaphase for the total duration of the observation period (10 hours) were not included in this analysis. These chronically arrested prometaphase cells often became non-adherent and/or died, as indicated by membrane blebbing and highly condensed chromatin (Video S2-1). Taken together, these results show that ATRX is required for the normal transition from prometaphase to metaphase during mitosis.

2.3.3 ATRX Depletion Affects Chromosome Congression

The mitotic delay in ATRX-depleted cells occurred primarily between prometaphase and metaphase, a time when condensed chromosomes are congressing toward the metaphase plate. We noticed that metaphase plates in transiently depleted cells and in the shATRX1 and shATRX2 stable cell lines were often characterized by misaligned chromosomes or by chromosomes that remained randomly distributed over the bipolar microtubule spindle (Figure 2-2C and Video S2-2), suggesting that the prometaphase-to-metaphase delay might be caused by impaired chromosome congression (chromosome movement mediated by the mitotic spindle) to the spindle equator. To evaluate the extent of this defect, we scored the number of metaphasic cells with misaligned chromosomes in control siRNA transfected and ATRX-depleted live cell cultures. A greater proportion of metaphase plates had misaligned chromosomes in the shATRX1 and shATRX2 depleted clones compared to control HG-pSuper cells (Figure 2-2C and 2-2E). In addition, we followed stably (shATRX1; $n=100$) and transiently (siATRX; $n\geq120$) depleted mitotic cells by videomicroscopy over a 10 hour period and observed an approximately 3-fold (stable depletion) and 4-fold (transient depletion) increase in the number of cells displaying congression defects in ATRX-depleted cells compared to control HG-pSuper cells during that time period (Figure 2-2D). In addition, metaphasic cells often appeared less condensed in ATRX-depleted cells and were sometimes observed to undergo decondensation/recondensation (or mitotic rotation) prior to anaphase onset by live-cell imaging (Figure 2-2E, middle panels and Video S2-3). We further confirmed the general

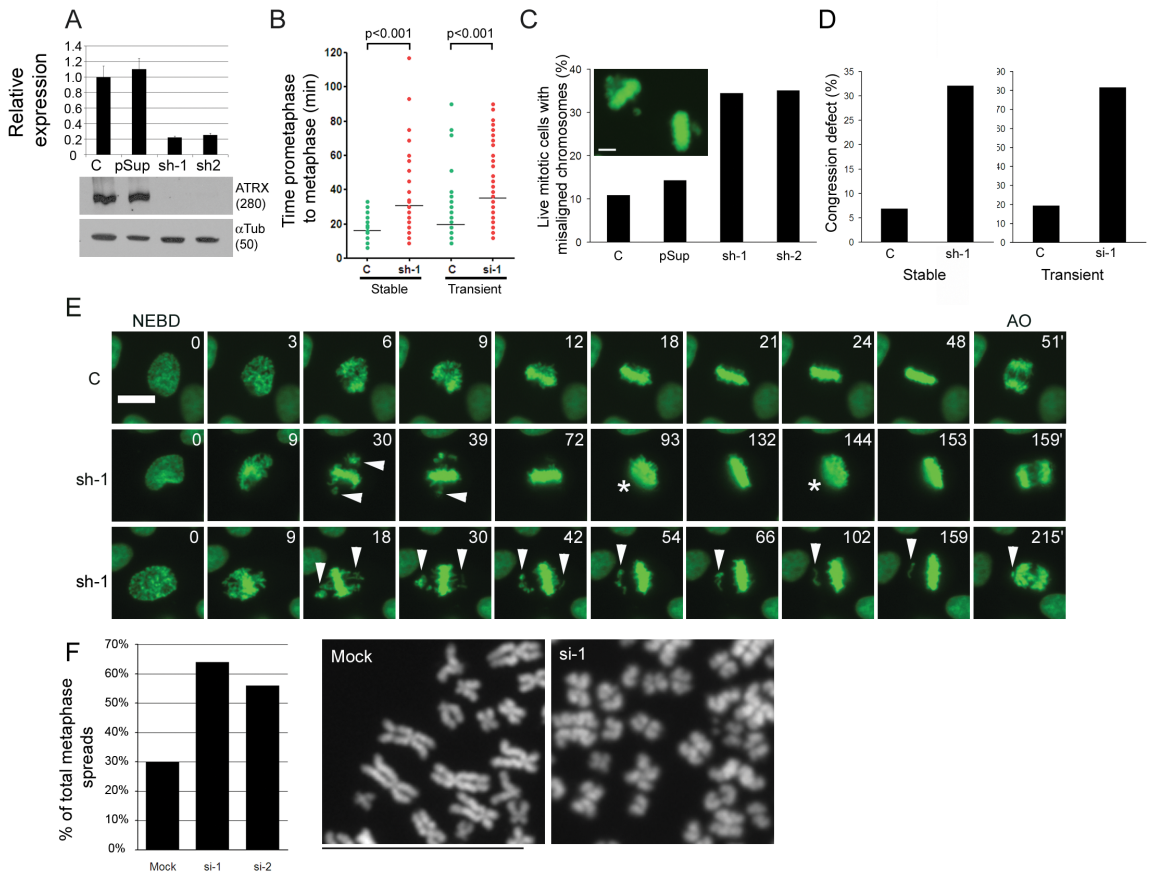

Figure 2-2. Stable and transient depletion of ATRX extends the transition to metaphase and induces congression defects.

(A) HeLa-HG cells that stably express pSuper-shATRX1, pSuper-shATRX2, or pSuper (empty vector control) were generated and the level of ATRX depletion was measured by Q-RT-PCR (top) and Western blot analysis (bottom). Q-RT-PCR results were normalized to GAPDH expression and protein loading on the Western blot was controlled with α-tubulin. Error bars represent the standard deviation from triplicate samples. (B) Mitotic cells were followed in real time by videomicroscopy and the duration of prometaphase was measured for pSuper control and HG-shATRX1 stably depleted cells (n = 50 each) and also in transient transfections with siATRX1 (n > 120). Horizontal lines indicate the mean value of each dataset. (C) The fraction of metaphasic cells with misaligned chromosomes (inset) was evaluated in live cell cultures of HeLa-HG, HG-pSuper, HG-shATRX1, and HG-shATRX2 stable clones (n = 100 for each). To score chromosome misalignment, any visibly discrete GFP-positive signal that was distinct from the metaphase plate was scored as a misaligned chromosome(s). (D) Live mitotic cells were followed over a 10 h period and scored for congression defects in stable (n = 50) and transient experiments (n > 120). (E) Selected panels from live cell videomicroscopy experiments of control HeLa-HG cells and ATRX-depleted cells from nuclear envelope breakdown (NEBD) to anaphase onset (AO). ATRX-depleted mitotic cells often displayed misaligned chromosomes (arrowheads) that resolved before the onset of

anaphase (middle), whereas, in some cases, anaphase was initiated despite the presence of misaligned chromosomes (bottom). A subset of metaphase chromosomes underwent cycles of general decondensation and recondensation, or mitotic rotation (the asterisk indicates a decondensed metaphase plate). Numbers indicate minutes after NEBD. (F) Morphological assessment of chromosome decondensation in control siRNA treated and cells transiently depleted of ATRX. Graph depicts the percentage of metaphase spreads that display a more decondensed appearance (far right). Bars: (C) 5 μm; (E) 16 μm, (F) 20 μm.

decondensed appearance of ATRX-depleted metaphasic chromosomes by staining chromosome spreads with DAPI. The frequency of spreads with a staining pattern indicative of more decondensed chromatin (wider chromosomes) was higher in cells transiently depleted of ATRX using siATRX1 and siATRX2 duplexes (Figure 2-2F) than in control siRNA treated cells. These results demonstrate that transient as well as stable silencing of ATRX interferes with normal prometaphase-to-metaphase progression, causes impaired chromosome congression and is sometimes accompanied by chromosome decondensation.

2.3.4 Sister Chromatid Cohesion is Compromised in ATRX Depleted Cells

Abnormal chromosomal congression could be caused by perturbed targeting of outer kinetochore proteins to the centromere, spindle defects, abnormal pericentromeric heterochromatin or reduced cohesion between sister chromatids. Congression defects have been reported upon depletion of the outer-kinetochore proteins CENP-E and CENP-F (mitosin) that are essential for stable MT-kinetochore capture (Yao et al., 1997; Wood et al., 1997; McEwen et al., 2001; Yang et al., 2005). We examined the ability of CENP-E and CENP-F to localize to kinetochores in ATRX depleted cells and found that both proteins localized normally at the kinetochore of metaphasic cells (Figure 2-3A). The loss of factors that control pericentromeric heterochromatin (PCH) structure can also cause aberrant mitosis (Melcher et al., 2000; Peters et al., 2001). Specific histone modifications that characterize PCH, including trimethylated H3K9 and H4K20 and monomethylated H3K27, were not visibly affected in ATRX-depleted cells (data not shown). Trimethylation of Lys9 on histone H3 (H3K9me3) by the Suv39H1 methyltransferase recruits HP1α and forms a compact heterochromatic structure. HP1α in turn interacts with several chromatin factors, including NIPBL, ATRX and CAF-1 (Lechner et al., 2005). However, we observed that nuclear HP1α as well as HP1β immunoreactivity was indistinguishable between transiently-depleted and control siRNA treated cells (Supplementary Figure 2-3), suggesting that ATRX is not required for proper targeting of these proteins to PCH.

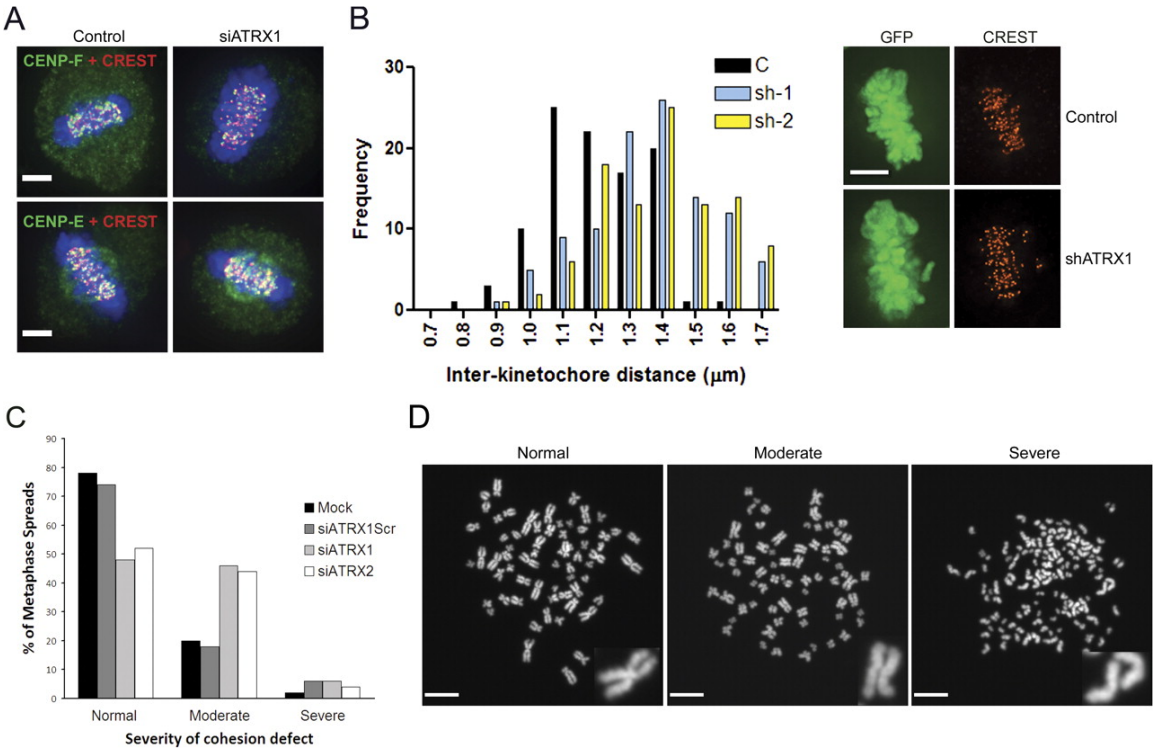

Figure 2-3. Increased interkinetochore distances and reduced cohesion in ATRX-depleted cells.

(A) ATRX-depleted metaphase cells were stained for the kinetochore proteins CENP-F or CENP-E (green) in combination with CREST (red) and imaged at different z planes. Images represent an extended focus rendering of deconvoluted z stacks. (B) Control and ATRX-depleted cells were stained with anti-CREST antibody to stain kinetochores. Distances between paired kinetochores (n = 100) were measured at individual z planes and were significantly increased in shATRX1 and shATRX2 cells compared with control HG-pSuper cells ($P < 0.05$ by ANOVA). (C) Mitotic HeLa cells were transiently transfected with either siATRX-Scr control or siATRX1 and siATRX2 duplexes. After mitotic shake-off to remove any cells in mitosis, cells were treated with colcemid and chromosome spreads were stained with DAPI and scored for the percentage of chromatids displaying cohesion defects (n = 50 per treatment). Chromosomes from ATRX-depleted cells showed reduced cohesion compared with control scrambled siRNA-treated cells. (D) Microscopic images of representative chromosome spreads scored as normal (<10% cohesion defect), moderate (10–90% cohesion defect), or severe (>90% cohesion defect). Insets show representative chromosomes from each spread with normal (left), moderate (middle), and severe (right) cohesion defects. Bars: (A and B) 5 μm; (C) 20 μm.

We next measured the distance between metaphasic sister kinetochores in ATRX-depleted cells using CREST immunostaining. Sister chromatid inter-kinetochore distances were significantly increased in both shATRX1 and shATRX2 aligned metaphases compared to control (HG-pSuper) metaphases (Figure 2-3B; $p<0.05$ ANOVA). Increased distance between sister chromatids could reflect a more decondensed state of chromatin and perhaps fewer nucleosomes associated with centric chromatin. Alternatively, increased interkinetochore distances could be explained by reduced cohesion between sister chromatids. We evaluated the extent of cohesion between the chromatid pairs in DAPI stained metaphase chromosome spreads following transient depletion using siATRX1 and siATRX2 duplexes in HeLa cells. To rule out possible effects of extended mitotic arrest (Figure 2-2B), we performed a mitotic shake-off to remove mitotic cells before colcemid treatment. As a control for non-specific siRNA effects, cells were transfected with an siATRX1 scrambled duplex. Mitotic chromosomes from control metaphase spreads exhibited an association of the chromosome arms with a primary constriction at the centromeres, resulting in the typical "X-shaped" chromosomal morphology (Figure 3D, left panel). In contrast, following transient ATRX interference, we observed a higher proportion of chromosomes that were separated along the chromosome length with no evidence of primary centromeric constrictions, indicating reduced centromeric cohesion (Figure 3C). To evaluate the extent of this defect, chromosome spreads (n=100 per treatment) were categorized as having a normal (<10%), moderate (10-90%) or severe (>90%) loss of chromatid cohesion (see examples in Figure 3D). We found that ATRX-depleted cells had a higher occurrence of spreads displaying cohesion defects compared to the mock-transfected and non-specific siRNA control (Figure 3C). Severe loss of cohesion (>90% of chromosome pairs displaying loss of cohesion) was observed at low levels in both controls and depleted cells (Figure 3C,D), indicating that ATRX depletion results in reduced but not complete loss of sister chromatin cohesion.

2.3.5 ATRX Depletion Transiently Activates the Spindle Checkpoint

The mitotic delay incurred by ATRX depletion prompted us to survey the status of the spindle checkpoint proteins in ATRX-depleted cells. As such, the pre-anaphase mitotic delay might result from continued mitotic checkpoint signaling at misaligned chromosomes. Activation of the spindle checkpoint was confirmed by staining for the checkpoint proteins BubR1 and Bub1 at misaligned chromosomes. We observed that both proteins were enriched at a subset of kinetochores in ATRX-depleted metaphases, with a strong signal at misaligned chromosomes (Figure 2-4A). We further tested the robustness of the spindle checkpoint by analyzing the fate of cells after exposure to nocodazole, a microtubule-depolymerizing agent. Nocodazole-induced mitotic arrest was robust in both control HG-pSuper and ATRX-depleted cells, demonstrating that ATRX is not required for spindle checkpoint activation (Figure 2-4B). We next selectively destabilized non-kinetochore fibers by cold treatment. The residual intact kinetochore fibers (K fibers) were visualized by α-tubulin staining. We observed that ATRX depleted cells were characterized by highly irregular arrays of K-fibers (Supplementary Figure 2-4).

2.3.6 Reduced Levels of ATRX Induce Chromosome Segregation Defects

Despite the activation of spindle checkpoint proteins, we observed a modest accumulation of mitotic cells in ATRX-depleted cultures by FACS analysis (Supplementary Figure 2-2B*)*, suggesting that the checkpoint activation could not be maintained completely in all cells. As a result, an increased number of cells with lagging chromosomes at anaphase, telophase, and G1 (Figure 2-4D and Video S2-4) were observed, indicating a problem with chromosome segregation. A 3 to 7 fold increase in the number of cells displaying interphase DNA bridges were observed at 48 to 96 hours post-transfection with ATRX siRNA duplexes compared to control non-targeting siRNA treated cells (Figure 2-4D and 2-4E). DNA bridges in mammalian cells produce micronuclei when the bridges resolve and reform as small membrane bound DNA bodies (Hoffelder et al., 2004). The number of micronuclei increased 3.4 fold compared to

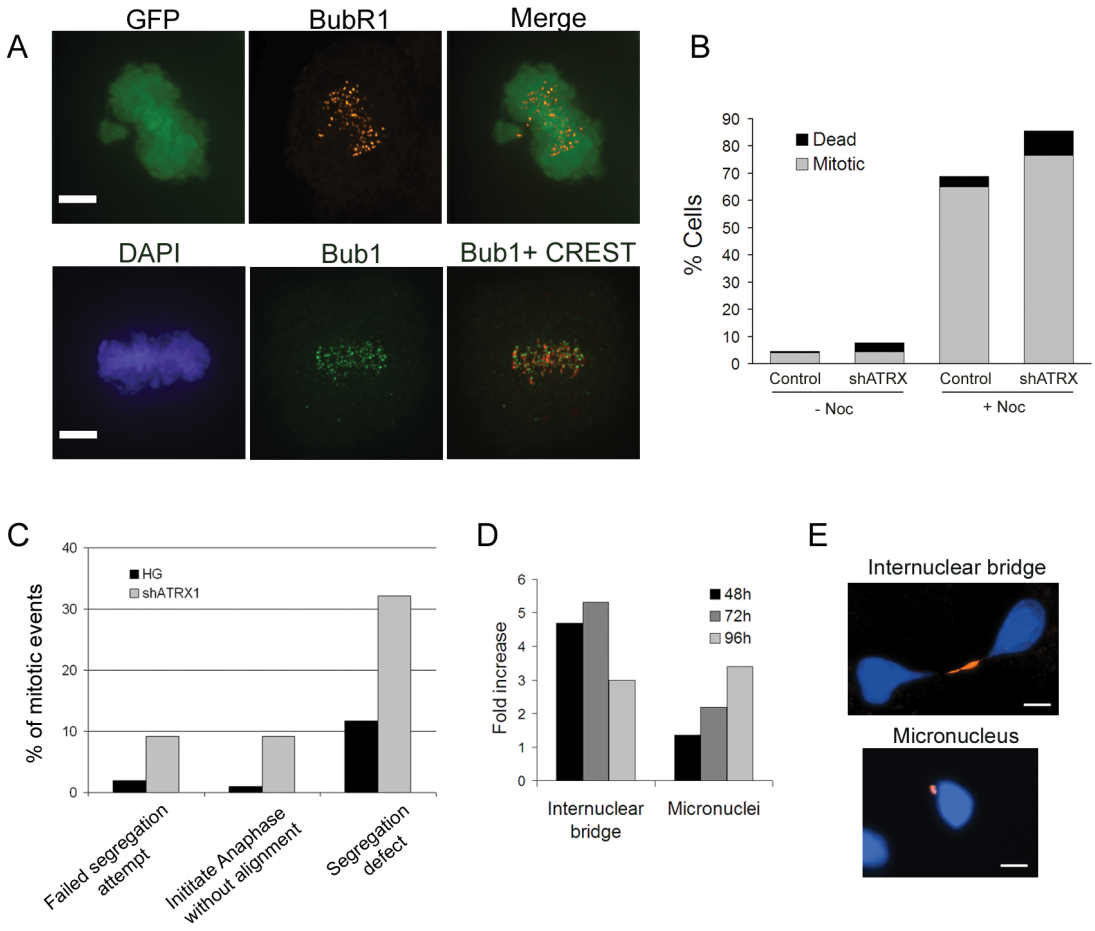

Figure 2-4. Spindle checkpoint activation and aberrant chromosome segregation in ATRX-depleted cells.

(A) The spindle checkpoint protein BubR1 was detected in ATRX-depleted metaphase cells at both aligned and misaligned chromosomes (top). Another checkpoint protein, Bub1, was also found to be adjacent to the centromeres (CREST staining) in ATRX-depleted metaphase cells. (B) Mitotic index of control HG-pSuper and ATRX-depleted cells after 16 h of nocodazole treatment. Control HG-pSuper and ATRX-depleted cells were cultured with or without nocodazole for 16 h and live cells were photographed and scored for the percentage of mitotic rounded cells by phase imaging (n > 1,000). (C) Live cell imaging of control HG-pSuper and ATRX-depleted mitotic cells (n = 100 for each cell line) revealed an increased number of cells that undergo repeated failed attempts at initiating anaphase, an increased number of cells that initiate anaphase without full chromosome alignment, and an increased incidence of segregation defects as indicated by the formation of chromosome DNA bridges and micronuclei. (D) The number of internuclear bridges and micronuclei indicative of chromosome missegregation were quantified at 2–4 d after transfection of the siATRX1 duplex and the fold difference between mock and depleted cells was calculated. (E) Fixed mitotic cells stained with DAPI (blue) and a phosphohistone H3S10 antibody (red) showing intranuclear DNA bridges and micronuclei in transiently depleted cells. Bars in (A) = 5 μm.

control cells by 96 hours after siRNA treatment (Figure 2-4D). Taken together, these data suggest that the spindle checkpoint control is compromised in a subset of cells, causing chromosome segregation errors characterized by lagging chromosomes, interphase DNA bridges and the subsequent formation of micronuclei.

2.3.7 Defective Mitosis *in vivo* in ATRX-null Neuroprogenitors

The Cre-mediated deletion of the *Atrx* gene in the developing mouse forebrain leads to a reduction in cortical and hippocampal size in newborn pups. In these mice, conditional deletion of the *Atrx* gene occurs in nearly 100% of cells in the developing forebrain starting at approximately embryonic day (E) 8.5 (Bérubé et al., 2005). The analysis of the mitotic defects by live cell videomicroscopy in ATRX-depleted HeLa cells now provided indicators of mitotic anomalies that could potentially occur in the *Atrx*-null developing mouse brain, and evidence of such abnormalities would indicate that ATRX contributes to corticogenesis in part by participating in progenitor cell mitosis. The primary progenitor cells in the developing cortex are the neuroepithelial (NE) cells in the proliferative ventricular zone (VZ). Due to the fact that cells undergo cyclical migration within the ventricular zone, mitotic progenitors are always localized at the edge of the VZ facing the lateral ventricle (LV). Cortical sections from normal embryos at E13.5 were first examined for the pattern of ATRX protein expression and localization. ATRX immunoreactivity was indeed enriched at condensed chromatin of mitotic neuroprogenitors lining the lateral ventricle, consistent with a mitotic function (Figure 2-5A, white arrows). ATRX was also expressed in cycling cortical progenitors in a punctate nuclear pattern characteristic of PCH in mouse cells and in differentiated neurons, as previously reported (McDowell et al., 1999; Bérubé et al., 2005). To evaluate the outcome of *Atrx* loss of function on mitotic cells *in vivo* during corticogenesis, brain sections from four different *Atrx*-null and littermate controls (Foxg1Cre) were fixed, stained with DAPI to visualize nuclei and chromatin, and the status of mitotic NE cells lining the ventricular space was evaluated. We observed a high occurrence of pyknotic nuclei, indicative of cells undergoing apoptosis in the vicinity of mitotic cells, which confirms previous findings (Bérubé et al., 2005). We also observed a very high incidence of micronuclei or misaligned chromosomes (Figure 2-5B).

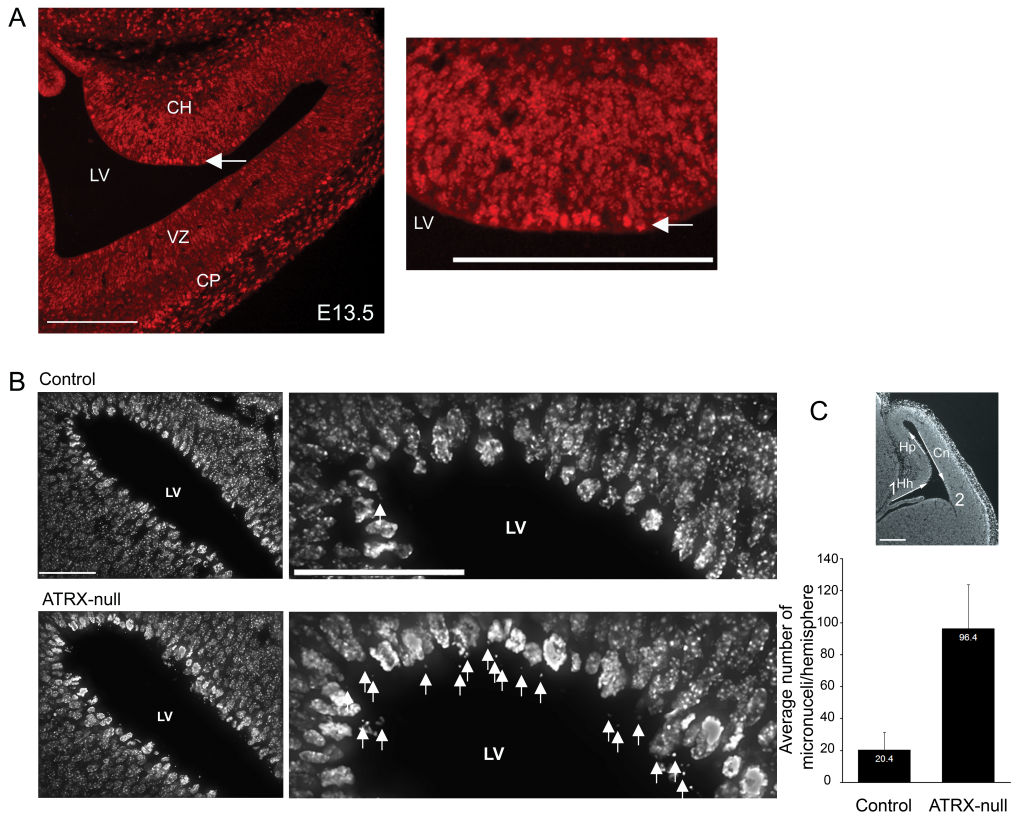

Figure 2-5. ATRX association with mitotic chromosomes and evidence of mitotic defects in ATRX-deficient neuroprogenitors *in vivo*.

(A) ATRX staining of the cortex at E13.5. ATRX is highly expressed in all cells but is highest in the cortical hem (CH), which gives rise to hippocampal structures. ATRX is also expressed at increased levels in the differentiated neurons of developing cortical plate (CP). Mitotic cells that line the lateral ventricle are highly enriched for ATRX protein (arrows). Higher magnification of the cortical hem (right) demonstrates ATRX staining of mitotic chromosomes in cells that line the lateral ventricle (arrow). Punctate nuclear staining of ATRX in cycling cells of the ventricular zone (VZ) is characteristic of ATRX localization at PCH. (B) Cryosections obtained from Foxg1Cre control and ATRX-null telencephalon were stained with DAPI to visualize mitotic chromosomes lining the lateral ventricle (LV) at E13.5. An increased incidence of micronuclei or dispersed chromosomes was detected in the vicinity of the mitotic layer (arrows) in the ATRX null embryonic brain. (C) The mean number of micronuclei or dispersed chromosomes were scored in the mitotic layer from point 1 to 2 as indicated by the white arrows (top) and are represented in the graph below ($n = 4$ for each control Foxg1Cre and ATRX-null brain; $P < 0.0001$ by nonpaired t test). Error bars represent the standard deviation of counts from a total of 24 cortical hemispheres from a total of four brains. Cn, cortical neuroepithelium; Hh, hippocampal hem; Hp, hippocampal primordium. Bars: (A) 100 μm; (B) 40 μm; (C) 200 μm.

We quantified the occurrence of micronulei/misaligned chromosomes by scoring both hemispheres in sections from four littermate *Atrx*-null and control Foxg1Cre embryos and limited our analysis to the mitotic layer that lines the hippocampal hem, hippocampal primordium and the dorsal cortical neuroepithelium (Figure 2-5C, between points 1 and 2). This analysis revealed a significant increase in the number of micronulei in *Atrx*-null mice compared to Foxg1Cre controls (Figure 2-5C), suggesting that *Atrx* loss of function *in vivo* in mouse neuroprogenitors causes mitotic defects that are similar to that observed by RNA interference in cultured human cells.

2.4 Discussion

It has been suggested that brain size is partly dictated by the correct expression of genes that control neuroprogenitor mitosis. Namely, MCPH1 (Alderton et al., 2006; Bartek, 2006), ASPM (Bond et al., 2002; Fish et al., 2006), CDK5RAP2 and CENPJ (Bond et al., 2005) all have roles in assembling, maintaining and orienting the mitotic spindle, and mutations of these genes in humans causes primary microcephaly. Our data now suggest that loss of both ATRX protein isoforms (full-length and truncated form), either by transient or stable depletion in HeLa cells causes defective sister chromatid cohesion and chromosome congression at the metaphase plate and that loss of ATRX in the mouse forebrain also results in mitotic defects. Although ATRX is highly enriched at PCH, we did not detect abnormal targeting of CENP-E, CENP-F, or HP1α, or in the enrichment of histone modifications that characterize condensed chromatin at PCH. However, we did observe a general effect on chromosome condensation in metaphasic chromosomes that will require further investigation. Misaligned chromosomes were also observed at meiosis II upon RNA interference of *Atrx* expression and by antibody injections in mouse oocytes (De La Fuente et al., 2004). It is unclear at present whether similar phenomenon are responsible for the meiotic and mitotic defects, but it is possible that loss of centromeric cohesion could explain misalignment of chromosomes at meiosis II. Further investigation of ATRX function on chromatin dynamics and architecture during meiosis will be required to clarify these issues.

Several genes involved in chromosome cohesion cause multiple developmental abnormalities when mutations arise in humans. The best examples to date include the *NIPBL (delangin), SMC1A,* and *SMC3* genes mutated in Cornelia de Lange syndrome (CdLS) and the *ESCO2* gene mutated in Robert's syndrome (Krantz et al., 2004; Vega et al., 2005; Musio et al., 2006; Borck et al., 2007; Deardorff et al., 2007). All of these factors are components of the cohesin complex or regulators of cohesin loading or unloading. Syndromes caused by *ATRX* mutations display partial phenotypic overlap with CdLS syndrome including cognitive delay, craniofacial dysmorphisms, microcephaly, gastrointestinal defects, problems in the genitourinary system, hearing and ocular development. Another similarity between ATRX and NIPBL is a shared protein motif that confers the ability to associate with the HP1α chromoshadow domain (CSD) (Lechner et al., 2005).

ATRX now joins other chromatin remodeling complexes, such as RSC and Snf2h/NURD implicated in cohesion, either by loading cohesin during DNA replication or by recruiting the cohesin complex to specific chromosomal regions (Hakimi et al., 2002; Baetz et al., 2004; Huang et al., 2004). While the cohesin complex is required for normal chromatid cohesion during mitosis, it also has a function in facilitating long-range enhancer-promoter interactions. The developmental abnormalities in CdLS and the ATR-X syndromes could therefore be explained by the specific deregulation of gene expression at loci that rely on long range enhancer interactions mediated by the cohesin complex and its regulators. An important focus of research will therefore be to identify such target genes and determine how chromosome cohesion might control their expression.

2.5 Supplementary figures

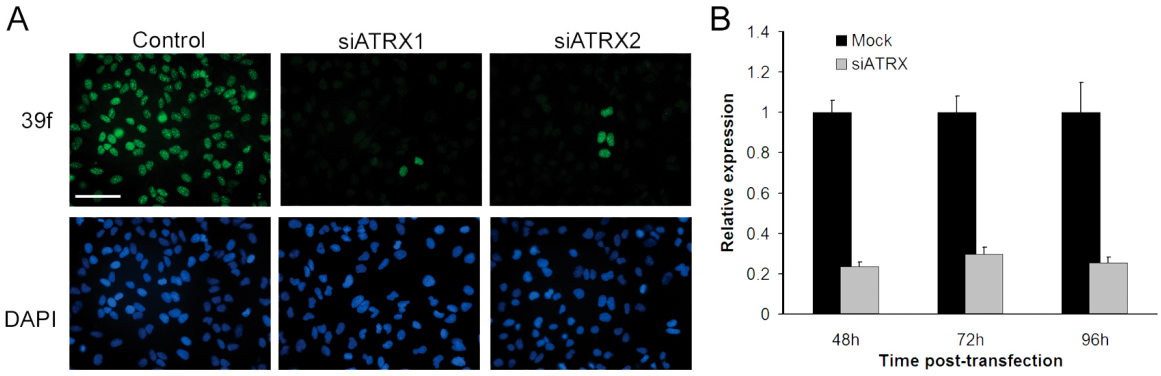

Supplementary Figure 2-1. Validation of ATRX depletion in HeLa cells.

(A) Indirect immunofluorescence detection of the ATRX protein in HeLa cells transfected with no siRNA (Mock) or with 8nM siATRX1 or siATRX2 siRNA duplexes. DAPI staining in the lower panels indicates cell confluence at the time of antibody staining. Bar, 100 μm. (B) ATRX expression was assessed by quantitative RT-PCR using primers that amplify both ATRX isoforms and the results were normalized to GAPDH expression. Error bars represent the standard deviation from triplicate samples.

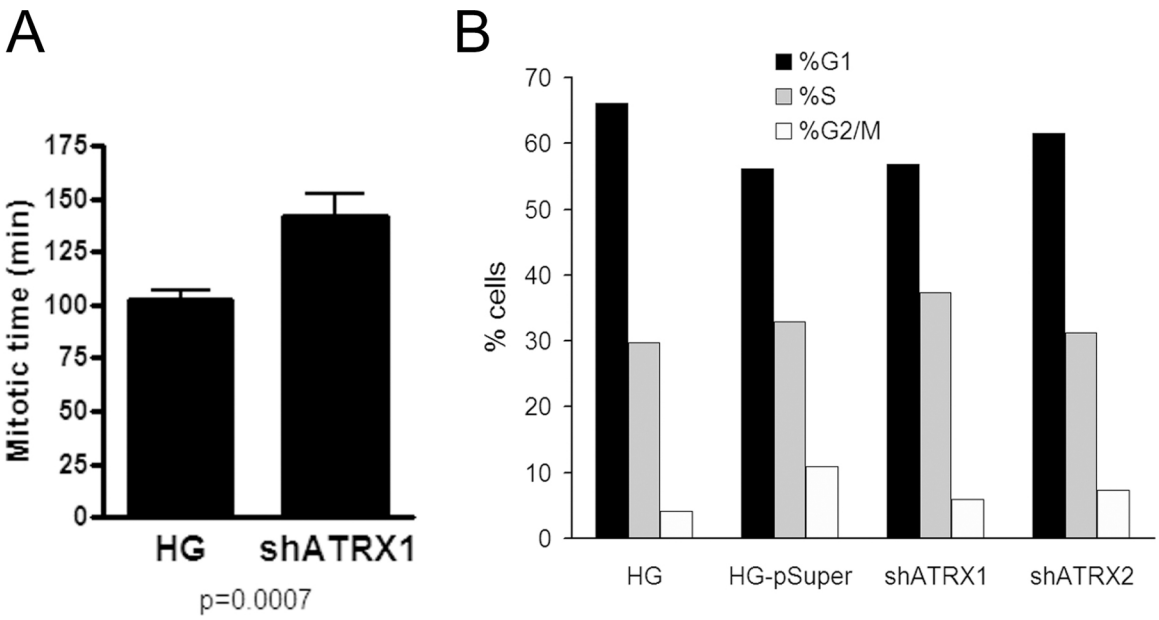

Supplementary Figure 2-2. ATRX depletion prolongs mitotic duration.

(A) Live cells in culture were followed for 10 h by time-lapse fluorescence microscopy and the total time from NEBD to G1 reentry was measured for control and ATRX-depleted cells. The error bars represent the SEM from mitoses (n = 50). (B) FACS analysis of cells stained for DNA content using propidium iodide shows ATRX depletion does not impact cell cycle progression.

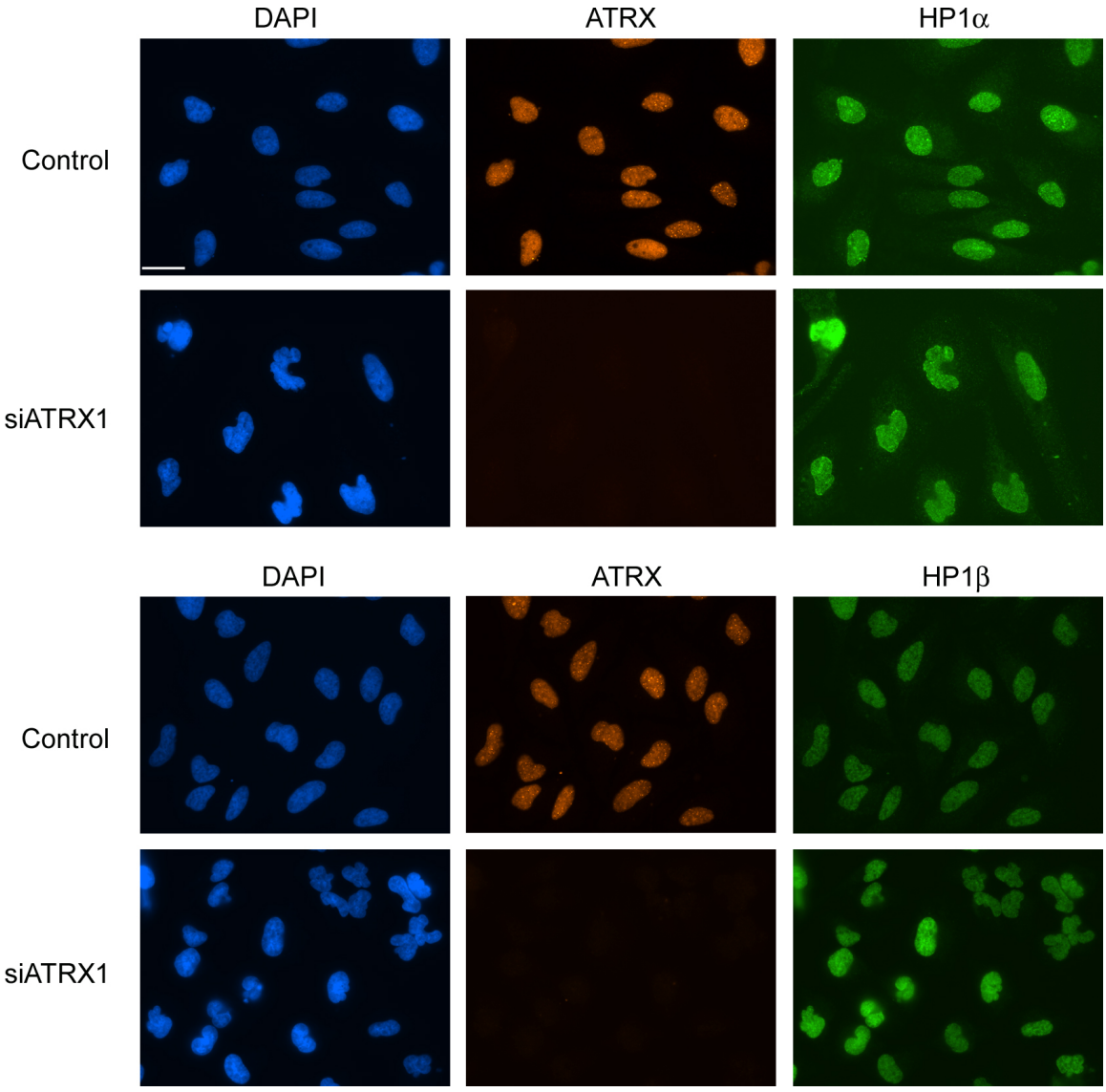

Supplementary Figure 2-3. HP1α and HP1β immunocytochemistry in ATRX-depleted cells.

HeLa cells were transfected with siATRX1 duplex (8 nM) and, 72 h after transfection, indirect immunofluorescence was performed using the anti-ATRX H-300, anti-HP1α, or anti-HP1β antibodies, and counterstained with DAPI. HP1α (top) and HP1β (bottom) proteins are unchanged after transient ATRX depletion when compared with wild-type untransfected cells. Bar, 20 μm.

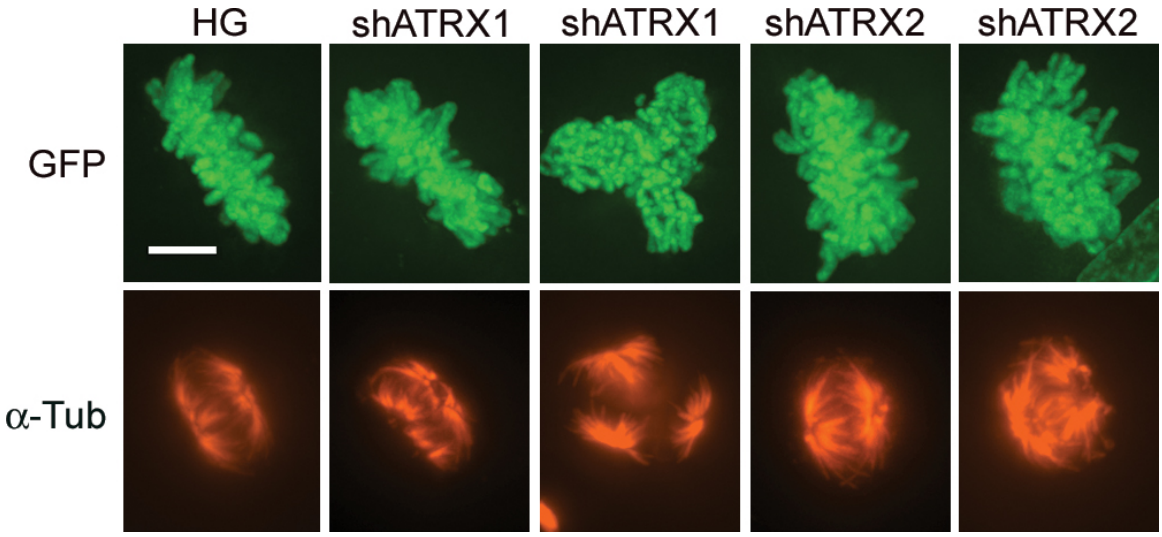

Supplementary Figure 2-4. Abnormal mitotic spindle morphology in ATRX-depleted cells.

Control (HG) and ATRX-depleted stable clones (shATRX1 and shATRX2) were cold-treated, fixed, and stained with anti–α-tubulin antibody to reveal kinetochore-bound microtubule fibers at metaphase (bottom). (top) Endogenous H2B-GFP fluorescence in these cells. Images represent extended focus of multiple z planes after deconvolution. Bar = 5 μm.

2.6 References

Alderton, G.K., Galbiati, L., Griffith, E., Surinya, K.H., Neitzel, H., Jackson, A.P., Jeggo, P.A., and O'Driscoll, M. (2006). Regulation of mitotic entry by microcephalin and its overlap with ATR signalling. Nat Cell Biol *8*, 725-733.

Baetz, K.K., Krogan, N.J., Emili, A., Greenblatt, J., and Hieter, P. (2004). The ctf13-30/CTF13 genomic haploinsufficiency modifier screen identifies the yeast chromatin remodeling complex RSC, which is required for the establishment of sister chromatid cohesion. Mol Cell Biol *24*, 1232-244.

Bartek, J. (2006). Microcephalin guards against small brains, genetic instability, and cancer. Cancer Cell *10*, 91-93.

Bérubé, N.G., Healy, J., Medina, C.F., Wu, S., Hodgson, T., Jagla, M., and Picketts, D.J. (2008). Patient mutations alter ATRX targeting to PML nuclear bodies. Eur J Hum Genet *16*, 192-201.

Bérubé, N.G., Mangelsdorf, M., Jagla, M., Vanderluit, J., Garrick, D., Gibbons, R.J., Higgs, D.R., Slack, R.S., and Picketts, D.J. (2005). The chromatin-remodeling protein ATRX is critical for neuronal survival during corticogenesis. J Clin Invest *115*, 258-267.

Bérubé, N.G., Smeenk, C.A., and Picketts, D.J. (2000). Cell cycle-dependent phosphorylation of the ATRX protein correlates with changes in nuclear matrix and chromatin association. Hum Mol Genet *9*, 539-547.

Bond, J., Roberts, E., Mochida, G.H., Hampshire, D.J., Scott, S., Askham, J.M., Springell, K., Mahadevan, M., Crow, Y.J., et al. (2002). ASPM is a major determinant of cerebral cortical size. Nat Genet *32*, 316-320.

Bond, J., Roberts, E., Springell, K., Lizarraga, S.B., Lizarraga, S., Scott, S., Higgins, J., Hampshire, D.J., Morrison, E.E., et al. (2005). A centrosomal mechanism involving CDK5RAP2 and CENPJ controls brain size. Nat Genet *37*, 353-55.

Borck, G., Zarhrate, M., Bonnefont, J.P., Munnich, A., Cormier-Daire, V., and Colleaux, L. (2007). Incidence and clinical features of X-linked Cornelia de Lange syndrome due to SMC1L1 mutations. Hum Mutat *28*, 205-06.

Ciosk, R., Shirayama, M., Shevchenko, A., Tanaka, T., Toth, A., Shevchenko, A., and Nasmyth, K. (2000). Cohesin's binding to chromosomes depends on a separate complex consisting of Scc2 and Scc4 proteins. Mol Cell *5*, 243-254.

Deardorff, M.A., Kaur, M., Yaeger, D., Rampuria, A., Korolev, S., Pie, J., Gil-Rodríguez, C., Arnedo, M., Loeys, B., et al. (2007). Mutations in cohesin complex members SMC3 and SMC1A cause a mild variant of cornelia de Lange syndrome with predominant mental retardation. Am J Hum Genet *80*, 485-494.

Fish, J.L., Kosodo, Y., Enard, W., Pääbo, S., and Huttner, W.B. (2006). Aspm specifically maintains symmetric proliferative divisions of neuroepithelial cells. Proc Natl Acad Sci U S A *103*, 10438-443.

Gandhi, R., Gillespie, P.J., and Hirano, T. (2006). Human Wapl is a cohesin-binding protein that promotes sister-chromatid resolution in mitotic prophase. Curr Biol *16*, 2406-417.

Garrick, D., Samara, V., McDowell, T.L., Smith, A.J., Dobbie, L., Higgs, D.R., and Gibbons, R.J. (2004). A conserved truncated isoform of the ATR-X syndrome protein lacking the SWI/SNF-homology domain. Gene *326*, 23-34.

Garrick, D., Sharpe, J.A., Arkell, R., Dobbie, L., Smith, A.J., Wood, W.G., Higgs, D.R., and Gibbons, R.J. (2006). Loss of Atrx affects trophoblast development and the pattern of X-inactivation in extraembryonic tissues. PLoS Genet *2*, e58.

Gibbons, R.J., Picketts, D.J., Villard, L., and Higgs, D.R. (1995). Mutations in a putative global transcriptional regulator cause X-linked mental retardation with alpha-thalassemia (ATR-X syndrome). Cell *80*, 837-845.

Hakimi, M.A., Bochar, D.A., Schmiesing, J.A., Dong, Y., Barak, O.G., Speicher, D.W., Yokomori, K., and Shiekhattar, R. (2002). A chromatin remodelling complex that loads cohesin onto human chromosomes. Nature *418*, 994-98.

Hirano, T. (2005). SMC proteins and chromosome mechanics: from bacteria to humans. Philos Trans R Soc Lond B Biol Sci *360*, 507-514.

Hoffelder, D.R., Luo, L., Burke, N.A., Watkins, S.C., Gollin, S.M., and Saunders, W.S. (2004). Resolution of anaphase bridges in cancer cells. Chromosoma *112*, 389-397.

Huang, J., Hsu, J.M., and Laurent, B.C. (2004). The RSC nucleosome-remodeling complex is required for Cohesin's association with chromosome arms. Mol Cell *13*, 739-750.

Kitajima, T.S., Sakuno, T., Ishiguro, K., Iemura, S., Natsume, T., Kawashima, S.A., and Watanabe, Y. (2006). Shugoshin collaborates with protein phosphatase 2A to protect cohesin. Nature *441*, 46-52.

Krantz, I.D., McCallum, J., DeScipio, C., Kaur, M., Gillis, L.A., Yaeger, D., Jukofsky, L., Wasserman, N., Bottani, A., et al. (2004). Cornelia de Lange syndrome is caused by mutations in NIPBL, the human homolog of Drosophila melanogaster Nipped-B. Nat Genet *36*, 631-35.

Kueng, S., Hegemann, B., Peters, B.H., Lipp, J.J., Schleiffer, A., Mechtler, K., and Peters, J.M. (2006). Wapl controls the dynamic association of cohesin with chromatin. Cell *127*, 955-967.

De La Fuente, R., Viveiros, M.M., Wigglesworth, K., and Eppig, J.J. (2004). ATRX, a member of the SNF2 family of helicase/ATPases, is required for chromosome alignment and meiotic spindle organization in metaphase II stage mouse oocytes. Dev Biol *272*, 1-14.

Lechner, M.S., Schultz, D.C., Negorev, D., Maul, G.G., and Rauscher, F.J. (2005). The mammalian heterochromatin protein 1 binds diverse nuclear proteins through a common

motif that targets the chromoshadow domain. Biochem Biophys Res Commun *331*, 929-937.

McDowell, T.L., Gibbons, R.J., Sutherland, H., O'Rourke, D.M., Bickmore, W.A., Pombo, A., Turley, H., Gatter, K., Picketts, D.J., et al. (1999). Localization of a putative transcriptional regulator (ATRX) at pericentromeric heterochromatin and the short arms of acrocentric chromosomes. Proc Natl Acad Sci U S A *96*, 13983-88.

McEwen, B.F., Chan, G.K., Zubrowski, B., Savoian, M.S., Sauer, M.T., and Yen, T.J. (2001). CENP-E is essential for reliable bioriented spindle attachment, but chromosome alignment can be achieved via redundant mechanisms in mammalian cells. Mol Biol Cell *12*, 2776-789.

McGuinness, B.E., Hirota, T., Kudo, N.R., Peters, J.M., and Nasmyth, K. (2005). Shugoshin prevents dissociation of cohesin from centromeres during mitosis in vertebrate cells. PLoS Biol *3*, e86.

Melcher, M., Schmid, M., Aagaard, L., Selenko, P., Laible, G., and Jenuwein, T. (2000). Structure-function analysis of SUV39H1 reveals a dominant role in heterochromatin organization, chromosome segregation, and mitotic progression. Mol Cell Biol *20*, 3728-741.

Musio, A., Selicorni, A., Focarelli, M.L., Gervasini, C., Milani, D., Russo, S., Vezzoni, P., and Larizza, L. (2006). X-linked Cornelia de Lange syndrome owing to SMC1L1 mutations. Nat Genet *38*, 528-530.

Peters, A.H., O'Carroll, D., Scherthan, H., Mechtler, K., Sauer, S., Schöfer, C., Weipoltshammer, K., Pagani, M., Lachner, M., et al. (2001). Loss of the Suv39h histone methyltransferases impairs mammalian heterochromatin and genome stability. Cell *107*, 323-337.

Picketts, D.J., Higgs, D.R., Bachoo, S., Blake, D.J., Quarrell, O.W., and Gibbons, R.J. (1996). ATRX encodes a novel member of the SNF2 family of proteins: mutations point

to a common mechanism underlying the ATR-X syndrome. Hum Mol Genet *5*, 1899-1907.

Ritchie, K., Seah, C., Moulin, J., Isaac, C., Dick, F., and Bérubé, N.G. (2008). Loss of ATRX leads to chromosome cohesion and congression defects. J Cell Biol *180*, 315-324.

Sumara, I., Vorlaufer, E., Stukenberg, P.T., Kelm, O., Redemann, N., Nigg, E.A., and Peters, J.M. (2002). The dissociation of cohesin from chromosomes in prophase is regulated by Polo-like kinase. Mol Cell *9*, 515-525.

Takata, H., Matsunaga, S., Morimoto, A., Ma, N., Kurihara, D., Ono-Maniwa, R., Nakagawa, M., Azuma, T., Uchiyama, S., and Fukui, K. (2007). PHB2 protects sister-chromatid cohesion in mitosis. Curr Biol *17*, 1356-361.

Vega, H., Waisfisz, Q., Gordillo, M., Sakai, N., Yanagihara, I., Yamada, M., van Gosliga, D., Kayserili, H., Xu, C., et al. (2005). Roberts syndrome is caused by mutations in ESCO2, a human homolog of yeast ECO1 that is essential for the establishment of sister chromatid cohesion. Nat Genet *37*, 468-470.

Watrin, E., Schleiffer, A., Tanaka, K., Eisenhaber, F., Nasmyth, K., and Peters, J.M. (2006). Human Scc4 is required for cohesin binding to chromatin, sister-chromatid cohesion, and mitotic progression. Curr Biol *16*, 863-874.

Wood, K.W., Sakowicz, R., Goldstein, L.S., and Cleveland, D.W. (1997). CENP-E is a plus end-directed kinetochore motor required for metaphase chromosome alignment. Cell *91*, 357-366.

Xue, Y., Gibbons, R., Yan, Z., Yang, D., McDowell, T.L., Sechi, S., Qin, J., Zhou, S., Higgs, D., and Wang, W. (2003). The ATRX syndrome protein forms a chromatin-remodeling complex with Daxx and localizes in promyelocytic leukemia nuclear bodies. Proc Natl Acad Sci U S A *100*, 10635-640.

Yang, Z., Guo, J., Chen, Q., Ding, C., Du, J., and Zhu, X. (2005). Silencing mitosin induces misaligned chromosomes, premature chromosome decondensation before anaphase onset, and mitotic cell death. Mol Cell Biol *25*, 4062-074.

Yao, X., Anderson, K.L., and Cleveland, D.W. (1997). The microtubule-dependent motor centromere-associated protein E (CENP-E) is an integral component of kinetochore corona fibers that link centromeres to spindle microtubules. J Cell Biol *139*, 435-447.

Chapter 3

3 Cytokinetic Abnormalities and Multinucleation Induced by ATRX Depletion

During the course of studying the mitotic cell division in ATRX-depleted HeLa cells, I consistently observed abnormalities during the terminal stages of cell division, during anaphase, telophase, and cytokinesis. I decided to more closely examine these stages of the cell cycle, and to investigate the effect of ATRX depletion on the outcome of a full cell division cycle. Interestingly, I found that ATRX depleted HeLa cells fail cytokinesis and produce multinucleated cells at a higher rate than control cells, suggesting an additional and important consequence of ATRX depletion on mitotic progression and cell biology.

3.1 Introduction

Cytokinesis is the final stage of the mitotic cell division cycle (M phase), when the newly generated daughter cells become physically separated following genome replication and partitioning. This event is achieved through the temporally and spatially co-ordinated actions of the cell cycle machinery (Wheatley et al., 1997), the cytoskeleton (Rappaport, 1997), and lipid membrane systems (Xu et al., 2002). Cytokinesis is an essential step in the proliferative program of eukaryotic cells, and is now recognized as a critical process by which complex organisms are able to achieve their precise morphological fates during development (Li, 2007). Not surprisingly, cytokinetic regulators are being increasingly implicated in the aetiology of diverse diseases including short stature (Rauch et al., 2008), primary microcephaly (Fish et al., 2006; Fu et al., 2007), and cancer (Fu et al., 2007; Andersen et al., 2007).

Microcephaly is characterized by a reduction of skull circumference and brain volume resulting primarily from disrupted neuroprogenitor proliferation (Woods et al., 2005) and survival (Chen et al., 2009) during cortical neurogenesis. Supporting this model, a number of human genes mutated in primary microcephaly are proposed regulators of cell division during neurogenesis, including abnormal spindle-like microcephaly-associated

(ASPM/MCPH5) (Bond et al., 2002), CDK5 regulatory subunit associated protein 2 (CDK5RAP2) (Cox et al., 2006), centromere protein J (CENPJ) (Bond et al., 2005), and pericentrin (Rauch et al., 2008). In addition, genes that specifically regulate neuroprogenitor cytokinesis in murine models have been implicated in achieving normal brain size, including the Rho-effector *Citron Kinase* (Di Cunto et al., 2000; LoTurco et al., 2003).

ATRX is a SWI/SNF chromatin remodelling protein required for the early development of several organs, particularly the central nervous system (CNS). In humans, *ATRX* gene mutations cause α-thalassemia/mental retardation X-linked (ATR-X) syndrome, characterized by postnatal microcephaly, severe cognitive and behavioural deficits, and skeletal and urogenital abnormalities. Affected patients also often display α-thalassemia caused by decreased levels of α-globin (Gibbons et al., 1995; Gibbons, 2006). *ATRX* mutant alleles have been identified in other X-linked mental retardations (XLMRs), including Carpenter-Waziri (Abidi et al., 1999), Juberg-Marsidi (Villard et al., 1996), Holmes-Gang (Stevenson et al., 2000), Smith-Fineman-Myers (Villard et al., 2000), and Chudley-Lowry syndromes (Abidi et al., 2005). In the mouse, *Atrx* loss of function from the 8- to 16-cell stage is lethal at embryonic day 9.5 (E9.5) due to defective formation of the extraembryonic trophoblast (Garrick et al., 2006). Targeted disruption of the full-length ATRX isoform in the mouse forebrain from E8.5 results in decreased forebrain size and elevated neuronal cell death, suggesting a role for ATRX in cortical expansion, and neuronal survival (Bérubé et al., 2005). ATRX deficiency is therefore detrimental to both mouse and human development, indicating a requirement for ATRX in basic cellular functions.

Although ATRX has been proposed to primarily regulate gene transcription, the protein is enriched at pericentromeric heterochromatin (McDowell et al., 1999), and appears hyperphosphorylated and highly enriched at condensed chromosomes during mitosis in human cells, suggesting an additional function during this stage of the cell cycle (Bérubé et al., 2000). ATRX is required for chromosome alignment on the metaphase II meiotic spindle in mouse oocytes (De La Fuente et al., 2004), and more recently we have shown a requirement for ATRX in mitotic chromosome congression, alignment, and cohesion in

human cells (Ritchie et al., 2008). We now extend our previous studies and report defects in the progression of cytokinetic events upon depletion of ATRX in HeLa cells. We show that RNAi-mediated depletion of ATRX results in an increased proportion of polynucleated cells and prolonged cytokinetic duration accompanied by morphological abnormalities of the cell membrane. These results show that ATRX loss of function can impede the cytokinesis process, either indirectly due to abnormal chromosome segregation, or directly by a yet unknown mechanism. Cytokinetic failure might provide an explanation for the increased cell death and size reduction observed in the ATRX-null mouse forebrain and some of the developmental abnormalities that characterize ATR-X patients.

3.2 Materials and Methods

3.2.1 Cell Culture and Generation of Stable Clones

All cell lines were grown in a humidified environment at 37 °C and 5 % CO_2. HeLa cells were grown in DME (Sigma) supplemented with 10 % FBS (Gibco). HeLa-HG cells were grown in DME supplemented with 10% FBS and 2 μg/ml Blasticidin S-HCl (Gibco) to maintain transgene expression. HeLa-HG-sh1 cells were grown in DME supplemented with 10% FBS and 2 μg/ml Blasticidin S-HCl and with 400 μg/ml G418/Geneticin (Invitrogen) to maintain short-hairpin RNA (shRNA) expression. Stable HeLa-HG clones expressing shRNA corresponding to the siATRX1 sequence (HeLa-HG-sh1) were generated and validated as described in (Ritchie et al., 2008). Briefly, pairs of sense 60-mer oligonucleotides corresponding to the 19-mer siATRX1 siRNA target sequences and their reverse complement (underlined sequences) were designed that contained 5' BglII and 3' HindIII restriction sites (Integrated DNA Technologies, Inc.) to facilitate cloning into the pSuper.retro.neo plasmid vector (Oligoengine Inc.): shATRX1 (sense) 5'-GATCCCCGAGGAAACCTTCAATTGTATTCAAGAGATACAATTGAAG GTTTCCTCTTTTTA-3'. The oligonucleotides were annealed to complementary anti-sense 60-mer oligonucleotides in buffer containing 10 mM Tris pH 7.5, 50 mM NaCl, and 1 mM EDTA at 90ºC for 4 min, followed by 70 ºC for 10 min, then step cooled to 37 ºC for 20 min using a thermocycler (MJ research) and cloned into the pSuper.retro.neo plasmid (Oligoengine Inc.) using the Quick Ligation Kit according to manufacturer's

instructions (New England Biolabs). The resulting vector construct, designated pSUPER-shATRX1, was subsequently sequenced to confirm sequence identity. Exponentially growing HeLa-H2B-GFP were transfected with empty pSuper vector or with pSuper-shATRX1 vector (1 μg/ml) using Lipofectamine 2000 (Invitrogen). Two days after transfection, cells were re-plated at low density and selection was applied 24 hours later (800 μg/ml Geneticin, Invitrogen). Drug-resistant colonies were picked and expanded in selection media (400 μg/ml Geneticin).

3.2.2 RNA Interference, Immunostaining and Microscopy

All siRNA transfections were conducted using 8nM siRNA and the cationic lipid reagent Lipofectamine 2000 (Invitrogen) according to manufacturer's instructions. The synthetic RNA oligonucleotides siATRX1 (5'-GAGGAAACCUUCAAUUGUAUU-3') was obtained from Dharmacon (Lafayette, CO). Control (non-targeting) duplex was obtained from Sigma Aldrich. Mock-transfected samples were treated similarly but without the addition of siRNA to the transfection mixture. For immunofluorescence experiments, cells were grown on 22 mm^2 glass coverslips (VWR Inc.) and fixed using ice cold 3:1 EtOH:MeOH up to 4 days following plating or 3 days following siRNA/mock transfection. Following fixation, coverslips were incubated with sequential dilutions of primary followed by fluorophore-conjugated secondary antibodies diluted in PBS + 0.3% TX-100. Primary antibodies used: rabbit anti-ATRX H300 (Santa Cruz Biotech, 1:200), mouse-anti-α-Tubulin (Sigma-Aldrich, 1:1000), mouse-anti-Plk1 (Upstate, 1:200), mouse-anti-Myosin II (Upstate, 1:200). Secondary antibodies used: Alexa Fluor 594 goat anti-mouse IgG, Alexa Fluor 488 goat anti-mouse IgG, Alexa Fluor 594 goat anti-rabbit IgG, and Alexa Fluor 488 goat anti-rabbit-IgG (Invitrogen, 1:1500). The DNA dye DAPI was used as a nuclear counterstain. Coverslips were mounted using Vectashield H-1000 antifade solution (Vector Labs). Imaging was performed using a DMI 6000b inverted microscope (Leica) and digital camera (ORCA ER; Hamamatsu). Image acquisition was performed using a Power Mac G5 computer (Apple Inc.) and Openlab imaging software (v5.0, Perkin-Elmer). Image analysis was performed using Volocity imaging software (v4.0, Perkin-Elmer) and Adobe Photoshop (vCS4, Adobe).

3.2.3 Live-Cell Video-Microscopy

HeLa-HG or HG-shATRX1 cells were grown in 35 mm dishes (Corning). Following a 24 hour incubation in a tissue culture incubator at 37°C and 5 % CO_2, growth media was replaced with CO_2 independent media (Gibco) supplemented with 10% FBS (Sigma) and 4mM L-Glutamine (Gibco). The culture dish was mounted on an inverted microscope (DMI 6000b; Leica) and maintained at 37°C using a Livecell incubator (Neue Biosciences). Phase-contrast and fluorescence images were captured at intervals between 2 and 10 minutes for up to 48 hours using the automation feature of Openlab and analyzed using Volocity. To measure cytokinetic duration, cells (N=100) were measured from anaphase onset (AO), characterized by the visible cytokinetic cleavage furrow and initiation of chromatid segregation, until the end of telophase, characterized by nuclear decondensation and cytoplasmic expansion.

3.3 Results

3.3.1 ATRX Depletion Causes Multinucleation

Actively growing HeLa cells were treated with a small interfering RNA (siATRX1) that specifically targets full-length ATRX transcripts. We have previously shown that RNA interference under these conditions results in substantial depletion of both ATRX mRNA and protein (Ritchie et al., 2008). Following transfection, staining for the microtubule protein α-tubulin revealed an increased number of cells connected to each other by cytoplasmic microtubule bridges at the cytokinetic midzone (Figure 1A, asterisk). Spindle midzone formation in ATRX depleted cells often appeared bent or narrow, while only minor variability in organization was observed in control cells expressing normal levels of ATRX (see example Fig 3-1A, asterisk). We also observed increased number of cells with more than one nucleus or with multilobular nuclei (Figure 3-1A, arrowheads). This phenotype was quantified and revealed a 3- to 4-fold increase in the number of bi- or multinucleated cells in HeLa cells transiently depleted of ATRX at 24 hours following siRNA transfection, and this effect persisted until at least 96 hours post transfection (Figure 3-1B).

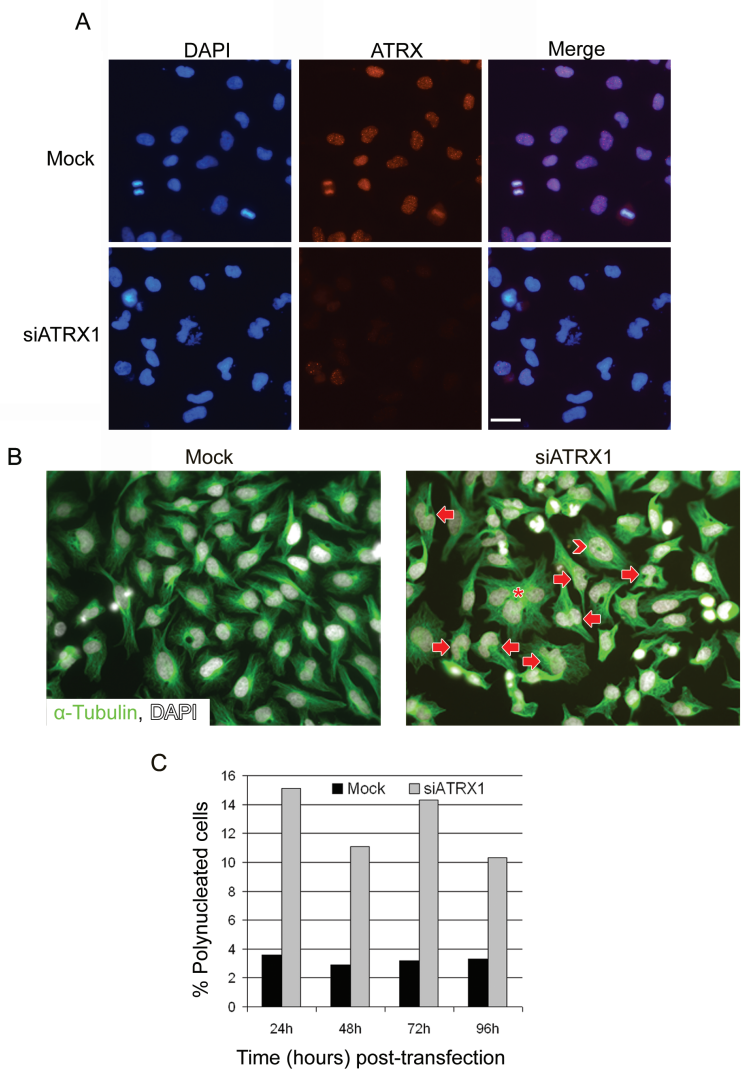

Figure 3-1. Transient ATRX depletion causes cellular multinucleation.

(A) HeLa cells were depleted of ATRX using transient siRNA (siATRX1) transfection, or mock transfected with Lipofectamine only (Mock). Immunostaining with anti-ATRX antibody confirmed ATRX depletion in the majority of cells treated with siATRX1 duplex. (B) Cells were immunostained with anti-α-tubulin antibody and the nuclear counterstain DAPI 48 hours following transfection. Cells treated with siATRX1 had a higher frequency of multinucleation (asterisk), lobulated nuclei (arrows), and nuclear holes (chevron) than controls. (C) Multinucleation was quantified in mock-treated and siATRX1-treated cells every 24 hours following siRNA transfection, up to 96 hours (n > 300 cells at each time point). Cells treated with siATRX1 showed increased levels of multinucleation at all time points examined following treatment.

3.3.2 ATRX-Depleted Cells Take Longer to Progress from Anaphase to G1

Increased levels of multinucleation in ATRX-depleted cells suggested that many cells fail to undergo cytokinesis following mitosis. To investigate the role of ATRX during cell cycle progression in live cells, we utilized HeLa cells that express Histone 2B fused with the green fluorescent protein (HeLa-HG cells). Using a combination of phase contrast and fluorescence microscopy, we were able to follow mitotic events in actively dividing HeLa-HG cells using time-lapse imaging. Stable ATRX depletion was achieved by generating a HeLa-HG clone (HG-shATRX1) that constitutively expresses a short hairpin RNA (shRNA) targeting the full length ATRX mRNA, yielding very good reduction of ATRX protein levels, as previously described (Ritchie et al., 2008). Using time-lapse microscopy, we measured the amount of time required for the mitotic cells to proceed from anaphase onset (first imaging frame with evidence of chromatid segregation) to re-entry into G1 (time of complete nuclear decondensation) (Figure 3-2A). This analysis demonstrated that the duration of anaphase to G1 transition was more than doubled in ATRX depleted HG-shATRX1 compared to wild type cells ($N=100$, $p<0.0001$, t-test), with an average of 74.1 min and 36.0 min, respectively (Figure 3-2A,B and Video S3-1 - HeLa-HG Normal Cytokinesis and additional file 2: Video S3-2 - HG-shATRX1 Membrane Instability).

3.3.3 Increased Cytokinetic Failure in ATRX-deficient Cells

The increased time required to reach G1 following chromosome segregation, as well as the higher levels of multinucleation, suggested that the process of cytokinesis might be disrupted in ATRX-depleted cells. We thus examined the cellular events of cytokinesis, including anaphase and telophase, and observed morphological abnormalities during the telophase and cytokinetic phases in ATRX-depleted cells. Cells lacking ATRX exhibited a high frequency of spontaneous disorganization of the lipid membrane. Immediately following ingression of the cleavage furrow during anaphase, the cell membrane frequently appeared disorganized and highly unstable (Figure 3-2A,C and additional file 2: Video S3-2 - HG-shATRX1 Membrane Instability). Plasma membrane disorganization was seen in 6.0% of control mitotic cells, but increased to 19.0% of

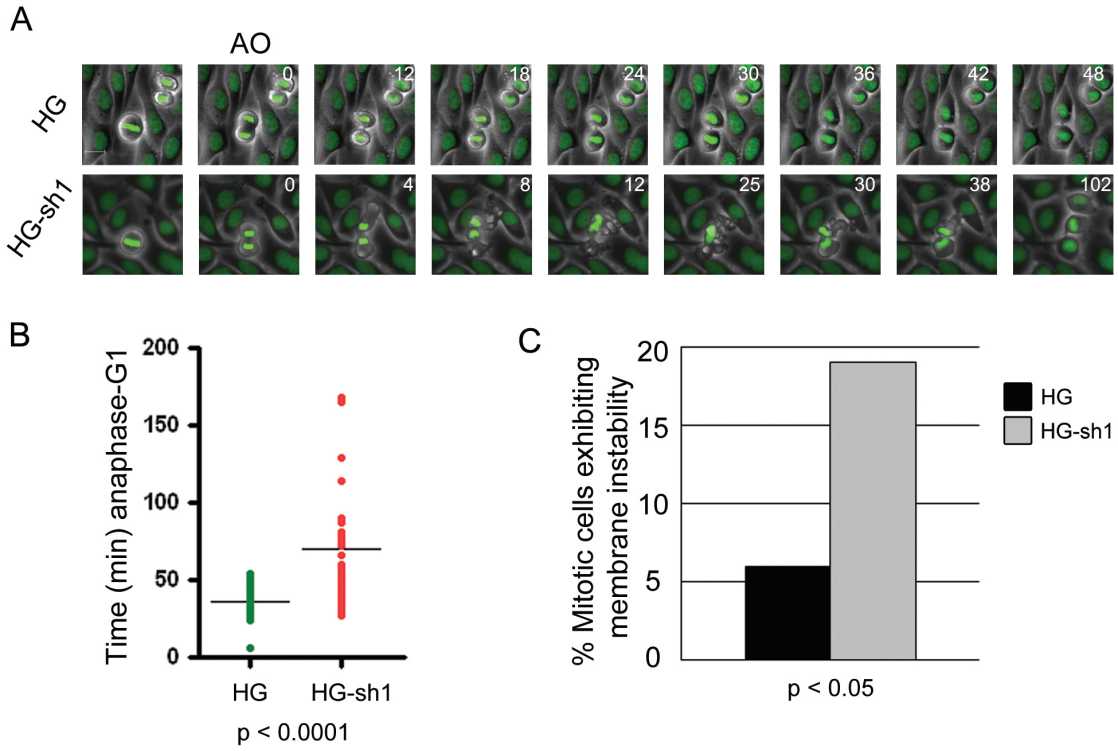

Figure 3-2. ATRX depletion causes delayed progression from anaphase to G1.

(A) Actively growing control (HG) cells and ATRX-depleted (HG-sh1) HeLa cells were visualized using time-lapse microscopy with a combination of phase and fluorescence microscopy from the onset of anaphase (AO, Time = 0 min) to G1 re-entry (nuclear decondensation, last frame shown in sequence). ATRX-depleted HG-sh1 cells were often delayed in reaching G1 phase after anaphase onset relative to control cells. (B) Cytokinetic duration was measured from time-lapse live-cell videomicroscopy experiments of control HG or ATRX-depleted HG-sh1 cells (n = 100), and was found to be significantly increased in HG-sh1 cells ($p < 0.0001$, t-test). (C) Membrane instability, defined as membrane blebbing between anaphase onset and the completion of cytokinesis (see panel A, HG-sh1), was found to be increased ($p < 0.05$, Yates' χ^2 test) in ATRX-depleted HG-sh1 cells (6%, N = 100) compared to controls (HG) (19%, N=100). Bar in (A) = 16 μm.

HG-shATRX1 mitotic cells (N=100, Figure 3-2C). In addition, we observed that ATRX depleted cells failed the terminal stages of cytokinesis and produced binucleated cells (Figure 3-3, additional file 3: Video S3-3 - HG-shATRX1 Failed Cytokinesis). Cytokinetic failure occurred in 5% of control HeLa-HG cells, and more than doubled to 11% of HG-shATRX1 cells (Figure 3-3B). We followed these binucleated cells using live-cell time-lapse video microscopy, and found that they often underwent programmed cell death several hours later (Figure 3-4, additional file 4: Video S3-4 - HG-shATRX1 Binucleate Cell Death).

3.3.4 Normal Midbody Organization in ATRX-depleted Cells

To determine if the observed cytokinetic defects were due to disruption of the midzone spindle or cytokinetic midbody, mock and siATRX1 treated cells were stained with an antibody against Polo-like kinase 1 (Plk1). Plk1 is normally localized to the midzone and midbody, where it phosphorylates a number of substrates, including kinesin (MKLP2) and dynein (NudC) subunits and is required for normal cytokinetic progression and termination. Plk1 localized to the midzone and midbody normally in *ATRX*-depleted cells, suggesting that the integrity of the central spindle and the associated Plk1-dependent signaling pathway is intact (Figure 3-5).

3.3.5 Relationship Between Cytokinetic Abnormalities and Chromosome Bridging

We have previously reported that ATRX depletion in HeLa cells causes chromosome congression, cohesion, and segregation defects during mitosis (Ritchie et al., 2008). It was therefore possible that chromosomal bridges are impeding cytokinetic progress in ATRX-depleted HeLa cells. To investigate this possibility, we conducted time-course live-cell microscopy of actively dividing HG and HG-sh1 cells, measured the number of mitotic cells that failed cytokinesis and determined whether this defect was preceded by the appearance of a chromosome bridge. We found that distinct chromosome bridges during anaphase and telophase often preceded cytokinetic failure and binucleation in ATRX depleted cells. Of 70 HG-sh1 cells that underwent cytokinesis, 11 were seen to

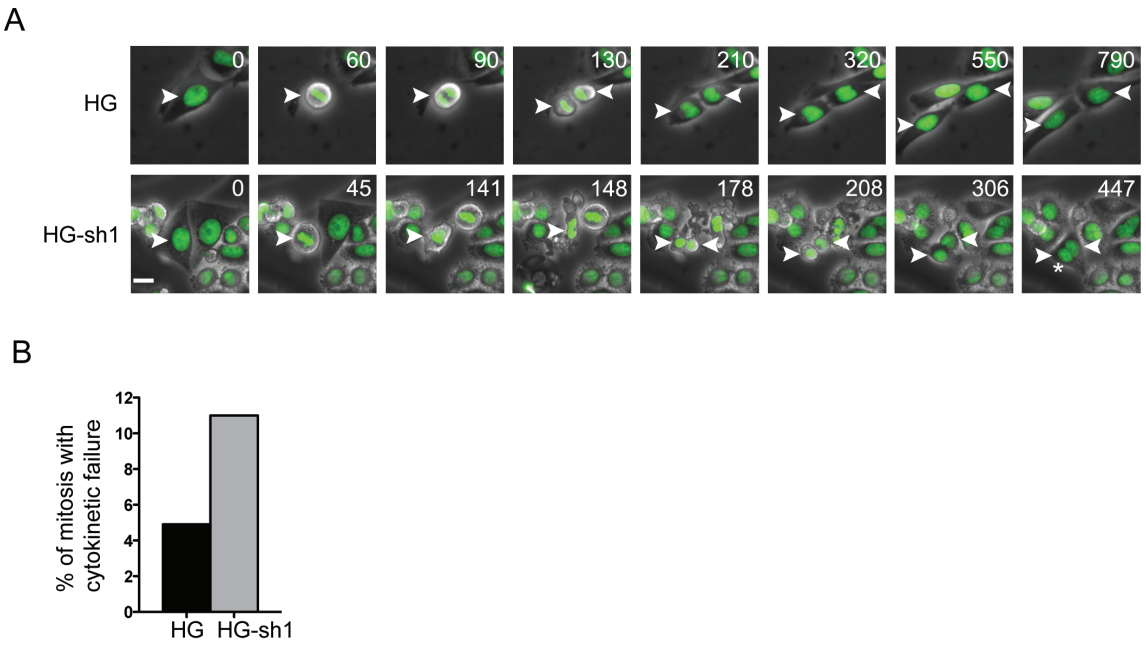

Figure 3-3. ATRX depleted cells show elevated levels of cytokinetic failure.

(A) ATRX-depleted (HG-sh1) cells more often failed cytokinesis (arrows, lower panel) than control (HG) cells. Cytokinetic failure was measured from time-lapse live-cell video microscopy and was defined as the generation of bi-nucleated cells following the end of M phase (asterisk, lower panel). Numbers indicate time in minutes following the first frame (Time = 0). (B) Successful completion or failure of cytokinesis was scored using time-lapse live-cell video microscopy. ATRX-depleted cells failed cytokinesis more often than control HG cells (11% vs. 5% of observed cytokinetic events respectively, n = 100 per genotype, not statistically significant). Bar in (A) = 16 µm.

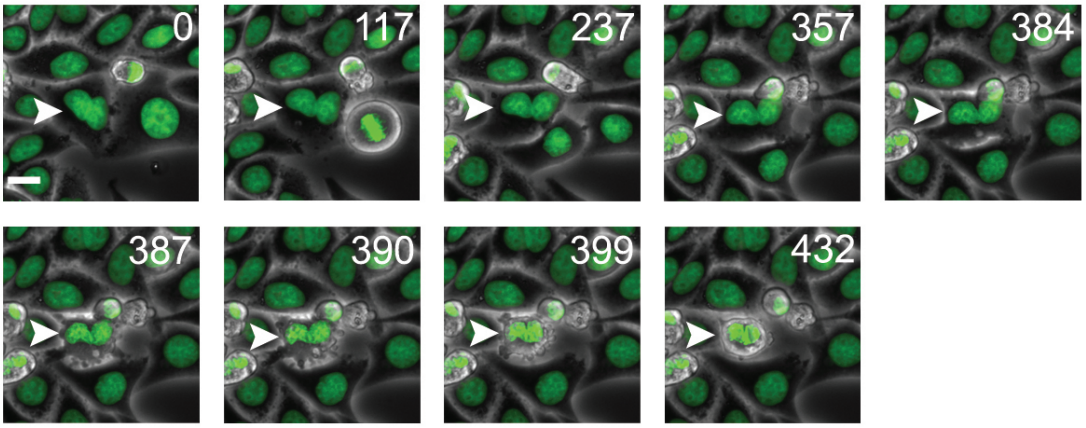

Figure 3-4. Cell death following cytokinetic failure and multinucleation.

Selected captured images from time-lapse videomicroscopy of ATRX depleted HG-shATRX1 cells. The arrow indicates a cell that failed cytokinesis and became multinucleated, and then underwent cell death. Numbers indicate time in minutes following the first frame (0 min). Bar = 16μm.

produce binucleated progeny, 8 (73%) of which were associated with the appearance of a chromosome bridge during anaphase, telophase, or cytokinesis. Notably, no apparent chromosomal abnormalities could be identified during cytokinesis in approximately 27% of the mitotic cells that failed cytokinesis. These results suggest that that failure to complete cytokinesis is often a consequence of chromosome bridges, possibly caused by ATRX dependent chromosome alignment and segregation, but that some cytokinetic abnormalities might result from alternative mechanisms.

3.4 Discussion

Our data demonstrate that decreased levels of ATRX can often result in cytokinetic defects or even failure. We used live cell microscopy to show that ATRX depletion causes a delay at the end of mitosis and during cytokinesis, morphological abnormalities of the plasma membrane, and cytokinetic failure. Our recent report that ATRX plays a critical role during mitosis in human cells suggests that altered chromatid cohesion and segregation in ATRX-deficient cells may indirectly impact normal cytokinetic progress (Ritchie et al., 2008). DNA bridges and poorly resolved chromatin masses pose a physical barrier to cytokinesis (Cutts et al., 1999), whereby the cell actively halts cytokinesis to prevent physical damage to its own genome. Notably, many ATRX-depleted cells displaying cytokinetic failure were accompanied by chromosome segregation defects, suggesting that the observed phenotypes may be dependent on chromosomal nondisjunction. Furthermore, the cytokinetic midzone and midbody are properly enriched for Plk1 in ATRX-depleted cells, suggesting that the cytokinetic abnormalities do not reflect a defect in general functional composition of the midzone or midbody. Regulatory proteins have now been identified that integrate early mitotic events with cytokinesis. Named the chromosome passenger complex (CPC) by virtue of its dynamic localization during M-phase, the core CPC complex is comprised of inner centromeric protein (INCENP), aurora B kinase, survivin, and borealin (Ruchaud et al., 2007). The CPC proteins are centromeric during early stages of M phase where they play an essential role in chromosome alignment (Mackay et al., 1998; Gassmann et al., 2004; Vong et al., 2005), but are shuttled to the spindle midzone and equatorial cell cortex upon anaphase commitment where they stabilize the central spindle and are essential

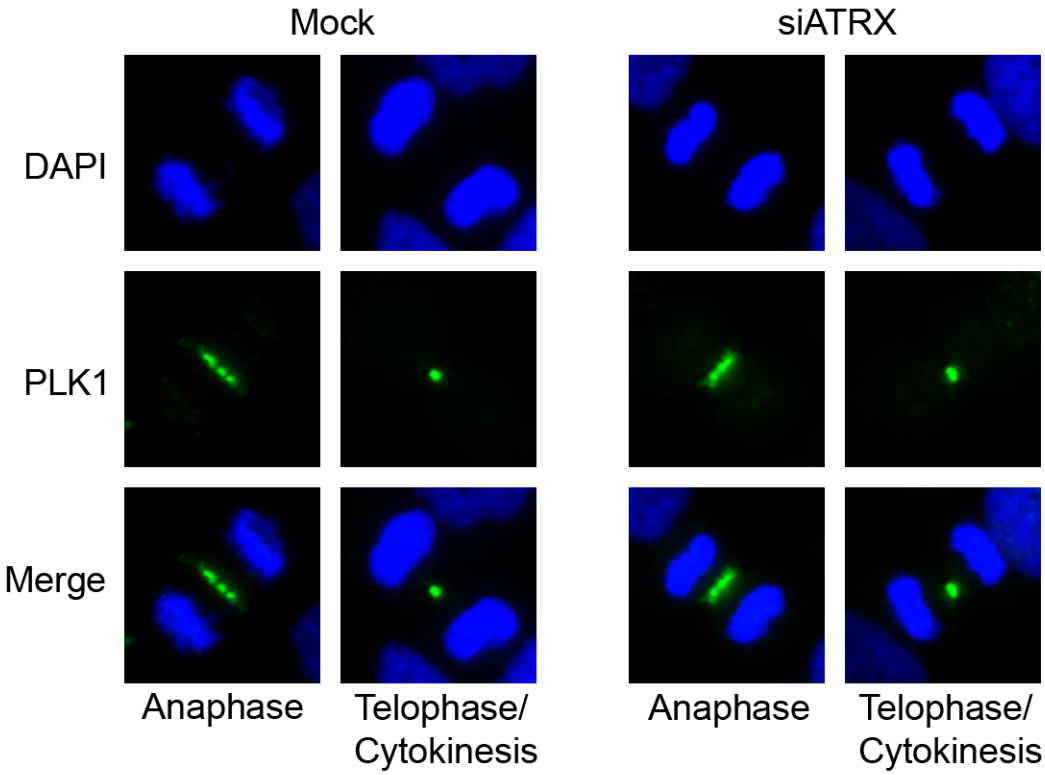

Figure 3-5. Plk1 normally localizes to the spindle midzone and midbody in *ATRX*-depleted cells.

HeLa cells were depleted of ATRX using transient RNAi (siATRX). After 72h, protein knockdown was confirmed using ATRX immunostaining. Cells were stained with an antibody against PLK1 (green). Different stages of the cell cycle were determined based on the pattern of Plk1 staining at the midzone (Anaphase) or midbody (Telophase/Cytokinesis).

for cytokinesis (Ruchaud et al., 2007). Other kinetochore-associated proteins have been implicated in both mitotic chromosome alignment and cytokinesis, including the DNA binding protein CENP-C (Kwon et al., 2007), the kinetochore motor protein CENP-E (Liu et al., 2006), and the large coiled-coil protein CENP-F/Mitosin (Holt et al., 2005). These examples demonstrate the relationship between centromeric proteins and cytokinesis, which may describe a novel function of the ATRX protein

Cytokinetic abnormalities caused by *Citron kinase* deficiency in the mouse brain result in strikingly similar morphological defects seen in the *Atrx*-null brain (Bérubé et al., 2005), including smaller forebrain (especially in the caudal areas), normal proliferation but increased cell death, and decreased numbers of superficial layer neurones (Di Cunto et al., 2000). ATRX is highly expressed in the neuroepithelial cells lining the lateral ventricles of the embryonic mouse forebrain. Based on the data presented in the present report, we speculate that ATRX could play a role during cytokinesis during neuroprogenitor proliferation. Loss of ATRX in the embryonic forebrain of the conditional knockout mouse may disrupt the proliferative divisions of the neuroprogenitor cells, depleting the pool of neuroprogenitors required for subsequent cortical expansion. These results provide a functional link between ATRX-dependent cell division and the cortical defects observed in the ATRX-null mouse forebrain.

In addition to a broad spectrum of developmental consequences, mitotic defects can be associated with oncogenic events and tumorigenesis due to genomic instability (Montgomery et al., 2003). To date there is no evidence that ATR-X patients exhibit mitotic defects or are prone to developing cancer, however there is increasing evidence for a role of ATRX in neoplasia outside of the context of ATR-X syndrome (Steensma et al., 2004). Recently, ATRX was found to be mutated in a large proportion of pancreatic neuroendocrine tumours (PanNETS), suggesting that it might have tumour suppressive functions (Jiao et al., 2011). All *ATRX* mutations correlated with loss of immunolabeling in these hyperplastic pancreatic islet cells, suggesting that complete loss of ATRX protein is associated with oncogenetic events in PanNETs. Furthermore, another recent study of PanNETs found substantial chromosomal alterations in 98% of samples (Hu et al., 2010), suggesting that genomic instability could contribute to PanNET oncogenesis.

Together these data suggest that ATRX might be a novel tumor suppressor gene, possibly through maintaining the accuracy of chromosome segregation during mitosis.

3.5 References

Abidi, F., Schwartz, C.E., Carpenter, N.J., Villard, L., Fontés, M., and Curtis, M. (1999). Carpenter-Waziri syndrome results from a mutation in XNP. Am J Med Genet *85*, 249-251.

Abidi, F.E., Cardoso, C., Lossi, A.M., Lowry, R.B., Depetris, D., Mattéi, M.G., Lubs, H.A., Stevenson, R.E., Fontes, M., et al. (2005). Mutation in the 5' alternatively spliced region of the XNP/ATR-X gene causes Chudley-Lowry syndrome. Eur J Hum Genet *13*, 176-183.

Andersen, M.H., Svane, I.M., Becker, J.C., and Straten, P.T. (2007). The universal character of the tumor-associated antigen survivin. Clin Cancer Res *13*, 5991-94.

Bérubé, N.G., Mangelsdorf, M., Jagla, M., Vanderluit, J., Garrick, D., Gibbons, R.J., Higgs, D.R., Slack, R.S., and Picketts, D.J. (2005). The chromatin-remodeling protein ATRX is critical for neuronal survival during corticogenesis. J Clin Invest *115*, 258-267.

Bérubé, N.G., Smeenk, C.A., and Picketts, D.J. (2000). Cell cycle-dependent phosphorylation of the ATRX protein correlates with changes in nuclear matrix and chromatin association. Hum Mol Genet *9*, 539-547.

Bond, J., Roberts, E., Mochida, G.H., Hampshire, D.J., Scott, S., Askham, J.M., Springell, K., Mahadevan, M., Crow, Y.J., et al. (2002). ASPM is a major determinant of cerebral cortical size. Nat Genet *32*, 316-320.

Bond, J., Roberts, E., Springell, K., Lizarraga, S.B., Lizarraga, S., Scott, S., Higgins, J., Hampshire, D.J., Morrison, E.E., et al. (2005). A centrosomal mechanism involving CDK5RAP2 and CENPJ controls brain size. Nat Genet *37*, 353-55.

Chen, L., Melendez, J., Campbell, K., Kuan, C.Y., and Zheng, Y. (2009). Rac1 deficiency in the forebrain results in neural progenitor reduction and microcephaly. Dev Biol *325*, 162-170.

Cox, J., Jackson, A.P., Bond, J., and Woods, C.G. (2006). What primary microcephaly can tell us about brain growth. Trends Mol Med *12*, 358-366.

Cutts, S.M., Fowler, K.J., Kile, B.T., Hii, L.L., O'Dowd, R.A., Hudson, D.F., Saffery, R., Kalitsis, P., Earle, E., and Choo, K.H. (1999). Defective chromosome segregation, microtubule bundling and nuclear bridging in inner centromere protein gene (Incenp)-disrupted mice. Hum Mol Genet *8*, 1145-155.

Di Cunto, F., Imarisio, S., Hirsch, E., Broccoli, V., Bulfone, A., Migheli, A., Atzori, C., Turco, E., Triolo, R., et al. (2000). Defective neurogenesis in citron kinase knockout mice by altered cytokinesis and massive apoptosis. Neuron *28*, 115-127.

Fish, J.L., Kosodo, Y., Enard, W., Pääbo, S., and Huttner, W.B. (2006). Aspm specifically maintains symmetric proliferative divisions of neuroepithelial cells. Proc Natl Acad Sci U S A *103*, 10438-443.

Fu, J., Bian, M., Jiang, Q., and Zhang, C. (2007). Roles of Aurora kinases in mitosis and tumorigenesis. Mol Cancer Res *5*, 1-10.

Garrick, D., Sharpe, J.A., Arkell, R., Dobbie, L., Smith, A.J., Wood, W.G., Higgs, D.R., and Gibbons, R.J. (2006). Loss of Atrx affects trophoblast development and the pattern of X-inactivation in extraembryonic tissues. PLoS Genet *2*, e58.

Gassmann, R., Carvalho, A., Henzing, A.J., Ruchaud, S., Hudson, D.F., Honda, R., Nigg, E.A., Gerloff, D.L., and Earnshaw, W.C. (2004). Borealin: a novel chromosomal passenger required for stability of the bipolar mitotic spindle. J Cell Biol *166*, 179-191.

Gibbons, R. (2006). Alpha thalassaemia-mental retardation, X linked. Orphanet J Rare Dis *1*, 15.

Gibbons, R.J., Picketts, D.J., Villard, L., and Higgs, D.R. (1995). Mutations in a putative global transcriptional regulator cause X-linked mental retardation with alpha-thalassemia (ATR-X syndrome). Cell *80*, 837-845.

Holt, S.V., Vergnolle, M.A., Hussein, D., Wozniak, M.J., Allan, V.J., and Taylor, S.S. (2005). Silencing Cenp-F weakens centromeric cohesion, prevents chromosome alignment and activates the spindle checkpoint. J Cell Sci *118*, 4889-4900.

Hu, W., Feng, Z., Modica, I., Klimstra, D.S., Song, L., Allen, P.J., Brennan, M.F., Levine, A.J., and Tang, L.H. (2010). Gene Amplifications in Well-Differentiated Pancreatic Neuroendocrine Tumors Inactivate the p53 Pathway. Genes Cancer *1*, 360-68.

Jiao, Y., Shi, C., Edil, B.H., de Wilde, R.F., Klimstra, D.S., Maitra, A., Schulick, R.D., Tang, L.H., Wolfgang, C.L., et al. (2011). DAXX/ATRX, MEN1, and mTOR pathway genes are frequently altered in pancreatic neuroendocrine tumors. Science *331*, 1199-1203.

Kwon, M.S., Hori, T., Okada, M., and Fukagawa, T. (2007). CENP-C is involved in chromosome segregation, mitotic checkpoint function, and kinetochore assembly. Mol Biol Cell *18*, 2155-168.

De La Fuente, R., Viveiros, M.M., Wigglesworth, K., and Eppig, J.J. (2004). ATRX, a member of the SNF2 family of helicase/ATPases, is required for chromosome alignment and meiotic spindle organization in metaphase II stage mouse oocytes. Dev Biol *272*, 1-14.

Li, R. (2007). Cytokinesis in development and disease: variations on a common theme. Cell Mol Life Sci *64*, 3044-058.

Liu, D., Zhang, N., Du, J., Cai, X., Zhu, M., Jin, C., Dou, Z., Feng, C., Yang, Y., et al. (2006). Interaction of Skp1 with CENP-E at the midbody is essential for cytokinesis. Biochem Biophys Res Commun *345*, 394-402.

LoTurco, J.J., Sarkisian, M.R., Cosker, L., and Bai, J. (2003). Citron kinase is a regulator of mitosis and neurogenic cytokinesis in the neocortical ventricular zone. Cereb Cortex *13*, 588-591.

Mackay, A.M., Ainsztein, A.M., Eckley, D.M., and Earnshaw, W.C. (1998). A dominant mutant of inner centromere protein (INCENP), a chromosomal protein, disrupts prometaphase congression and cytokinesis. J Cell Biol *140*, 991-1002.

McDowell, T.L., Gibbons, R.J., Sutherland, H., O'Rourke, D.M., Bickmore, W.A., Pombo, A., Turley, H., Gatter, K., Picketts, D.J., et al. (1999). Localization of a putative transcriptional regulator (ATRX) at pericentromeric heterochromatin and the short arms of acrocentric chromosomes. Proc Natl Acad Sci U S A *96*, 13983-88.

Montgomery, E., Wilentz, R.E., Argani, P., Fisher, C., Hruban, R.H., Kern, S.E., and Lengauer, C. (2003). Analysis of anaphase figures in routine histologic sections distinguishes chromosomally unstable from chromosomally stable malignancies. Cancer Biol Ther *2*, 248-252.

Rappaport, R. (1997). Cleavage furrow establishment by the moving mitotic apparatus. Dev Growth Differ *39*, 221-26.

Rauch, A., Thiel, C.T., Schindler, D., Wick, U., Crow, Y.J., Ekici, A.B., van Essen, A.J., Goecke, T.O., Al-Gazali, L., et al. (2008). Mutations in the pericentrin (PCNT) gene cause primordial dwarfism. Science *319*, 816-19.

Ritchie, K., Seah, C., Moulin, J., Isaac, C., Dick, F., and Bérubé, N.G. (2008). Loss of ATRX leads to chromosome cohesion and congression defects. J Cell Biol *180*, 315-324.

Ruchaud, S., Carmena, M., and Earnshaw, W.C. (2007). Chromosomal passengers: conducting cell division. Nat Rev Mol Cell Biol *8*, 798-812.

Steensma, D.P., Higgs, D.R., Fisher, C.A., and Gibbons, R.J. (2004). Acquired somatic ATRX mutations in myelodysplastic syndrome associated with alpha thalassemia (ATMDS) convey a more severe hematologic phenotype than germline ATRX mutations. Blood *103*, 2019-026.

Stevenson, R.E., Abidi, F., Schwartz, C.E., Lubs, H.A., and Holmes, L.B. (2000). Holmes-Gang syndrome is allelic with XLMR-hypotonic face syndrome. Am J Med Genet *94*, 383-85.

Villard, L., Fontès, M., Adès, L.C., and Gecz, J. (2000). Identification of a mutation in the XNP/ATR-X gene in a family reported as Smith-Fineman-Myers syndrome. Am J Med Genet *91*, 83-85.

Villard, L., Gecz, J., Mattéi, J.F., Fontés, M., Saugier-Veber, P., Munnich, A., and Lyonnet, S. (1996). XNP mutation in a large family with Juberg-Marsidi syndrome. Nat Genet *12*, 359-360.

Vong, Q.P., Cao, K., Li, H.Y., Iglesias, P.A., and Zheng, Y. (2005). Chromosome alignment and segregation regulated by ubiquitination of survivin. Science *310*, 1499-1504.

Wheatley, S.P., Hinchcliffe, E.H., Glotzer, M., Hyman, A.A., Sluder, G., and Wang, Y. (1997). CDK1 inactivation regulates anaphase spindle dynamics and cytokinesis in vivo. J Cell Biol *138*, 385-393.

Woods, C.G., Bond, J., and Enard, W. (2005). Autosomal recessive primary microcephaly (MCPH): a review of clinical, molecular, and evolutionary findings. Am J Hum Genet *76*, 717-728.

Xu, H., Boulianne, G.L., and Trimble, W.S. (2002). Membrane trafficking in cytokinesis. Semin Cell Dev Biol *13*, 77-82.

Chapter 4

4 ATRX Regulates Cortical Development Through Control of Neural Progenitor Cell Division

Mitotic cell division is considered one of the primary mechanisms used by neural progenitor cells to initiate the neuronal/glial fate commitment. Studies of the Atrx-null mouse cortex had previously identified cortical defects, including a reduction in the volume of the forebrain, and reduction in the radial and tangential dimensions of the cortex, suggesting a broad neurodevelopmental defect. This phenotype is similar to those observed in rodent models deficient for other genes involved in neural progenitor cell division (*Cit*){LoTurco 2003; Di Cunto 2000;Chang 2010}. Importantly, disruption of neural progenitor cell division can lead to changes in the regulation of neuron production, and lead to altered patterns of cortical layering and imbalances in the proportions of different neuronal layers, something that had not yet been investigated in the Atrx-null mouse.

4.1 Introduction

Inherited mutations of the *ATRX* gene, encoding the SWI/SNF2 family chromatin remodeling protein ATRX, are associated with a spectrum of syndromic and non-syndromic mental retardations characterized by developmental delay, cognitive deficits and microcephaly (Gibbons, 2006). ATRX utilizes the energy of ATP hydrolysis to disrupt histone-DNA interactions, and has strong DNA translocase activity (Xue et al., 2003), suggesting a role for ATRX in chromatin remodeling and regulation of gene transcription. Supporting this, ATRX has been shown to regulate the expression of a number of imprinted target genes in the mouse brain (Kernohan et al., 2010), to bind tandem repetitive DNA elements in telomeric and euchromatic regions as a means to regulate gene expression (Law et al., 2010), and to deposit the histone variant H3.3 at telomeric and pericentric heterochromatin in cooperation with the histone chaperone Daxx (Goldberg et al., 2010; Drané et al., 2010; Lewis et al., 2010). ATRX is highly enriched at pericentromeric heterochromatin in mouse and human cells throughout the cell cycle (McDowell et al., 1999) where it becomes hyperphosphorylated at the onset of

the mitotic phase (Bérubé et al., 2000), and is required for normal chromosome alignment during both mitosis and meiosis (De La Fuente et al., 2004; Ritchie et al., 2008; Baumann et al., 2010). Conditional inactivation of *Atrx* in the developing mouse forebrain prior to the onset of neurogenesis leads to reduced forebrain size, hippocampal dysgenesis, and elevated p53-dependent neuronal apoptosis (Bérubé et al., 2005; Seah et al., 2008). Inactivation of p53 leads only to a partial rescue of cortical size, indicating that additional mechanisms contribute to the *Atrx*-dependent cortical phenotype in this model (Seah et al., 2008).

The mature mammalian cerebral cortex is laminated into six stratified layers, each populated by distinct neuronal subtypes with unique cell morphologies, gene expression profiles, and neuronal connectivites (Campbell, 2005). Excitatory glutamatergic projection neurons constitute the large majority of cortical neurons, and are produced by apical and basal neural progenitor cells (NPCs) in the germinal ventricular and subventricular zones, respectively, adjacent to the lateral ventricles in the dorsal telencephalon (Gorski et al., 2002; Noctor et al., 2004). In the mouse, cortical development is characterized by an initial expansion of the neural progenitor cell population through symmetric proliferative cell divisions, followed by a transition to asymmetric neurogenic cell divisions at embryonic day (E) 14 (McConnell, 1995). These new neurons migrate radially away from the lateral ventricle along a scaffold of radial glia projections to their final cortical destinations in a temporally determined inside-out fashion, with the earliest born neurons populating the deep cortical layers (V-VI), and late born neurons found in the superficial layers (II-IV) (Rakic, 1974). Throughout cortical neurogenesis the appropriate balance of neural progenitor self-renewal, differentiation, and survival is required to achieve proper cortical size and functional organization (Rakic, 1995; Haydar et al., 1999; Kriegstein et al., 2006). Ultimately, the fate of a daughter cell born from a dividing apical NP depends in part upon the inheritance of the relatively small apical membrane and its associated factors, including m-Numb (Petersen et al., 2002; Shen et al., 2002; Petersen et al., 2004) and Par-3 (Kosodo et al., 2004; Bultje et al., 2009), which likely specify cell fate through the notch signaling pathway. Inheritance of the apical domain by the two daughter cells during symmetric cell division yields two NPCs, resulting in a proliferative expansion of the

progenitor pool during the early stages of neurogenesis**.** Conversely, inheritance of the apical domain by only one daughter cell during asymmetric cell division leads to the differentiation of the daughter cell lacking the apical domain**.** Certain proteins implicated in cortical development and microcephaly have been shown to regulate the orientation of the mitotic spindle during apical neural progenitor mitosis (Woods et al., 2005), including ASPM (Fish et al., 2006), and CDK5RAP2 (Lizarraga et al., 2010). In these cases it is thought that disrupted mitotic spindle and cleavage plane orientation increases the proportion of asymmetric NPC divisions, prematurely depleting the NPC pool and leading to a loss of late-born neurons and a smaller cortex.

In the present report, we show that isolated *Atrx*-null neuroprogenitors display mitotic chromosome misalignment and missegregation phenotypes similar to those observed in an *ATRX* depleted human somatic cell line (Ritchie et al., 2008). Dividing apical neural progenitors in the *Atrx*-null embryonic forebrain are more often seen in an asymmetric orientation, suggesting that the absence of ATRX might affect the timing and balance of apical progenitor cell differentiation. Indeed, we observed an overproduction of Tbr1 expressing layer VI neurons in the postnatal *Atrx*-null cortex, and fewer Brn2 expressing neurons in the superficial cortical layers. Furthermore, the NPC pool was reduced in the late-stage *Atrx*-null forebrain. We propose that loss of *Atrx* early in neurogenesis disrupts the ability of apical progenitor cells to maintain the highly regulated symmetric orientation of the mitotic spindle, possibly due to failed mitotic chromosome alignment and segregation, consequently disrupting the balance of progenitor cell proliferation and neuronal differentiation, and ultimately leading to abnormal cortical architecture.

4.2 Materials and Methods

4.2.1 Animal Husbandry

Conditional deletion of *Atrx* in the mouse forebrain was achieved by crossing $Atrx^{loxP}$ females with heterozygous *Foxg1Cre* knock-in males, as previously described (Bérubé et al., 2005; Ritchie et al., 2008; Seah et al., 2008). The $Atrx^{loxP}$ line was kindly provided by D. Higgs and R.J. Gibbons (Weatherall Institute of Molecular Medicine, John Radcliffe Hospital, Oxford, United Kingdom). For embryonic studies, vaginal plugs were checked

at 9 am and midday of positive plugs were considered E0.5. All animal studies were conducted in compliance with the regulations of The Animals for Research Act of the province of Ontario, the guidelines of the Canadian Council on Animal Care, and the policies and procedures approved by the University of Western Ontario Council on Animal Care.

4.2.2 Western Blot Analysis

Protein was extracted from mouse forebrain cortical tissues of *Atrx*-null ($Atrx^{f/y}$ $Foxg1^{Cre}$) and control ($Atrx^{wt/y}$ $Foxg1^{Cre}$) littermates at P7 and P10 using RIPA buffer (150 mM NaCl, 1 % NP-40, 50 mM Tris, pH 8.0, 0.5 % deoxycholic acid, 0.1 % SDS, 0.2 mM PMSF, 0.5 mM NaF, 0.1 mM Na_3VO_4, and 1 % protease inhibitor cocktail tablet [Complete mini, EDTA-free; Roche]) for 30 minutes on ice (for Tbr1 and Ctip2), or using the NE-PER nuclear and cytoplasmic protein extraction kit (for Brn2) (Thermo Scientific) and protein concentration was quantified from 280 nm absorbance measurements using a NanoDrop ND-1000 Spectrophotometer (Thermo Scientific). Isolated total protein (10-30 μg) was resolved using 8 % SDS-PAGE and transferred onto nitrocellulose membranes (Bio-Rad Laboratories). The membranes were probed with goat anti-Brn2 (1:1000, Santa Cruz Biotechnology, Inc.), rabbit anti-Tbr1 (1:1000, Abcam), and rabbit anti-Ctip2 (1:1000, Abcam) followed by the appropriate horseradish peroxidase (HRP)–conjugated secondary antibody (1:5,000; GE Healthcare). The membranes were incubated in enhanced chemiluminescence reagent (ECL) before exposure to x-ray film (Amersham). The membranes were reprobed with mouse anti-α-tubulin (1:40,000; Sigma-Aldrich) or anti-INCENP as a loading control. Band intensities were quantified from developed film using a Fluorchem 8800 gel documentation system (Alpha Innotech Corp., San Leandro, CA)

4.2.3 Neuroprogenitor Cultures

Embryos were isolated at E13.5 days of gestation, measured after the observation of a mating plug (E0.5). Pregnant dams were euthanized by CO_2 asphyxiation. Embryonic cortices were dissected into ice-cold Hank's Balanced Salt Solution (HBSS, Sigma), dissociated by trituration and plated in Neurobasal media (Gibco) supplemented with 1 %

Penicillin-Streptomycin, 1 % Glutamax (Gibco), 1 % N2 supplement, and 25 ng/ml bFGF in 4-well plates (Nunc). Cultures were maintained in a humidified tissue culture incubator at 37 °C and 5 % CO_2.

4.2.4 Cryosectioning

For embryonic time points, whole mouse embryos were collected from CO_2 euthanized pregnant dams at specific gestational ages (E13.5, E16.5) and stored in phosphate buffered saline (PBS) pH 7.4 with 4 % paraformaldehyde (PFA) at 4 °C for 16-24 hours. For postnatal day P7, mice were lethally sedated with CO_2 and were transcardially perfused with 4 % PFA-PBS pH 7.4. Brains were then dissected and stored in 4 % PFA-PBS pH 7.4 at 4 °C for 16-24 hours. Samples were cryoprotected in 10-30 % sucrose-PBS pH 7.4, embedded in Shandon Cryomatrix (Thermo Scientific), sectioned using a Leica cryostat (CM 3050S), and collected on Superfrost+ glass microscope slides (VWR).

4.2.5 Immunofluorescence Staining and Quantification

Prior to immunostaining, tissue cryosections were heated for 10 minutes in 10 mM Na-Citrate (pH 6.0) in a microwave to unmask antibody binding-sites. Cryosections were incubated with primary antibodies diluted in PBS + 0.3 % Triton X-100 overnight at 4 °C in a Shandon Sequenza slide rack (Thermo), rinsed in PBS, incubated with secondary antibodies diluted in PBS + 0.3 % Triton X-100 for 1 hour, followed by a 5 minute incubation with DAPI (1 μg/ml in PBS, Sigma) as a nuclear counterstain, rinsed with PBS and mounted in SlowFade Gold (Invitrogen) or Vectashield H-1000 (Vector Labs) fluorescent mounting media. Antibodies used were anti-γ-Tubulin, anti-Ctip2 (1:500, Abcam), anti-Tbr1 (1:200, Abcam), anti-Brn2 (1:50, Santa Cruz), anti-Tbr2 (1:500, Abcam), anti-Pax6 (1:50, Santa Cruz). Immunofluorescence images were captured using a Leica DMI-6000B inverted microscope (Leica Microsystems) equipped with a digital camera (ORCA-ER, Hammamatsu). Image capture was achieved using Openlab v5.0 (Perkin Elmer) and processed using Volocity v5.4 (Perkin Elmer) and Photoshop CS3 (Adobe). To analyze P7 cortical layer thickness, three different measurements separated by 100 μm were made perpendicular to the lateral cortical axis in equivalent regions from

three sequential cryosections per brain from n = 5 mice for both control and Atrx-null samples. For P7 cortical cell quantifications, 200 μm-wide columns perpendicular to the lateral cortical axis were quantified for specific immunopositive cells in equivalent areas from 3 adjacent cryosections per brain from n = 5 mice for control and Atrx-null samples. Statistical analysis of the sample means was performed using student's t-test. For neuroprogenitor mitotic figure analysis, cultures were fixed with 2 % PFA in PBS pH 7.4 after 2-3 days in culture, immunostained with anti-Atrx (Santa Cruz) and counterstained with DAPI (1 μg/ml in PBS), and mounted in Vectashield H-1000 mounting media (Vector labs). Cells were quantified from n = 3 mice for control and n = 4 for Atrx-null.

4.3 Results

4.3.1 Abnormal Chromosome Alignment and Segregation in Cultured Atrx-null Neuroprogenitors

A mouse model of Cre-mediated *Atrx* inactivation in the developing embryonic mouse forebrain has been previously described (Bérubé et al., 2005) ($Atrx^{Foxg1Cre}$ mice, defined as Atrx-null hereafter). In this model, *Atrx* is inactivated in cortical NPCs at age E8.5, prior to the onset of neurogenesis, resulting in loss of *Atrx* expression in all cortical neurons. The *Atrx*-null forebrain is reduced in size at birth, with elevated P53-dependent cortical cell death (Bérubé et al., 2005; Seah et al., 2008). We have previously reported that the *Atrx*-null embryonic forebrain displays dispersed chromatin fragments in close association with the mitotic NPCs of the ventricular zone lining the embryonic lateral ventricles (Ritchie et al., 2008). To determine whether this phenotype reflects disrupted mitotic chromosome alignment in the NPCs of the developing neuroepithelium, we established primary cell cultures of control and *Atrx*-null NPCs isolated from E13.5 telencephalon. Isolated cells were cultured in Neurobasal media supplemented with N2 and bFGF to allow for colony growth of dividing NPCs, and the cultures were fixed and stained with DAPI two days after plating. Mitotic figures were identified by characteristic condensed chromatin morphologies, and scored for evidence of abnormalities. We found that embryonic NPCs isolated from *Atrx*-null cortices were more often seen with abnormal mitotic figures, including misaligned chromosomes during metaphase and chromatin bridges during anaphase/telophase (Control = 10/161

(6.21%), *Atrx*-null = 23/114 (20.18%)) (Figure 4-1A, B). These results indicate that Atrx is required for proper chromosome dynamics during mitotic cell division of cortical NPCs.

4.3.2 Disrupted Angle of Division in Atrx-null Apical Neuroprogenitors Lining the Ventricular Zone

Normal neocortical development relies on the temporally choreographed balance of progenitor cell divisions. Initially the progenitor population is expanded through symmetric proliferative cell divisions, which is then followed by a shift to asymmetric differentiative divisions that yield the variety of cell types found in the mature cortex. The balance and timing of these two modes of division are critical to achieve normal cortical size and patterning (Kriegstein et al., 2006). The differential inheritance of the apical plasma membrane is considered a key determinant in the ultimate fate decision of daughter neuroprogenitor cells. This mechanism is achieved by controlling the orientation of the mitotic spindle and cytokinetic cleavage furrow to orient that axis of cell division relative to the apical cell surface. Disruption of spindle orientation or cleavage angle has been linked to microcephalic phenotypes in murine models. To assess whether ATRX is required to achieve a normally oriented mitotic axis, we cryosectioned control and *Atrx*-null E13.5 embryos and scored the orientation of the mitotic spindle axis relative to the ventricular surface in apical NPCs. Angular measurements of the mitotic spindle were achieved by staining cryosections with the DNA counterstain DAPI in conjunction with an antibody against the centrosomal marker γ-Tubulin, an indicator of the mitotic spindle poles (Figure 4-1C). In control forebrains (n = 3), we observed that in 84% of dividing cells, the mitotic spindles were oriented in a near-parallel (0-20°) angle to the apical surface, only 63 % of dividing cells in the *Atrx*-null forebrain were oriented in this manner. In contrast, mitotic apical NPCs in the *Atrx*-null forebrain (n = 3) were more frequently oriented in asymmetrically, with 25.3 % between 20-39° and 11.3 % between 40-90° relative to the apical surface, in contrast only 12% of control NPCs were between 20-29° and 4% between 40-90°.

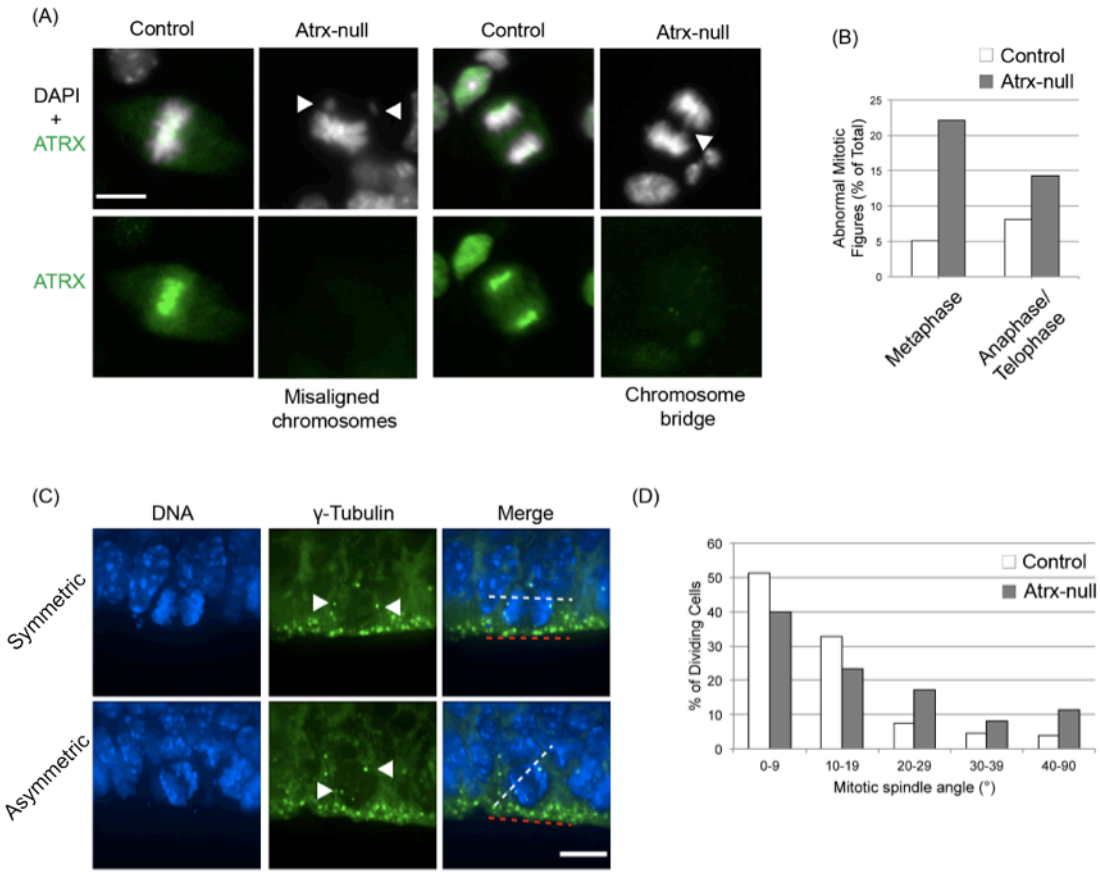

Figure 4-1. *Atrx*-null neuroprogenitors exhibit mitotic defects *in vitro* and altered cell division axis *in vivo*.

(A) Cultured neural progenitors from E13.5 control and *Atrx*-null forebrain were fixed, immunostained with an anti-ATRX antibody and counterstained with DAPI to detect DNA. (B) Mitotic cells were scored for mitotic defects (control n = 161 from 3 mice, *Atrx*-null n = 114 from 4 mice), specifically for misaligned chromosomes at the metaphase plate and chromosome bridges or lagging chromosomes at anaphase/telophase. (C) Cryosections of E13.5 control and *Atrx*-null cortex were labeled with anti-γ-Tubulin antibody to detect the centrosomes (arrowheads), and counterstained with DAPI to detect DNA. The axis of neural progenitor cell division at the neuroepithelial surface was measured using the axis between centrosomes (white dashed line) relative to the neuroepithelial surface (red dashed line) (D) Orientation of the cell division axis relative to the axis of the apical neuroepithelial surface was scored in control and Atrx-null cortex (n = 50 cells/mouse, 3 mice/genotype). Scale in (A) & (C) = 10 μm.

These findings demonstrate that dividing apical neuroprogenitors of the *Atrx*-null embryonic forebrain were aligned more often in an asymmetric mode of cell division, which may alter the inheritance of the apical plasma membrane and disturb the pattern of neuronal differentiation.

4.3.3 Altered Cortical Architecture in the Postnatal *Atrx*-null Forebrain

Our observation of increased asymmetrically oriented mitotic NPCs in the embryonic *Atrx*-null neuroepithelium suggested a potential defect in the timing and balance of projection neuron differentiation during this stage of neurogenesis. Our observation of increased asymmetric cell divisions at E13.5 would initially cause an overproduction of deep layer neurons (layers V-VI), eventually leading to a depletion of the progenitor pool and thus reduced capacity to produce superficial layer neurons (Layers II-IV). To test this, we examined cortical lamination and the different neuronal subpopulations in the *Atrx*-null P7 cortex, when most cortical neurons have been produced and have migrated to their final laminar positions. We first examined the status of the deep layer VI neurons, which are born following the splitting of the preplate into the subplate and marginal zone. Corticothalamic projection neurons of the deep cortical layer VI are characterized by expression of the T-box transcription factor Tbr1 (Bulfone et al., 1995). Consistent with increased asymmetric neurogenic cell divisions at E13.5, we found that the postnatal *Atrx*-null cortex was characterized by an increased population of deep cortical layer VI neurons, as assessed by immunofluorescence staining for Tbr1-expressing cells (Control = 130.93 ± 20.37 cells, *Atrx*-null = 211.80 ± 27.18 cells, $p < 0.01$, $n = 5$) (Figure 4-2). In the *Atrx*-null cortex, this deep layer of Tbr1 expressing cells was dramatically expanded along the dorsal-ventral axis (Control = 259.26 ± 34.94 μm, Atrx-null = 352.78 ± 66.91 μm, $p < 0.05$, $n = 5$) (Figure 4-2). Surprisingly, total cortical thickness was not significantly changed in this cortical region (Control = 754.09 ± 65.05 μm, *Atrx*-null = 767.46 ± 124.49 μm, $p = 0.83$, $n = 5$), though the depth of layer VI relative to the entire depth of the cortex was significantly increased in the *Atrx*-null forebrain (Figure 4-2). These results indicate a disproportionate increase in the number

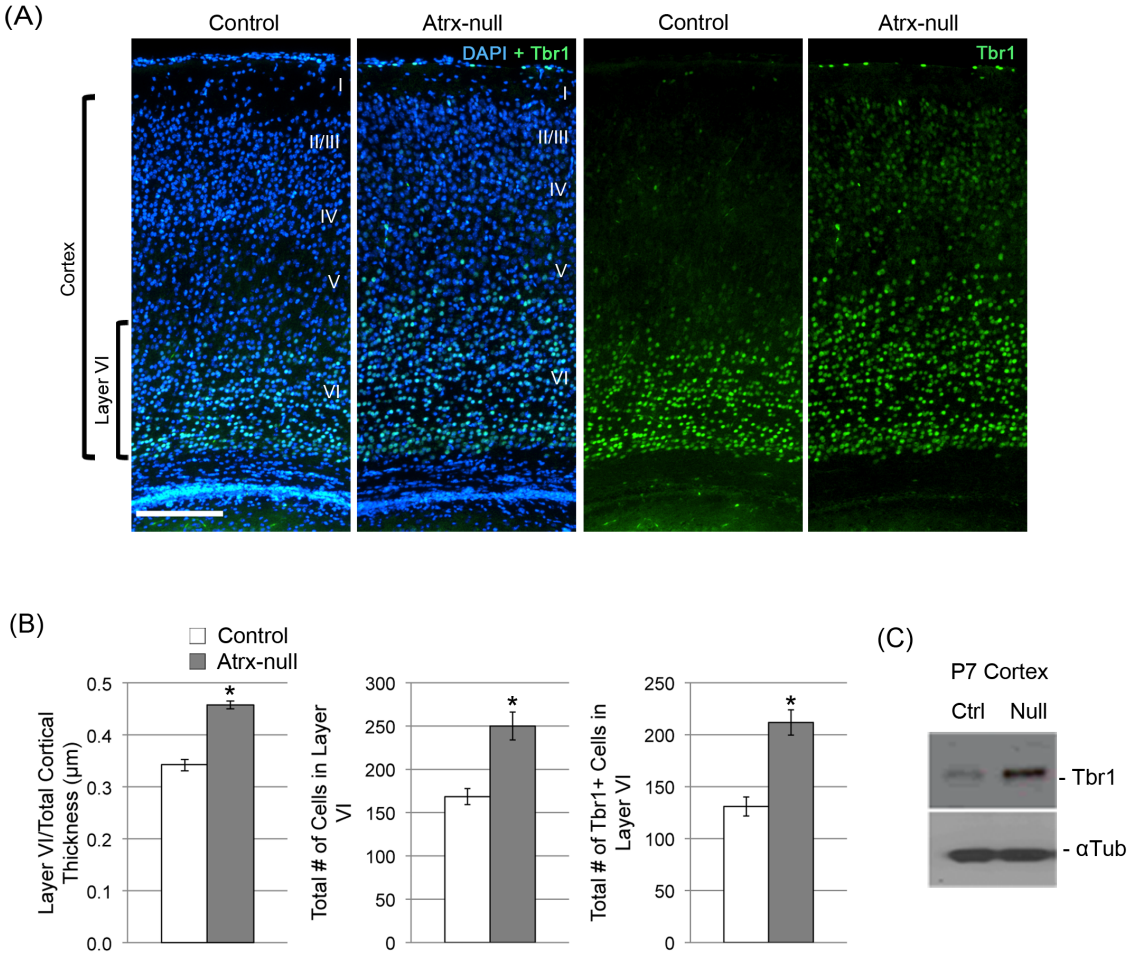

Figure 4-2. Cortical layer IV is expanded in the postnatal *Atrx*-null forebrain.

(A) Cortical sections at P7 from control and *Atrx*-null mice were stained with an anti-Tbr1 antibody to detect deep cortical layer VI projection neurons. (B) Results in (A) were quantified by measuring the thickness of the domain of Tbr1 expressing deep cortical layer neurons and total cortical thickness. Layer VI represents an increased proportion of the total cortical depth in the *Atrx*-null mouse. Measurements were taken from 3 points 100 µm apart in 3 sequential sections per animal (n = 5 mice per genotype). The total number of Tbr1 expressing cells in cortical layer VI is increased in the *Atrx*-null mouse, along with the total number of layer VI cells ($p < 0.01$), as determined by DAPI coutnerstaining. Cells counts were quantified from single 200 µm-wide columns spanning the entire depth of the cortex from 3 sequential sections (n = 5 mice for both control and Atrx-null genotypes). Scale in (A) = 200 µm. Error bars represent mean +/- s.e.m. Single asterisk = $P < 0.01$. (C) Western blot analysis of total protein from P7 cortices shows an increase in the amount of Tbr1 protein in the Atrx-null (Null) forebrain relative to the Foxg1Cre control (Ctrl) forebrain.

of Tbr1 expressing neurons within the deep cortical layers of the postnatal *Atrx*-null cortex. The expansion of layer VI and concurrent increase in the number of Tbr1-expressing cells was confirmed by semi-quantitative Western Blot analysis of P7 cortex, which showed an increase in Tbr1 protein levels in the *Atrx*-null cortex relative to control samples (Fig 4-2C).

4.3.4 The Neural Progenitor Population is Reduced in the Late Embryonic *Atrx*-null Cortex

Because we observed a dramatic increase in the number of Tbr1 expressing layer VI cortical projection neurons in the P7 *Atrx*-null forebrain, in conjunction with an increase in asymmetrically oriented neural progenitor cell divisions during mid-neurogenesis, we theorized that the late-embryonic progenitor pool might be prematurely depleted as a consequence. We investigated the populations of neural progenitor cells in E16.5 control and *Atrx*-null forebrain by immunostaining cryosections with antibodies against the transcription factors Pax6 and Tbr2, markers of apical and basal progenitors, respectively (Figure 4-3). Both progenitor populations appeared reduced in the *Atrx*-null forebrain, however the Tbr2 expressing basal progenitors were more severely affected. This effect was consistent at both caudal (Figure 4-3A) and rostral (Figure 4-3B) cortical depths, and affected both the dorsal cortical progenitors and hippocampal progenitors, consistent with the hippocampus being a severely affected cerebral structure in the post-natal *Atrx*-null forebrain. These results suggest that the overproduction of early born, deep cortical projection neurons in the *Atrx*-null forebrain comes at the expense of the late-embryonic neural progenitor population.

4.3.5 Superficial Cortical Projection Neurons are Depleted in the *Atrx*-null Forebrain

The depletion of both neural progenitor populations at E16.5, especially of the basal progenitor cells, suggested that the neural output during the later stages of neurogenesis might be limited in the *Atrx*-null cortex. At E16.5, the projection neurons destined for the most superficial cortical layers (II/III) are being produced, primarily by the basal progenitor cells of the SVZ. The corticospinal projection neurons of cortical layer V express high levels of the C2H2-type zinc finger transcription factor Ctip2. Control and

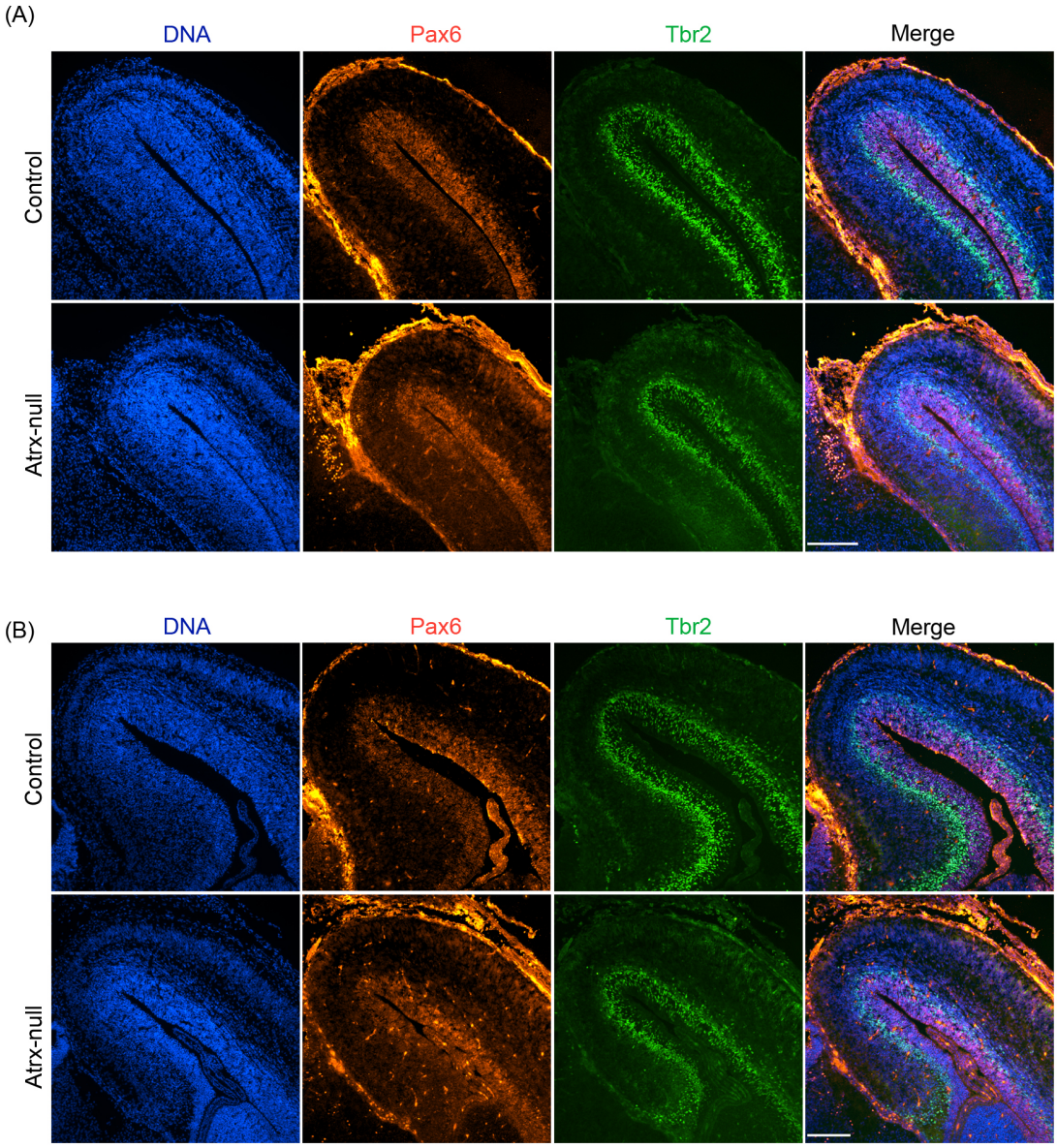

Figure 4-3. Neural progenitor cells are depleted in the late-embryonic *Atrx*-null cortex.

Cryosections of E16.5 control and *Atrx*-null forebrain were immunostained with antibodies against Pax6 and Tbr2 to detect apical and basal neural progenitor cells, respectively, at both rostral (A) and caudal (B) cortical depths. The *Atrx*-null cortex shows a small reduction of Pax6 and more severe reduction of Tbr2 expressing cells in the germinal VZ and SVZ. Scale in (A) & (B) = 200 μm.

Atrx-null P7 forebrain cryosections were immunostained with an antibody against Ctip2to identify the projection neurons of layer V. Interestingly, we found no change in the number of cells in layer V (Control: 113 ± 21.03 cells, *Atrx*-null 113.60 ± 19.23 cells, p = 0.98, n = 5), or Ctip2-positive cells in layer V (Control = 56.60 ± 9.61 cells, *Atrx*-null = 63.00 ± 12.25 cells, p = 0.38, n = 5), or of overall layer V thickness (Control: 228.11 ± 23.24 μm, *Atrx*-null: 199.37 ± 31.29 μm, p = 0.14, n = 5) however the entire layer was shifted dorsally, possibly to accommodate the expansion of the deeper cortical layer VI (Figure 4-4A, C)(Figure 4-2). We next examined the status of the corticocortical projection neurons of the superficial layers (II-IV) that express the class III POU domain transcription factor Brn2. Control and *Atrx*-null P7 forebrain cryosections were immunostained with an antibody against Brn2 to identify superficial layer projection neurons. Indeed, most Brn2 positive cells were observed in the superficial cortical region corresponding to layer II-IV in both control and *Atrx*-null cortices (Fig 4-4A). In the *Atrx*-null cortex, this upper layer (Cortical layers II-IV) of strong Brn2 expressing cells was dramatically reduced in thickness along the dorsal-ventral axis (Control: 359.08 ± 42.49 μm, Atrx-null 256.63 ± 26.76 μm, $p < 0.01$, n = 5) (Fig 4-4B). This decrease in layer thickness was accompanied by a reduction in the number of Brn2 expressing cells within the superficial cortical layers (Control = 208.60 ± 45.97 cells, *Atrx*-null = 116.40 ± 31.41 cells, n = 5, $p < 0.01$) (Figure 4-4B). Together these results show that the *Atrx*-null cortex is specifically depleted of late-born superficial cortical projection neurons.

4.4 Discussion

Using a conditional model of *Atrx* inactivation, we have shown altered cerebral cortical patterning and neuron production in the post-natal *Atrx*-null mouse forebrain. In addition we show that when cultured under proliferative conditions, NPCs isolated from the embryonic *Atrx*-null cortex exhibit characteristic mitotic defects, including chromosome misalignment at metaphase, and chromatin bridges at anaphase/telophase, supporting the proposal that the DNA fragments observed in the embryonic lateral ventricles lining the apical ventricular zone represent mitotic defects *in vivo* (Ritchie et al., 2008). We have previously reported mitotic abnormalities in ATRX depleted HeLa cells, characterized by

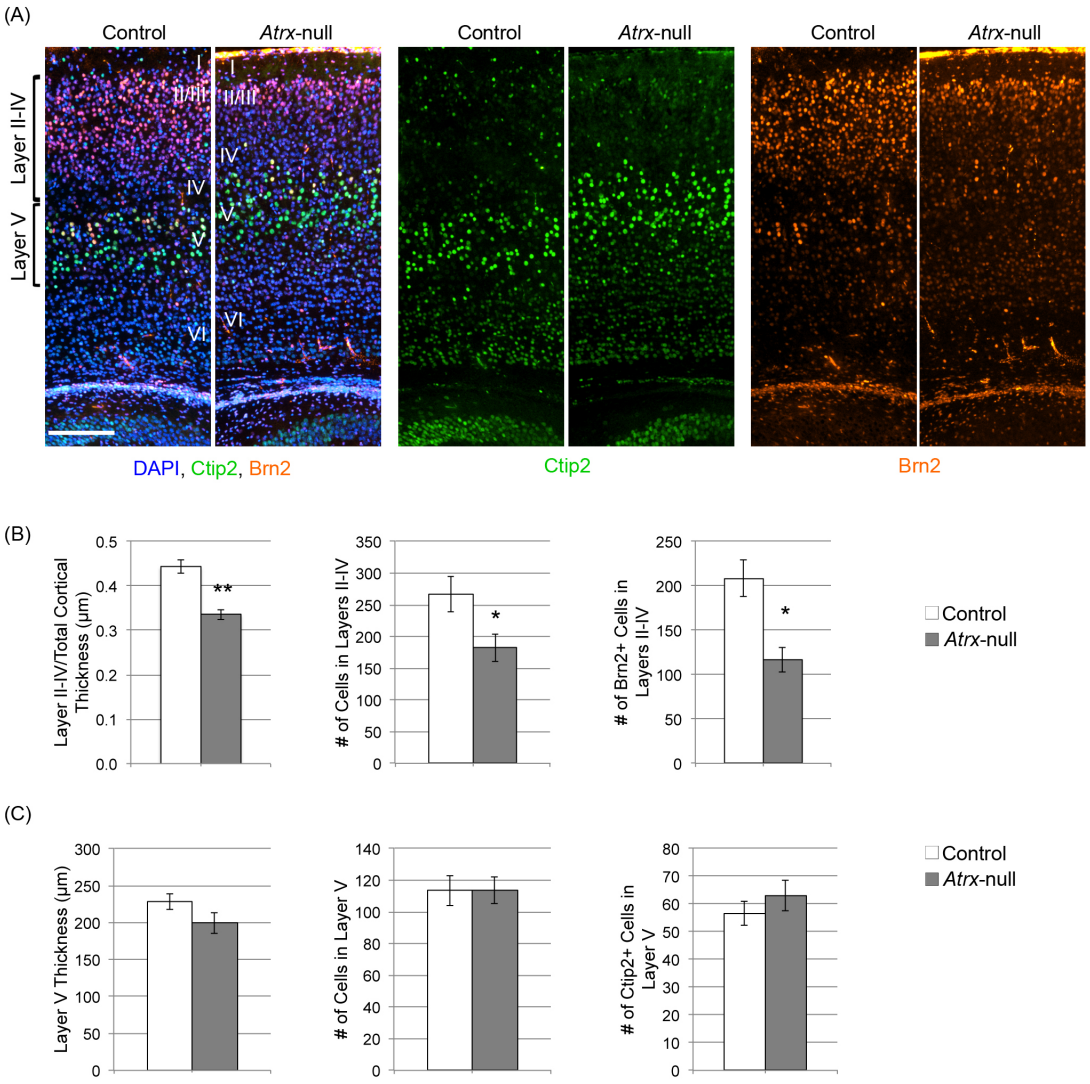

Figure 4-4. Superficial cortical layers are reduced in the *Atrx*-null cortex.

(A) Forebrain cryosections from P7 control and *Atrx*-null mice were immunostained with antibodies against CTIP2 and BRN2. (B) Superficial cortical layers II-IV in the Atrx-null mouse are thinner, and have a reduced number of BRN2+ cells (C) Cortical layer V is unaffected in the Atrx-null mouse, showing conserved thickness, total cell number, and CTIP2+ cell number. Measurements represent n = 5 mice per genotype. Single asterisk = P<0.05, double asterisk= P<0.01. Error bars are mean ± s.e.m. Scale in (A) = 200 µm.

chromosome congression defects during prometaphase, chromosome misalignment during metaphase, and chromosome bridging during telophase/anaphase (Ritchie et al., 2008). Taken together our data suggests that ATRX may regulate mitotic division in a variety of cell types.

Loss of *Atrx* increased the proportion of apical progenitor cell divisions that exhibited asymmetrically oriented mitotic spindles during early neurogenesis (E13.5), suggesting a possible disruption of the normal timing of neuronal differentiation in the *Atrx*-null cortex, as the mode of cell division is postulated to ultimately direct the choice of cell differentiation or self-renewal. In the *Atrx*-null cortex at P7, cortical layer VI contained significantly more cells and was much thicker along the dorsoventral axis compared to equivalent control cortices, indicating an overproduction of early born deep-layer neurons. As these cells are produced during the early stages of cortical neurogenesis (E11-E14), this observation supports the hypothesis that increased asymmetric apical progenitor cell divisions during this period increases the amount of early neuronal differentiation. Notably, the overall cell density of layer VI was unchanged in the *Atrx*-null mouse, suggesting that overall cell packing density was largely unaffected by loss of ATRX expression. In contrast to the deep cortical layers, the superficial cortical layers (Layers II-IV) of the *Atrx*-null cortex were significantly reduced in thickness along the dorsal-ventral axis, and contained fewer superficial Brn2+ neurons. Upper cortical layer neurons are produced during the later period of cortical neurogenesis (E14.5-E18.5), and are derived primarily from neurogenic cell divisions of basal progenitors in the embryonic subventricular zone. In the *Atrx*-null cortex, excessive asymmetric cell division during the early developmental stages might result in a consequent loss of late-born superficial layer neurons due to the depletion of the late-stage population of cortical progenitor cells in both the ventricular and subventricular zones. Immunostaining of the late (E16.5) progenitor population showed a reduction in the domain of Pax6 and Tbr2-expression in the progenitor populations in the ventricular and subventricular zones. These results show that the late-embryonic apical (Pax6 positive) and basal (Tbr2

positive) progenitor populations are depleted in the *Atrx*-null forebrain, likely as a consequence of excessive neurogenesis during the early stages of development.

Studies of the primary microcephaly-associated gene cyclin-dependent kinase 5 regulatory subunits 2 (*CDK5RAP2*) have found that the forebrain of the knockout mouse is severely dysmorphic, with cortical hypoplasia, and reduction in brain and hippocampal size (Lizarraga et al., 2010). The cortex is characterized by a loss of later born superficial layer (II/III) neurons and an increase in early born neurons of the deep cortical layer (VI), a phenotype strikingly similar to that of the *Atrx*-null mouse, albeit more severe. The neural progenitors of the embryonic cortex are characterized by mitotic defects, including delayed mitotic progression and abnormal mitotic spindles with supernumerary spindle poles, and increased levels of cell death. These progenitors also show defects in mitotic spindle positioning, with an increase in the proportion of horizontal/asymmetric cell divisions and a premature depletion of the neural progenitor cell population. A premature increase in cell cycle exit in neural progenitors is predicted to increase the amount of early born neurons, and decrease the amount of later born neurons in a predictable way (Caviness et al., 2003), matching the observations in the *cdk5rap2* deficient mouse, and the *Atrx*-null mouse here. Defects in spindle orientation have also been shown to correlate with increased cell death during neuroepithelial stem cell divisions (Yingling et al., 2008), pointing to a possible mechanism leading to the phenotype in the *Atrx*-null forebrain.

It has recently been shown that ATRX partners with DAXX in the deposition the H3.3 histone variant at specific genomic loci, including telomeric repeats and pericentromeric heterochromatin (Goldberg et al., 2010; Drané et al., 2010; Lewis et al., 2010). Interestingly, reduced ATRX-dependent H3.3 deposition at pericentromeric chromatin inhibits the expression of pericentromeric transcripts in mouse embryonic fibroblasts (Drané et al., 2010). In fission yeast, these transcripts are required for the formation of heterochromatin and sister chromatid cohesion (Zaratiegui et al., 2007), however a role in mammalian cells remains unclear. The mitotic defects induced by *Atrx* disruption may suggest that the incorporation of histone H3.3 is important for the organization and

function of pericentromeric heterochromatin, with ramifications on mitotic division and cell type ratios in the developing cerebral cortex.

These observations demonstrate a novel requirement for *Atrx* in the generation of specific neuronal subtypes in the developing mouse cortex. Importantly, they show that *Atrx* is required to maintain the appropriate level of symmetric neural progenitor cell divisions during corticogenesis. The regulation of pericentromeric heterochromatin and mitotic cell division by *Atrx* may be a critical feature in the control of neurogenesis, and may help us understand the disease mechanisms related to ATRX deficiency.

4.5 References

Baumann, C., Viveiros, M.M., and De La Fuente, R. (2010). Loss of maternal ATRX results in centromere instability and aneuploidy in the mammalian oocyte and pre-implantation embryo. PLoS Genet *6*

*B*érubé, N.G., Mangelsdorf, M., Jagla, M., Vanderluit, J., Garrick, D., Gibbons, R.J., Higgs, D.R., Slack, R.S., and Picketts, D.J. (2005). The chromatin-remodeling protein ATRX is critical for neuronal survival during corticogenesis. J Clin Invest *115*, 258-267.

Bérubé, N.G., Smeenk, C.A., and Picketts, D.J. (2000). Cell cycle-dependent phosphorylation of the ATRX protein correlates with changes in nuclear matrix and chromatin association. Hum Mol Genet *9*, 539-547.

Bulfone, A., Smiga, S.M., Shimamura, K., Peterson, A., Puelles, L., and Rubenstein, J.L. (1995). T-brain-1: a homolog of Brachyury whose expression defines molecularly distinct domains within the cerebral cortex. Neuron *15*, 63-78.

Bultje, R.S., Castaneda-Castellanos, D.R., Jan, L.Y., Jan, Y.N., Kriegstein, A.R., and Shi, S.H. (2009). Mammalian Par3 regulates progenitor cell asymmetric division via notch signaling in the developing neocortex. Neuron *63*, 189-202.

Campbell, K. (2005). Cortical neuron specification: it has its time and place. Neuron *46*, 373-76.

Caviness, V.S., Goto, T., Tarui, T., Takahashi, T., Bhide, P.G., and Nowakowski, R.S. (2003). Cell output, cell cycle duration and neuronal specification: a model of integrated mechanisms of the neocortical proliferative process. Cereb Cortex *13*, 592-98.

Drané, P., Ouararhni, K., Depaux, A., Shuaib, M., and Hamiche, A. (2010). The death-associated protein DAXX is a novel histone chaperone involved in the replication-independent deposition of H3.3. Genes Dev *24*, 1253-265.

Fish, J.L., Kosodo, Y., Enard, W., Pääbo, S., and Huttner, W.B. (2006). Aspm specifically maintains symmetric proliferative divisions of neuroepithelial cells. Proc Natl Acad Sci U S A *103*, 10438-443.

Gibbons, R. (2006). Alpha thalassaemia-mental retardation, X linked. Orphanet J Rare Dis *1*, 15.

Goldberg, A.D., Banaszynski, L.A., Noh, K.M., Lewis, P.W., Elsaesser, S.J., Stadler, S., Dewell, S., Law, M., Guo, X., et al. (2010). Distinct factors control histone variant H3.3 localization at specific genomic regions. Cell *140*, 678-691.

Gorski, J.A., Talley, T., Qiu, M., Puelles, L., Rubenstein, J.L., and Jones, K.R. (2002). Cortical excitatory neurons and glia, but not GABAergic neurons, are produced in the Emx1-expressing lineage. J Neurosci *22*, 6309-314.

Haydar, T.F., Kuan, C.Y., Flavell, R.A., and Rakic, P. (1999). The role of cell death in regulating the size and shape of the mammalian forebrain. Cereb Cortex *9*, 621-26.

Kernohan, K.D., Jiang, Y., Tremblay, D.C., Bonvissuto, A.C., Eubanks, J.H., Mann, M.R., and Bérubé, N.G. (2010). ATRX partners with cohesin and MeCP2 and contributes to developmental silencing of imprinted genes in the brain. Dev Cell *18*, 191-202.

Kosodo, Y., Röper, K., Haubensak, W., Marzesco, A.M., Corbeil, D., and Huttner, W.B. (2004). Asymmetric distribution of the apical plasma membrane during neurogenic divisions of mammalian neuroepithelial cells. EMBO J *23*, 2314-324.

Kriegstein, A., Noctor, S., and Martínez-Cerdeño, V. (2006). Patterns of neural stem and progenitor cell division may underlie evolutionary cortical expansion. Nat Rev Neurosci *7*, 883-890.

De La Fuente, R., Viveiros, M.M., Wigglesworth, K., and Eppig, J.J. (2004). ATRX, a member of the SNF2 family of helicase/ATPases, is required for chromosome alignment and meiotic spindle organization in metaphase II stage mouse oocytes. Dev Biol *272*, 1-14.

Law, M.J., Lower, K.M., Voon, H.P., Hughes, J.R., Garrick, D., Viprakasit, V., Mitson, M., De Gobbi, M., Marra, M., et al. (2010). ATR-X syndrome protein targets tandem repeats and influences allele-specific expression in a size-dependent manner. Cell *143*, 367-378.

Lewis, P.W., Elsaesser, S.J., Noh, K.M., Stadler, S.C., and Allis, C.D. (2010). Daxx is an H3.3-specific histone chaperone and cooperates with ATRX in replication-independent chromatin assembly at telomeres. Proc Natl Acad Sci U S A *107*, 14075-080.

Lizarraga, S.B., Margossian, S.P., Harris, M.H., Campagna, D.R., Han, A.P., Blevins, S., Mudbhary, R., Barker, J.E., Walsh, C.A., and Fleming, M.D. (2010). Cdk5rap2 regulates centrosome function and chromosome segregation in neuronal progenitors. Development *137*, 1907-917.

McConnell, S.K. (1995). Strategies for the generation of neuronal diversity in the developing central nervous system. J Neurosci *15*, 6987-998.

McDowell, T.L., Gibbons, R.J., Sutherland, H., O'Rourke, D.M., Bickmore, W.A., Pombo, A., Turley, H., Gatter, K., Picketts, D.J., et al. (1999). Localization of a putative transcriptional regulator (ATRX) at pericentromeric heterochromatin and the short arms of acrocentric chromosomes. Proc Natl Acad Sci U S A *96*, 13983-88.

Noctor, S.C., Martínez-Cerdeño, V., Ivic, L., and Kriegstein, A.R. (2004). Cortical neurons arise in symmetric and asymmetric division zones and migrate through specific phases. Nat Neurosci *7*, 136-144.

Petersen, P.H., Zou, K., Hwang, J.K., Jan, Y.N., and Zhong, W. (2002). Progenitor cell maintenance requires numb and numblike during mouse neurogenesis. Nature *419*, 929-934.

Petersen, P.H., Zou, K., Krauss, S., and Zhong, W. (2004). Continuing role for mouse Numb and Numbl in maintaining progenitor cells during cortical neurogenesis. Nat Neurosci *7*, 803-811.

Rakic, P. (1974). Neurons in rhesus monkey visual cortex: systematic relation between time of origin and eventual disposition. Science *183*, 425-27.

Rakic, P. (1995). A small step for the cell, a giant leap for mankind: a hypothesis of neocortical expansion during evolution. Trends Neurosci *18*, 383-88.

Ritchie, K., Seah, C., Moulin, J., Isaac, C., Dick, F., and Bérubé, N.G. (2008). Loss of ATRX leads to chromosome cohesion and congression defects. J Cell Biol *180*, 315-324.

Seah, C., Levy, M.A., Jiang, Y., Mokhtarzada, S., Higgs, D.R., Gibbons, R.J., and Bérubé, N.G. (2008). Neuronal death resulting from targeted disruption of the Snf2 protein ATRX is mediated by p53. J Neurosci *28*, 12570-580.

Shen, Q., Zhong, W., Jan, Y.N., and Temple, S. (2002). Asymmetric Numb distribution is critical for asymmetric cell division of mouse cerebral cortical stem cells and neuroblasts. Development *129*, 4843-853.

Woods, C.G., Bond, J., and Enard, W. (2005). Autosomal recessive primary microcephaly (MCPH): a review of clinical, molecular, and evolutionary findings. Am J Hum Genet *76*, 717-728.

Xue, Y., Gibbons, R., Yan, Z., Yang, D., McDowell, T.L., Sechi, S., Qin, J., Zhou, S., Higgs, D., and Wang, W. (2003). The ATRX syndrome protein forms a chromatin-remodeling complex with Daxx and localizes in promyelocytic leukemia nuclear bodies. Proc Natl Acad Sci U S A *100*, 10635-640.

Yingling, J., Youn, Y.H., Darling, D., Toyo-Oka, K., Pramparo, T., Hirotsune, S., and Wynshaw-Boris, A. (2008). Neuroepithelial stem cell proliferation requires LIS1 for precise spindle orientation and symmetric division. Cell *132*, 474-486.

Zaratiegui, M., Irvine, D.V., and Martienssen, R.A. (2007). Noncoding RNAs and gene silencing. Cell *128*, 763-776.

Chapter 5

5 General Discussion and Future Directions

The body of work presented in this thesis describes a novel role for the chromatin remodeling protein ATRX in mitotic cell division and mammalian cortical neurogenesis. Based on the results presented in chapters two and three, I conclude that ATRX is required for normal mitotic progression, sister chromatid cohesion, and cytokinesis in human somatic cells. Furthermore, chapter four shows that in the developing mouse brain, ATRX regulates cortical neurogenesis by maintaining mitotic fidelity in dividing neuronal progenitor cells and promoting accurate symmetric proliferative cell divisions.

5.1 Thesis Summary

The ATRX protein belongs to the Snf2 family of chromatin remodeling proteins, and although ATRX was originally presumed to function primarily as a transcriptional regulator, my work has revealed a novel role for ATRX in mitotic cell division. In both human and mouse cells, ATRX is enriched at the gene-sparse PCH domains throughout the cell cycle, raising the possibility that it might have additional functions beyond transcriptional control of gene expression. There, ATRX interacts with other factors implicated in the establishment and maintenance of PCH, including HP1 (McDowell et al., 1999), MeCP2 (Nan et al., 2007; Kernohan et al., 2010), Daxx (Xue et al., 2003), and H3.3 (Goldberg et al., 2010; Wong et al., 2010; Drané et al., 2010; Lewis et al., 2010), suggesting that it may also perform a specific function at this heterochromatic domain. Proper assembly of PCH is required for normal centromere function and chromatid cohesion during mitotic cell division, with disturbances leading to errors in chromosome biorientation and segregation during mitosis.

In Chapter two, I tested the hypothesis that ATRX is required to maintain mitotic fidelity in mammalian somatic cells. I found that RNAi mediated depletion of *ATRX* expression in a human cancer cell line (HeLa) leads to increased levels of mitotic abnormalities, including chromosome congression, alignment, and segregation errors. This phenotype was accompanied by reduced sister-chromatid cohesion at metaphase, pointing to a

potential mechanism underlying these defects. Importantly, I reported evidence of mitotic abnormalities in *Atrx*-null embryonic cortical neuronal progenitor cells *in vivo*, suggesting that a requirement for ATRX in mitotic cell division might extend to a physiologically relevant tissue.

In Chapter three, I reported a further disturbance of the terminal stages of mitotic cell division in *ATRX* depleted HeLa cells, notably cytokinetic failure, multinucleation, and cell death. There were two possible explanations for this phenotype; firstly that unresolved chromosome bridges or lagging chromosomes were inhibiting the cellular cleavage through mechanical hindrance, or secondly, that the cytokinetic cleavage furrow or midbody were functionally impaired, perhaps due to an unidentified role for ATRX in regulating the expression of factors related to the function of these cellular structures. It appears that the cytokinetic midbody and cleavage furrow are correctly assembled and functional in these cells, suggesting that this phenotype may be a consequence of chromosome segregation errors during mitosis.

In Chapter four, I investigated more thoroughly the effect of *Atrx* loss on neuronal progenitor cell division and cerebral cortical organization and neurogenesis in the developing mouse forebrain. I found that cultured neuronal progenitor cells from the embryonic *Atrx*-null cortex displayed elevated levels of mitotic defects, including chromosome misalignment on the metaphase spindle; reminiscent of the phenotype observed in *ATRX* depleted HeLa cells. The apical neuronal progenitors within the embryonic *Atrx*-null cortex were more often asymmetrically oriented during cell division, suggesting an increase in neuronal differentiation. Consistent with these findings, the postnatal *Atrx*-null cortex was characterized by a significant increase in early-born deep cortical projection neurons. Furthermore the late-embryonic neuronal progenitor population was depleted, accompanied by a decrease in the late-born neurons of the superficial cortical layers. These findings specifically identify a functional role for ATRX in cerebral cortical development, and contribute partly to the cortical phenotype of the conditional *Atrx*-null mouse used in this study.

5.2 A Novel Function for ATRX in Cell Division

The initial goal of my research was to investigate a potential requirement of ATRX for normal mitotic cell division by virtue of its seemingly ubiquitous enrichment at PCH in both human and mouse somatic cells. To meet these ends I depleted HeLa cells of ATRX using transient small interfering RNA (siRNA) and stable short hairpin RNA (shRNA) mediated RNAi. These experiments revealed a general mitotic defect in proliferating ATRX deficient cells, associated with reduced chromatid cohesion and a transient delay in mitotic progression. Other groups have also reported a requirement for ATRX in normal meiotic progression. In the fully-grown mouse oocyte, ATRX is found at PCH, and functional ablation *in vitro* using RNAi severely disrupts chromosome alignment at the metaphase II (MII) meiotic spindle (De La Fuente et al., 2004). More recently, further work showed that mouse oocytes depleted of ATRX by RNAi using a stably expressing *zona pellucida 3* (*ZP3*)-driven *Atrx*-short hairpin vector had chromosome segregation defects with lagging chromosomes, loss of sister chromatid cohesion at MII and greatly increased incidence of aneuploidy (Baumann et al., 2010). Meiotic spindle abnormalities and faulty chromosome congression to the metaphase plate are associated with advanced maternal age and are suspected of contributing to the observed age-related increases of aneuploid eggs in humans (Battaglia et al., 1996). In addition, an age-associated decrease in chromosome cohesion has also been reported, and could also contribute to the observed increase in aneuploidy (Hodges et al., 2005). Furthermore, a study by Pan et al. revealed that ATRX expression is reduced in eggs obtained from old female mice, which have up to a 6-fold increase in hyperploidy, associated with reduced fidelity of the metaphase I (MI) spindle assembly checkpoint (SAC) (Pan et al., 2008).

Earlier this year, Bagheri-Fam et al. investigated the role of ATRX in testis development, as ATR-X patients often display urogenital abnormalities, including small testis (Bagheri-Fam et al., 2011). In this study, *Atrx* was conditionally inactivated in the supporting cell lineage (Sertoli cells) of the mouse testis, and it was found that these *Atrx*-negative Sertoli cells exhibit prolonged G2/M phase, and elevated levels of apoptosis during development, leading to tubule dysgenesis. However, it was not clear whether the

decrease in cell viability was related to the mitotic delay or an alternative cause like impaired cellular maturation.

In addition to broad developmental consequences, mitotic defects can be associated with oncogenic events and tumorigenesis due to genomic instability (Montgomery et al., 2003). To date there is no evidence that ATR-X patients exhibit mitotic defects or are prone to developing cancer, however there is increasing evidence for a role of ATRX in neoplasia outside of the context of ATR-X syndrome (Steensma et al., 2004). Recently, ATRX and DAXX mutations were found in a large proportion of pancreatic neuroendocrine tumours (PanNETS), suggesting that they have tumour suppressive functions. Although rare, PanNETs are the second most common malignancy of the pancreas, with a 10-year survival rate of only 40%. Exomic sequencing of 68 pancreatic PanNETS identified mutations in both ATRX and Daxx in 17.6% (12/68) and 25% (17/68) of the samples, respectively, but never together, suggesting that they act through the same biological pathway in this context (Jiao et al., 2011). All *ATRX* mutations correlated with loss of immunolabeling in these hyperplastic pancreatic islet cells, suggesting that complete loss of ATRX protein is associated with oncogenetic events in PanNETs. Furthermore, another recent study of PanNETs found substantial chromosomal alterations in 98% of samples (Hu et al., 2010), suggesting that genomic instability could contribute to PanNET oncogenesis. It may be that null mutations in *ATRX* lead to more severe genomic instability with a much higher propensity for oncogenesis than hypomorphic mutations. Although I observed mitotic defects in human cells retaining low levels of *ATRX* transcript (20% of control levels), both full-length and ATRXt protein were not detectable using western blots analysis (see Figure 2-2), suggesting that this approach may produce an effect more similar to a null-allele rather than a hypomorphic allele.

A growing number of reports have now linked ATRX and cancer. In a study of 132 adults with de novo acute myeloid leukemia (AML), low *ATRX* expression correlated with high-risk karyotype and poor clinical outcome (Serrano et al., 2006). Altered ATRX expression levels have also been reported in gene expression profiling experiments using prostate cancer primary cells (Coutinho-Camillo et al., 2006), esophageal squamous cell

carcinoma cell lines (Bo et al., 2004), chronic lymphocytic leukemia primary cells, and irradiated breast cancer cell lines (Roy et al., 2008).

Myelodysplastic syndromes (MDS) are a diverse group of neoplastic bone marrow disorders, associated with a diverse array of cytogenetic abnormalities (Davids and Steensma, 2010). Acquired somatic *ATRX* mutations were identified in the bone marrow or blood cells of nearly all cases of alpha thalassemia myelodysplastic syndrome (ATMDS) (Steensma et al., 2004), a pre-leukemic condition accompanied by alpha thalassemia, typically observed in elderly men. It has not yet been determined whether *ATRX* mutations in this context are the cause of the myeloproliferative syndrome, or are acquired passenger mutations affecting only α-globin synthesis (Steensma et al., 2004; Higgs and Weatherall, 2009). In some ATMDS cases, the α-thalassemia has been found to be more severe than that associated with germline ATRX mutations, suggesting that these somatic mutations may produce a null-allele, or that disparate mechanisms govern this phenotype depending on the context of the mutation (Steensma et al., 2004).

Although ATRX deficiency induces a general mitotic or meiotic phenotype in some types of actively dividing cells, the potential mechanisms leading to this defect have not yet been determined. This may soon change after a number of recent reports identified a novel role for ATRX, together with its binding partner DAXX, in the specific deposition of H3.3 containing nucleosomes at discrete heterochromatic domains (Goldberg et al., 2010; Wong et al., 2010), including PCH (Drané et al., 2010). Depletion of *Atrx* in MEFs resulted in reduced H3.3 incorporation at pericentric repeats, and a decrease in the abundance of pericentric transcripts (Drané et al., 2010). It is speculated that H3.3 facilitates transcription by reducing the stability of nucleosomes into which it is incorporated, facilitating removal from the DNA template (Jin and Felsenfeld, 2007). Interestingly, contrary to previous assumptions, the repetitive and heterochromatic pericentric repeats are highly transcribed in fission yeast (Cam et al., 2005; Djupedal et al., 2005) and mammals (Lu and Gilbert, 2007), and these transcripts are in fact required for the formation of pericentric DNA as condensed heterochromatin through an RNAi mediated mechanism (Maison et al., 2002; Djupedal et al., 2005). Importantly, pericentric heterochromatin structure is essential for kinetochore assembly (Gieni et al.,

2008), centromeric cohesion (Nonaka et al., 2002), and accurate chromosome segregation during mitosis (Peters et al., 2001; Pidoux and Allshire, 2004). In the ATRX depleted HeLa cells described in my thesis, the kinetochore appears to be assembled properly as CREST immunoreactivity [CREST is a human autoimmune anti-centromere antiserum, predominantly detecting CENPA and CENPB (Brenner et al., 1981; Earnshaw and Migeon, 1985)] appeared identical in control and ATRX deficient cells. Loss of the H3K9me3 methyltransferase, Suv39h1, results in abnormal assembly of PCH, and aberrant chromosome segregation and premature sister chromatid separation (Lehnertz et al., 2003; García-Cao et al., 2004). This raises the possibility that the mitotic defects I have described in *ATRX* compromised HeLa cells and mouse embryonic neuronal progenitors are due to abnormal PCH assembly, perhaps due to the lack of H3.3 deposition and pericentric transcription, and subsequent failure to recruit or retain appropriate amount of cohesin at PCH. To continue these studies, it will be important to investigate the composition of PCH in these cells using immunofluorescence and ChIP analysis to measure the presence of PCH antigens like HP1 and H3K9me3. In addition, it would be useful to examine the level of pericentric repeat transcripts produced in these cells, to confirm a disturbance in the RNAi-mediated pathway of PCH assembly. Other studies conducted in the Bérubé lab have found that ATRX interacts with members of the cohesin protein complex and recruits them to discrete gene regulatory regions of the genome (Kernohan et al., 2010). A logical next step will be to determine whether ATRX is required for the localization of cohesin to PCH in HeLa cells or cortical progenitors, as this may provide a mechanism to explain the chromatid cohesion and mitotic defects. I predict that ATRX is also required for normal enrichment of cohesin at PCH, as it is at discrete gene loci. A chromatin ChIP approach to examine cohesin enrichment at the human α-satellite or mouse major satellite pericentric repeats in ATRX deficient cells could be used to address this question. To determine if this is a direct recruitment of cohesin or an indirect mechanism through the maintenance of PCH structure by ATRX, the domains of interaction between ATRX and cohesin will need to be identified. Directed mutagenesis of ATRX and/or cohesin could be used to localize the interacting regions, and *in vivo* reconstitution of these mutant isoforms could help distinguish between these possibilities, for example if ATRX directly recruits cohesin to PCH,

disrupting the interacting domains on either protein should lead to loss of recruitment. In fission yeast, cohesin is primarily recruited to PCH by the HP1 homolog, Swi6 (Nonaka et al., 2002). Because of the similarities in centromere regulation between mammals and yeast, it was assumed that similar mechanisms of cohesin recruitment were active in both systems. In fact, researchers have been unable to identify an interaction between cohesin and mouse HP1 (Koch et al., 2008), suggesting that novel mechanisms of cohesin recruitment may have evolved in the mammalian system (Gartenberg, 2009).

In Chapter three I presented evidence that ATRX-depletion induces cytokinetic instability, whereby human cells depleted of *ATRX* more frequently fail cytokinesis, producing multinucleated progeny. This phenotype may indicate a direct effect of ATRX in the transcriptional regulation of genes required for the normal function of the cytokinetic midbody or cleavage furrow, or a potential secondary effect of chromosome instability during mitosis. To investigate this we conducted an examination of midbody and cleavage furrow formation in these cells by immunostaining for specific proteins associated with these cellular features, but were unable to identify any difference between the control and ATRX depleted cells. However, this analysis was not exhaustive, and did not include all potential protein targets involved in this complex process. I would continue this study by expanding the cohort of protein candidates to achieve a more detailed profile of the cleavage furrow and cytokinetic midbody in ATRX deficient cells. One protein candidate we investigated was Plk1, a serine/threonine kinase enriched at the cytokinetic midzone during anaphase, telophase, and at the cytokinetic midbody. Elegant studies using a selectively inhibitable Plk1 isoform have shown that Plk1 activity is required for cleavage furrow formation (Burkard et al., 2007; Petronczki et al., 2007; Santamaria et al., 2007; Brennan et al., 2007). It will be worthwhile to investigate the recruitment of downstream Plk1 cofactors, such as RhoA, and the RhoA GTP exchange factor ECT2, to the central spindle and midbody, to confirm that the Plk1 pathway is intact in ATRX-deficient cells. The phenotype observed in the *Atrx* depleted HeLa cells suggested a failure to complete the terminal stage of cytokinesis, a process known as cellular abscission. Abscission is the least well-understood reaction in cytokinesis, but is believed to involve membrane trafficking to remodel the midbody (Glotzer, 2001). Therefore it may be informative to assess lipid membrane composition, focusing on the

phospholipid phosphatidylethanolamine (PE), a required component of the lipid membrane at the midbody (Emoto et al., 1996), and the syntaxin 2 membrane trafficking proteins (Low et al., 2003), as the cytoplasmic membrane if often highly disorganized in *ATRX*-depleted HeLa cells undergoing cytokinesis. Cytokinesis can also be blocked by the presence of chromosome bridges that might signal via DNA damage response pathways to block and reverse the ingression of the cleavage furrow, resulting in aneuploidy or tetraploidy. Because chromosome bridges were observed in *ATRX*-depleted HeLa cells, and *Atrx*-null neuroprogenitors, it is possible that cytokinetic failure is due strictly to chromosome nondisjunction. To investigate this, it would be important to first examine the activation or post-translational modification of specific DNA-damage signaling proteins such as BRCA2 phosphorylation, and Aurora B poly-ADP-ribosylation, both implicated in cytokinetic regulation [Reviewed in (Normand and King, 2010)].

5.3 ATRX and the Control of Cell Division in Neurodevelopment

The severe developmental consequences of *ATRX* mutations on the human CNS highlight the importance of characterizing the role of ATRX in mammalian neurodevelopment. After observing mitotic defects in ATRX deficient human cells and mouse neuronal progenitors, and because of the direct relationship connecting cell division and cortical neurogenesis, I chose to investigate progenitor cell division in the conditional *Atrx*-null mouse forebrain.

In Chapter four, I reported that apical neuronal progenitors in the embryonic *Atrx*-null forebrain are more often oriented asymmetrically during cell division, suggesting an increase in the proportion of neurogenic divisions during cortical development. It is likely that abnormalities in the progression or completion of mitosis or cytokinesis in these cells, such as in the ATRX depleted HeLa cells described in chapter two, promote deviation of mitotic spindle positioning and/or cleavage furrow ingression, resulting in aberrant mitotic orientation relative to the apical ventricular surface and altered cell fate commitment. The murine animal model system has been used to identify a number of genes that are specifically involved in neuronal progenitor cell division, many of which

have human homologs associated with neurodevelopmental abnormalities, including MCPH. One such gene is abnormal spindle microcephaly (*ASPM*), in which mutations are the leading cause of human MCPH. ASPM is localized to the spindle poles (centrosomes) of mitotic cells (Fish et al., 2006; Higgins et al., 2010), and is downregulated by apical neuronal progenitors undergoing neurogenic divisions (Fish et al., 2006). Knockdown of ASPM expression using *in vivo* RNAi electroporation in developing embryonic mouse forebrain resulted in more asymmetrically oriented mitotic progenitor cells and an increase of non-progenitor daughter cell fate (Fish et al., 2006). In addition, the products of the other characterized MCPH associated genes are also centrosomal components, including CDK5RAP2, CENP-J, and Microcephalin, suggesting a common mechanism linking mitotic regulation, neurogenesis, and cortical size.

Striking results have been obtained from studies of one such MCPH-associated gene, cyclin-dependent kinase 5 regulatory subunits 2 (*CDK5RAP2*), encoding a centrosomal protein with a role in γ-tubulin ring complex (γ-TuRC) recruitment and microtubule nucleation at the centrosome (Fong et al., 2008). Interestingly, this gene is mutated in the *Hertwig's anemia* (an) mouse line, where homozygous mutant animals have a hypoproliferative anemia and leukopenia (Barker and Bernstein, 1983). These mice have germ cell deficiencies with meiotic defects in embryonic germ cells and a high level of spontaneous aneuploidy in primary cultures of hematopoietic fetal liver, bone marrow and kidney epithelial cells (Eppig and Barker, 1984). More recently it was found that the forebrain of this mouse is severely dysmorphic, with cortical hypoplasia, and reduction in brain and hippocampal size (Lizarraga et al., 2010). The cortex is characterized by a loss of later born superficial layer (II/III) neurons and an increase in early born neurons of the deep cortical layer (VI), a phenotype strikingly similar to that of the *Atrx*-null mouse, albeit more severe. The neuronal progenitors of the embryonic cortex are characterized by mitotic defects, including delayed mitotic progression and abnormal mitotic spindles with supernumerary spindle poles, and increased levels of cell death. These progenitors also show defects in mitotic spindle positioning, with an increase in the proportion of horizontal/asymmetric cell divisions and a premature depletion of the neuronal progenitor cell population. Defects in spindle orientation have also been shown to correlate with

increased cell death during neuroepithelial stem cell divisions (Yingling et al., 2008), pointing to a possible mechanism leading to this phenotype in the *Atrx*-null forebrain. A premature increase in cell cycle exit in neuronal progenitors is predicted to increase the amount of early born neurons, and decrease the amount of later born neurons in a predictable way (Caviness et al., 2003), matching the observations in the *cdk5rap2* deficient mouse, as well as my results presented in chapter four.

Cytokinesis is also a critical step in the cellular control of cortical development, exemplified by mutations in the *CIT* gene encoding the serine-threonine kinase Citron (CitK). Initial functional studies found that overexpression of truncation mutations causes erratic cytokinetic behaviour and cytokinesis failure when overexpressed in HeLa cells (Madaule et al., 2000). Citron kinase is specifically found at the cytokinetic midzone spindle and cleavage furrow during anaphase/telophase, where it then translocates to the midbody during cytokinesis (Di Cunto et al., 1998; Eda et al., 2001). The only known substrate of citron kinase is the regulatory light chain of myosin II, a subunit of the ATP-dependent +-end actin motor protein that helps to organize actin filaments into the contractile ring. In rodent models, *cit* null mutations lead to microcephaly, cellular binucleation, cytokinetic failure, and massive apoptosis in the proliferative zones of the embryonic cortex (Di Cunto et al., 2000; Sarkisian et al., 2002). Together these data demonstrate the critical role of cytokinetic regulation in cortical development. Notably, the cortical phenotype of the *Cit*-null mouse is similar to that of the conditional *Atrx*-null mouse studied in this thesis, with microcephaly, neuronal apoptosis, and abnormal cell division. In addition to the phenotype described in Chapter four, previous studies have shown that the embryonic *Atrx*-null cortex is also characterized by elevated levels of p53-dependent apoptosis (Seah et al., 2008). It may be that deficiency of ATRX in the developing cortex could lead to aneuploidy, which could reduce cell viability and result in elevated apoptosis. It will be important for future studies of the *Atrx*-null cortex to investigate the occurrence of neuronal binucleation *in vivo*.

The *Atrx*-null forebrain used in this study retains normal expression of the truncated ATRXt isoform. This isoform is not affected by the loxP-mediated recombination of

Atrx exon 18, as this isoform naturally truncates at exon 11, producing a protein that lacks the SWI/SNF homology domain. The function of ATRXt is not known, but it may be useful to study a null allele of this isoform, or both isoforms in conjunction, to further extend our understanding of the developmental and biological function of this gene. I predict that a complete knockout of both alleles will be more severe than either single allele in isolation, but might be difficult to study in the mouse if it leads to lethality when induced in the developing brain. The RNAi-mediated depletion of *ATRX* in HeLa cells described in chapter two targeted both full-length and *ATRXt* transcripts, therefore the mitotic phenotype might also have been made more severe by a deficiency of both proteins (versus only full length in the Atrx-null mouse). Furthermore, the *Atrx*-null allele used here may produce a more profound effect than that of a more biologically appropriate hypomorphic allele, because pathological mutations in ATRX are always hypomorphic (with relation to ATR-X syndrome). This is supported by the observation that somatic ATRX mutations associated with ATMDS can confer a more severe hematological phenotype than inherited germline mutations associated with ATR-X (Steensma et al., 2004). One explanation is that the somatic mutations produce null-alleles that would otherwise be developmentally lethal, but can be tolerated in a clonal population of erythrocytes. However, since some mutations associated with this disparity are identical to those found in ATR-X patients, who typically display less severe α-thalassemia, other contributing factors must be important, for instance the polymorphic G-rich VNTRs adjacent to the α-globin locus that are thought to be resolved by ATRX as a means to regulate gene expression. Although the approaches presented in this thesis are useful for the study of ATRX function, it will be important to introduce hypomorphic patient mutations into the endogenous *Atrx* allele in the mouse followed by a study of neurodevelopment to more accurately model the human disease.

5.4 Proposed model: The Role of ATRX in Mitosis and Neurogenesis

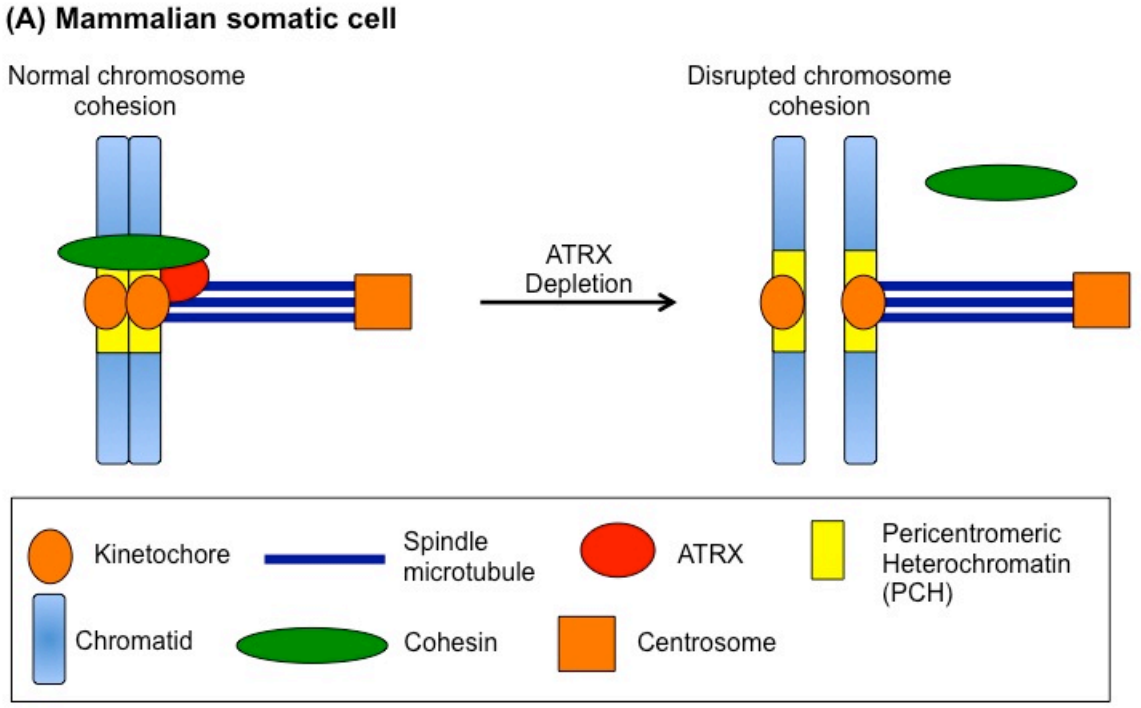

Figure 5-1. Proposed model of ATRX function in mitosis and neurogenesis.

(A) In mammalian somatic cells, ATRX is required for normal sister chromatid cohesion, possibly through the recruitment of the cohesin protein complex to pericentromeric heterochromatin (PCH). In ATRX-deficient cells, cohesin occupancy (or function) might be disrupted at PCH, resulting in reduced centromeric sister chromatid cohesion. During mitosis in ATRX-deficient cells, the spindle microtubules exert a force on the kinetochores, pulling the sister chromatids towards opposing centrosomes prematurely, resulting in mitotic defects. (B) In the embryonic *Atrx*-null mouse cortex, mitotic neural progenitors in the neuroepithelium, which line the lateral ventricles, are less often symmetrically oriented during cell division, suggesting abnormally elevated levels of neurogenic cell division. Mitotic abnormalities due to loss of ATRX-dependent sister chromatid cohesion might disrupt the precise symmetric orientation of the mitotic spindle. The postnatal *Atrx*-null cortex is characterized by an expansion of the deep cortical layers and a reduction of the superficial cortical layers, suggesting excessive production of early-born deep-layer neurons at the expense of later-born superficial layer neurons, consistent with excessive neuron production during the earlier stages of neurogenesis.

5.5 Concluding Remarks

The work presented in this thesis identifies a novel role for the Snf2 chromatin remodeling protein in the process of mitotic cell division both in cultured human cells and in the neuronal progenitors of the developing mouse brain. The observation that *ATRX* depleted cells exhibit chromatid cohesion defects contributes to the rapidly expanding role for ATRX at constitutively condensed pericentromeric heterochromatin. In addition to regulating the expression of a subset of genes, different lines of research now point to a likely role for ATRX in maintaining the structure and function of PCH. Together with the growing list of malignancies associated with somatic ATRX mutations, these data suggest a possible mechanism contributing to genomic instability in certain cases of severe ATRX deficiency. Furthermore, *ATRX* now joins a growing list of genes that are implicated in neurodevelopment through the regulation of cell division.

5.6 References

Bagheri-Fam, S., Argentaro, A., Svingen, T., Combes, A.N., Sinclair, A.H., Koopman, P., and Harley, V.R. (2011). Defective survival of proliferating Sertoli cells and androgen receptor function in a mouse model of the ATR-X syndrome. Hum Mol Genet *20*, 2213-224.

Barker, J.E., and Bernstein, S.E. (1983). Hertwig's anemia: characterization of the stem cell defect. Blood *61*, 765-69.

Battaglia, D.E., Goodwin, P., Klein, N.A., and Soules, M.R. (1996). Influence of maternal age on meiotic spindle assembly in oocytes from naturally cycling women. Hum Reprod *11*, 2217-222.

Baumann, C., Viveiros, M.M., and De La Fuente, R. (2010). Loss of maternal ATRX results in centromere instability and aneuploidy in the mammalian oocyte and pre-implantation embryo. PLoS Genet *6*

*B*o, H., Ghazizadeh, M., Shimizu, H., Kurihara, Y., Egawa, S., Moriyama, Y., Tajiri, T., and Kawanami, O. (2004). Effect of ionizing irradiation on human esophageal cancer cell lines by cDNA microarray gene expression analysis. J Nippon Med Sch *71*, 172-180.

Brennan, I.M., Peters, U., Kapoor, T.M., and Straight, A.F. (2007). Polo-like kinase controls vertebrate spindle elongation and cytokinesis. PLoS One *2*, e409.

Brenner, S., Pepper, D., Berns, M.W., Tan, E., and Brinkley, B.R. (1981). Kinetochore structure, duplication, and distribution in mammalian cells: analysis by human autoantibodies from scleroderma patients. J Cell Biol *91*, 95-102.

Burkard, M.E., Randall, C.L., Larochelle, S., Zhang, C., Shokat, K.M., Fisher, R.P., and Jallepalli, P.V. (2007). Chemical genetics reveals the requirement for Polo-like kinase 1 activity in positioning RhoA and triggering cytokinesis in human cells. Proc Natl Acad Sci U S A *104*, 4383-88.

Cam, H.P., Sugiyama, T., Chen, E.S., Chen, X., FitzGerald, P.C., and Grewal, S.I. (2005). Comprehensive analysis of heterochromatin- and RNAi-mediated epigenetic control of the fission yeast genome. Nat Genet *37*, 809-819.

Caviness, V.S., Goto, T., Tarui, T., Takahashi, T., Bhide, P.G., and Nowakowski, R.S. (2003). Cell output, cell cycle duration and neuronal specification: a model of integrated mechanisms of the neocortical proliferative process. Cereb Cortex *13*, 592-98.

Coutinho-Camillo, C.M., Miracca, E.C., dos Santos, M.L., Salaorni, S., Sarkis, A.S., and Nagai, M.A. (2006). Identification of differentially expressed genes in prostatic epithelium in relation to androgen receptor CAG repeat length. Int J Biol Markers *21*, 96-105.

Davids, M.S., and Steensma, D.P. (2010). The molecular pathogenesis of myelodysplastic syndromes. Cancer Biol Ther *10*, 309-319.

Di Cunto, F., Calautti, E., Hsiao, J., Ong, L., Topley, G., Turco, E., and Dotto, G.P. (1998). Citron rho-interacting kinase, a novel tissue-specific ser/thr kinase encompassing the Rho-Rac-binding protein Citron. J Biol Chem *273*, 29706-711.

Di Cunto, F., Imarisio, S., Hirsch, E., Broccoli, V., Bulfone, A., Migheli, A., Atzori, C., Turco, E., Triolo, R., et al. (2000). Defective neurogenesis in citron kinase knockout mice by altered cytokinesis and massive apoptosis. Neuron *28*, 115-127.

Djupedal, I., Portoso, M., Spåhr, H., Bonilla, C., Gustafsson, C.M., Allshire, R.C., and Ekwall, K. (2005). RNA Pol II subunit Rpb7 promotes centromeric transcription and RNAi-directed chromatin silencing. Genes Dev *19*, 2301-06.

Drané, P., Ouararhni, K., Depaux, A., Shuaib, M., and Hamiche, A. (2010). The death-associated protein DAXX is a novel histone chaperone involved in the replication-independent deposition of H3.3. Genes Dev *24*, 1253-265.

Earnshaw, W.C., and Migeon, B.R. (1985). Three related centromere proteins are absent from the inactive centromere of a stable isodicentric chromosome. Chromosoma *92*, 290-96.

Eda, M., Yonemura, S., Kato, T., Watanabe, N., Ishizaki, T., Madaule, P., and Narumiya, S. (2001). Rho-dependent transfer of Citron-kinase to the cleavage furrow of dividing cells. J Cell Sci *114*, 3273-284.

Emoto, K., Kobayashi, T., Yamaji, A., Aizawa, H., Yahara, I., Inoue, K., and Umeda, M. (1996). Redistribution of phosphatidylethanolamine at the cleavage furrow of dividing cells during cytokinesis. Proc Natl Acad Sci U S A *93*, 12867-872.

Eppig, J.T., and Barker, J.E. (1984). Chromosome abnormalities in mice with Hertwig's anemia. Blood *64*, 727-732.

Fish, J.L., Kosodo, Y., Enard, W., Pääbo, S., and Huttner, W.B. (2006). Aspm specifically maintains symmetric proliferative divisions of neuroepithelial cells. Proc Natl Acad Sci U S A *103*, 10438-443.

Fong, K.W., Choi, Y.K., Rattner, J.B., and Qi, R.Z. (2008). CDK5RAP2 is a pericentriolar protein that functions in centrosomal attachment of the gamma-tubulin ring complex. Mol Biol Cell *19*, 115-125.

García-Cao, M., O'Sullivan, R., Peters, A.H., Jenuwein, T., and Blasco, M.A. (2004). Epigenetic regulation of telomere length in mammalian cells by the Suv39h1 and Suv39h2 histone methyltransferases. Nat Genet *36*, 94-99.

Gartenberg, M. (2009). Heterochromatin and the cohesion of sister chromatids. Chromosome Res *17*, 229-238.

Gieni, R.S., Chan, G.K., and Hendzel, M.J. (2008). Epigenetics regulate centromere formation and kinetochore function. J Cell Biochem *104*, 2027-039.

Glotzer, M. (2001) Animal cell cytokinesis. Cell and Dev Biol *17*, 351-386.

Goldberg, A.D., Banaszynski, L.A., Noh, K.M., Lewis, P.W., Elsaesser, S.J., Stadler, S., Dewell, S., Law, M., Guo, X., et al. (2010). Distinct factors control histone variant H3.3 localization at specific genomic regions. Cell *140*, 678-691.

Higgins, J., Midgley, C., Bergh, A.M., Bell, S.M., Askham, J.M., Roberts, E., Binns, R.K., Sharif, S.M., Bennett, C., et al. (2010). Human ASPM participates in spindle organisation, spindle orientation and cytokinesis. BMC Cell Biol *11*, 85.

Higgs, D.R., and Weatherall, D.J. (2009). The alpha thalassaemias. Cell Mol Life Sci *66*, 1154-162.

Hodges, C.A., Revenkova, E., Jessberger, R., Hassold, T.J., and Hunt, P.A. (2005). SMC1beta-deficient female mice provide evidence that cohesins are a missing link in age-related nondisjunction. Nat Genet *37*, 1351-55.

Hu, W., Feng, Z., Modica, I., Klimstra, D.S., Song, L., Allen, P.J., Brennan, M.F., Levine, A.J., and Tang, L.H. (2010). Gene Amplifications in Well-Differentiated Pancreatic Neuroendocrine Tumors Inactivate the p53 Pathway. Genes Cancer *1*, 360-68.

Jiao, Y., Shi, C., Edil, B.H., de Wilde, R.F., Klimstra, D.S., Maitra, A., Schulick, R.D., Tang, L.H., Wolfgang, C.L., et al. (2011). DAXX/ATRX, MEN1, and mTOR pathway genes are frequently altered in pancreatic neuroendocrine tumors. Science *331*, 1199-1203.

Jin, C., and Felsenfeld, G. (2007). Nucleosome stability mediated by histone variants H3.3 and H2A.Z. Genes Dev *21*, 1519-529.

Kernohan, K.D., Jiang, Y., Tremblay, D.C., Bonvissuto, A.C., Eubanks, J.H., Mann, M.R., and Bérubé, N.G. (2010). ATRX partners with cohesin and MeCP2 and contributes to developmental silencing of imprinted genes in the brain. Dev Cell *18*, 191-202.

Koch, B., Kueng, S., Ruckenbauer, C., Wendt, K.S., and Peters, J.M. (2008). The Suv39h-HP1 histone methylation pathway is dispensable for enrichment and protection of cohesin at centromeres in mammalian cells. Chromosoma *117*, 199-210.

De La Fuente, R., Viveiros, M.M., Wigglesworth, K., and Eppig, J.J. (2004). ATRX, a member of the SNF2 family of helicase/ATPases, is required for chromosome alignment and meiotic spindle organization in metaphase II stage mouse oocytes. Dev Biol *272*, 1-14.

Lehnertz, B., Ueda, Y., Derijck, A.A., Braunschweig, U., Perez-Burgos, L., Kubicek, S., Chen, T., Li, E., Jenuwein, T., and Peters, A.H. (2003). Suv39h-mediated histone H3 lysine 9 methylation directs DNA methylation to major satellite repeats at pericentric heterochromatin. Curr Biol *13*, 1192-1200.

Lewis, P.W., Elsaesser, S.J., Noh, K.M., Stadler, S.C., and Allis, C.D. (2010). Daxx is an H3.3-specific histone chaperone and cooperates with ATRX in replication-independent chromatin assembly at telomeres. Proc Natl Acad Sci U S A *107*, 14075-080.

Lizarraga, S.B., Margossian, S.P., Harris, M.H., Campagna, D.R., Han, A.P., Blevins, S., Mudbhary, R., Barker, J.E., Walsh, C.A., and Fleming, M.D. (2010). Cdk5rap2 regulates centrosome function and chromosome segregation in neuronal progenitors. Development *137*, 1907-917.

Low, S.H., Li, X., Miura, M., Kudo, N., Quiñones, B., and Weimbs, T. (2003). Syntaxin 2 and endobrevin are required for the terminal step of cytokinesis in mammalian cells. Dev Cell *4*, 753-59.

Lu, J., and Gilbert, D.M. (2007). Proliferation-dependent and cell cycle regulated transcription of mouse pericentric heterochromatin. J Cell Biol *179*, 411-421.

Madaule, P., Furuyashiki, T., Eda, M., Bito, H., Ishizaki, T., and Narumiya, S. (2000). Citron, a Rho target that affects contractility during cytokinesis. Microsc Res Tech *49*, 123-26.

Maison, C., Bailly, D., Peters, A.H., Quivy, J.P., Roche, D., Taddei, A., Lachner, M., Jenuwein, T., and Almouzni, G. (2002). Higher-order structure in pericentric heterochromatin involves a distinct pattern of histone modification and an RNA component. Nat Genet *30*, 329-334.

McDowell, T.L., Gibbons, R.J., Sutherland, H., O'Rourke, D.M., Bickmore, W.A., Pombo, A., Turley, H., Gatter, K., Picketts, D.J., et al. (1999). Localization of a putative transcriptional regulator (ATRX) at pericentromeric heterochromatin and the short arms of acrocentric chromosomes. Proc Natl Acad Sci U S A *96*, 13983-88.

Montgomery, E., Wilentz, R.E., Argani, P., Fisher, C., Hruban, R.H., Kern, S.E., and Lengauer, C. (2003). Analysis of anaphase figures in routine histologic sections distinguishes chromosomally unstable from chromosomally stable malignancies. Cancer Biol Ther *2*, 248-252.

Nan, X., Hou, J., Maclean, A., Nasir, J., Lafuente, M.J., Shu, X., Kriaucionis, S., and Bird, A. (2007). Interaction between chromatin proteins MECP2 and ATRX is disrupted by mutations that cause inherited mental retardation. Proc Natl Acad Sci U S A *104*, 2709-714.

Nonaka, N., Kitajima, T., Yokobayashi, S., Xiao, G., Yamamoto, M., Grewal, S.I., and Watanabe, Y. (2002). Recruitment of cohesin to heterochromatic regions by Swi6/HP1 in fission yeast. Nat Cell Biol *4*, 89-93.

Normand, G., and King, R.W. (2010). Understanding cytokinesis failure. Adv Exp Med Biol *676*, 27-55.

Pan, H., Ma, P., Zhu, W., and Schultz, R.M. (2008). Age-associated increase in aneuploidy and changes in gene expression in mouse eggs. Dev Biol *316*, 397-407.

Peters, A.H., O'Carroll, D., Scherthan, H., Mechtler, K., Sauer, S., Schöfer, C., Weipoltshammer, K., Pagani, M., Lachner, M., et al. (2001). Loss of the Suv39h histone methyltransferases impairs mammalian heterochromatin and genome stability. Cell *107*, 323-337.

Petronczki, M., Glotzer, M., Kraut, N., and Peters, J.M. (2007). Polo-like kinase 1 triggers the initiation of cytokinesis in human cells by promoting recruitment of the RhoGEF Ect2 to the central spindle. Dev Cell *12*, 713-725.

Pidoux, A.L., and Allshire, R.C. (2004). Kinetochore and heterochromatin domains of the fission yeast centromere. Chromosome Res *12*, 521-534.

Roy, D., Guida, P., Zhou, G., Echiburu-Chau, C., and Calaf, G.M. (2008). Gene expression profiling of breast cells induced by X-rays and heavy ions. Int J Mol Med *21*, 627-636.

Santamaria, A., Neef, R., Eberspächer, U., Eis, K., Husemann, M., Mumberg, D., Prechtl, S., Schulze, V., Siemeister, G., et al. (2007). Use of the novel Plk1 inhibitor ZK-thiazolidinone to elucidate functions of Plk1 in early and late stages of mitosis. Mol Biol Cell *18*, 4024-036.

Sarkisian, M.R., Li, W., Di Cunto, F., D'Mello, S.R., and LoTurco, J.J. (2002). Citron-kinase, a protein essential to cytokinesis in neuronal progenitors, is deleted in the flathead mutant rat. J Neurosci *22*, RC217.

Seah, C., Levy, M.A., Jiang, Y., Mokhtarzada, S., Higgs, D.R., Gibbons, R.J., and Bérubé, N.G. (2008). Neuronal death resulting from targeted disruption of the Snf2 protein ATRX is mediated by p53. J Neurosci *28*, 12570-580.

Serrano, E., Lasa, A., Perea, G., Carnicer, M.J., Brunet, S., Aventín, A., Sierra, J., and Nomdedéu, J.F. (2006). Acute myeloid leukemia subgroups identified by pathway-restricted gene expression signatures. Acta Haematol *116*, 77-89.

Steensma, D.P., Higgs, D.R., Fisher, C.A., and Gibbons, R.J. (2004). Acquired somatic ATRX mutations in myelodysplastic syndrome associated with alpha thalassemia (ATMDS) convey a more severe hematologic phenotype than germline ATRX mutations. Blood *103*, 2019-026.

Wong, L.H., McGhie, J.D., Sim, M., Anderson, M.A., Ahn, S., Hannan, R.D., George, A.J., Morgan, K.A., Mann, J.R., and Choo, K.H. (2010). ATRX interacts with H3.3 in maintaining telomere structural integrity in pluripotent embryonic stem cells. Genome Res *20*, 351-360.

Xue, Y., Gibbons, R., Yan, Z., Yang, D., McDowell, T.L., Sechi, S., Qin, J., Zhou, S., Higgs, D., and Wang, W. (2003). The ATRX syndrome protein forms a chromatin-remodeling complex with Daxx and localizes in promyelocytic leukemia nuclear bodies. Proc Natl Acad Sci U S A *100*, 10635-640.

Yingling, J., Youn, Y.H., Darling, D., Toyo-Oka, K., Pramparo, T., Hirotsune, S., and Wynshaw-Boris, A. (2008). Neuroepithelial stem cell proliferation requires LIS1 for precise spindle orientation and symmetric division. Cell *132*, 474-486.

Appendices

Appendix A: Statement of permission for the reproduction of copyrighted material.

This thesis contains figures from previously published manuscripts:

> Figure 1-1: Gibbons, R.J., Wada, T., Fisher, C.A., Malik, N., Mitson, M.J., Steensma, D.P., Fryer, A., Goudie, D.R., Krantz, I.D., and Traeger-Synodinos, J. (2008). Mutations in the chromatin-associated protein ATRX. Hum Mutat *29*, 796-802.
>
> Figure 1-2: Farkas, L.M., and Huttner, W.B. (2008). The cell biology of neural stem and progenitor cells and its significance for their proliferation versus differentiation during mammalian brain development. Curr Opin Cell Biol *20*, 707-715.
>
> Figure 1-3: Götz, M., and Huttner, W.B. (2005). The cell biology of neurogenesis. Nat Rev Mol Cell Biol *6*, 777-788.

All previously published figures that have been reproduced in this thesis have been granted permission from the copyright holder (see Appendices B to D).

Chapter 2 of this thesis represents a previously published manuscript:

> Ritchie, K., Seah, C., Moulin, J., Isaac, C., Dick, F., and Bérubé, NG (2008) Loss of ATRX leads to chromosome cohesion and congression defects. JCB Jan 28;**180**(2):315-24.

The material in chapter two was reproduced in this thesis in accordance with the policy of Rockefeller University Press, which states that authors are free to use their own published work for any purpose without express permission (see Appendix E).

Appendix B: License for the reproduction of the previously published figure represented as Figure 1-1 in this thesis.

JOHN WILEY AND SONS LICENSE TERMS AND CONDITIONS

Jun 08, 2011

This is a License Agreement between Kieran L Ritchie ("You") and John Wiley and Sons ("John Wiley and Sons") provided by Copyright Clearance Center ("CCC"). The license consists of your order details, the terms and conditions provided by John Wiley and Sons, and the payment terms and conditions.

All payments must be made in full to CCC. For payment instructions, please see information listed at the bottom of this form.

License Number	2684341317715
License date	Jun 08, 2011
Licensed content publisher	John Wiley and Sons
Licensed content publication	Human Mutation
Licensed content title	Mutations in the chromatin-associated protein ATRX
Licensed content author	Richard J. Gibbons,Takahito Wada,Christopher A. Fisher,Nicola Malik,Matthew J. Mitson,David P. Steensma,Alan Fryer,David R. Goudie,Ian D. Krantz,Joanne Traeger-Synodinos
Licensed content date	Jun 1, 2008
Start page	796
End page	802
Type of use	Dissertation/Thesis
Requestor type	University/Academic
Format	Print and electronic
Portion	Figure/table
Number of figures/tables	1
Number of extracts	
Original Wiley figure/table number(s)	Figure 1
Will you be translating?	No

Appendix C: License for the reproduction of the previously published figure represented as Figure 1-2 in this thesis.

ELSEVIER LICENSE
TERMS AND CONDITIONS

Jun 08, 2011

This is a License Agreement between Kieran L Ritchie ("You") and Elsevier ("Elsevier") provided by Copyright Clearance Center ("CCC"). The license consists of your order details, the terms and conditions provided by Elsevier, and the payment terms and conditions.

All payments must be made in full to CCC. For payment instructions, please see information listed at the bottom of this form.

Supplier	Elsevier Limited The Boulevard,Langford Lane Kidlington,Oxford,OX5 1GB,UK
Registered Company Number	1982084
Customer name	Kieran L Ritchie
Customer address	800 Commissioners Road East London, ON N6C 2V5
License number	2684351138918
License date	Jun 08, 2011
Licensed content publisher	Elsevier
Licensed content publication	Current Opinion in Cell Biology
Licensed content title	The cell biology of neural stem and progenitor cells and its significance for their proliferation versus differentiation during mammalian brain development
Licensed content author	Lilla M Farkas, Wieland B Huttner
Licensed content date	December 2008
Licensed content volume number	20
Licensed content issue number	6
Number of pages	9
Start Page	707
End Page	715
Type of Use	reuse in a thesis/dissertation
Portion	figures/tables/illustrations
Number of figures/tables/illustrations	1
Format	both print and electronic
Are you the author of this Elsevier article?	No
Will you be translating?	No
Order reference number	
Title of your thesis/dissertation	THE REGULATION OF CELL DIVISION AND NEUROGENESIS BY THE CHROMATIN REMODELING PROTEIN ATRX
Expected completion date	Jul 2011
Estimated size (number of pages)	170
Elsevier VAT number	GB 494 6272 12

Appendix D: License for reproduction of the previously published figure represented as Figure 1-3 in this thesis.

NATURE PUBLISHING GROUP LICENSE TERMS AND CONDITIONS

Jun 08, 2011

This is a License Agreement between Kieran L Ritchie ("You") and Nature Publishing Group ("Nature Publishing Group") provided by Copyright Clearance Center ("CCC"). The license consists of your order details, the terms and conditions provided by Nature Publishing Group, and the payment terms and conditions.

All payments must be made in full to CCC. For payment instructions, please see information listed at the bottom of this form.

License Number	2684360063668
License date	Jun 08, 2011
Licensed content publisher	Nature Publishing Group
Licensed content publication	Nature Reviews Molecular Cell Biology
Licensed content title	The cell biology of neurogenesis
Licensed content author	Magdalena Gotz and Wieland B. Huttner
Licensed content date	Oct 1, 2005
Volume number	6
Issue number	10
Type of Use	reuse in a thesis/dissertation
Requestor type	academic/educational
Format	print and electronic
Portion	figures/tables/illustrations
Number of figures/tables/illustrations	1
High-res required	no
Figures	Figure 4
Author of this NPG article	no
Your reference number	
Title of your thesis / dissertation	THE REGULATION OF CELL DIVISION AND NEUROGENESIS BY THE CHROMATIN REMODELING PROTEIN ATRX
Expected completion date	Jul 2011
Estimated size (number of pages)	170

Appendix E: Permission and licensing policy of Rockefeller University Press for the reproduction of the published manuscript represented in Chapter 5.

Source: http://www.rupress.org/site/misc/permissions.xhtml

Permissions and Licensing

Rockefeller University Press Home > Permissions

It is the mission of The Rockefeller University Press to promote widespread reuse and distribution of the articles and data we publish. In this spirit, authors retain copyright to their own work and can reuse it for any purpose as long as proper attribution is provided. Third parties may use our published materials undera Creative Commons Attribution-Noncommercial-Share Alike 3.0 Unported License six months after publication. Within the first six months, the same conditions for reuse apply, except we prohibit the creation of mirror sites. Commercial reuse must be requested as described below and will incur a fee.

We encourage you to read more about our permission policies and the Creative Commons License terms:

- You wrote it; you own it! (Hill and Rossner, 2008)
- RUP Copyright Policy

Requesting Permission Licensing

Please read below to determine if you must obtain permission for your specific reuse.

Original author reuse (commercial and noncommercial)

Ownership of copyright remains with RUP authors, who may reuse their own material forany purpose, including commercial profit, as long as they provide proper attribution. The permission does not extend to the institution.

- Note that our preferred citation style is as follows:
- ©AUTHOR et al., YEAR. Originally published in *JOURNAL NAME*. doi:########.
- If an article does not carry a doi, our preferred citation style is as follows:
- ©AUTHOR et al., YEAR. Originally published in *JOURNAL NAME*. VOL:PP–PP.

Noncommercial third-party reuse

Third parties may reuse our content for noncommercial purposes without specific permission as long as they provide proper attribution (see citation preferences provided above). Within the first 6 months after publication, the creation of mirror sites is prohibited.

Appendix F: Statement of permission for the use of animals for experimental research.

All animal experimentation was conducted in compliance with the animal use protocol 2008-041-02 held by Dr. Nathalie Bérubé, principal investigator at the Schulich School of Medicine and Dentistry and the department of Paediatrics at the University of Western Ontario in London, Ontario, Canada.

Curriculum Vitae

Name: Kieran L Ritchie

Post-secondary Education and Degrees:
The University of Western Ontario
London, Ontario, Canada
2001-2005 BSc Hon. Genetics

Honours and Awards:

Winner - Best oral presentation (Senior basic sciences division) Paediatrics Research Day. Lawson Health Research Institute, London, Ontario, Canada. 2010

Winner - Best poster presentation (Senior basic sciences divison) Paediatrics Research Day. Lawson Health Research Institute, London, Ontario, Canada. 2009

Ontario Graduate Scholarship (15,000$/1 year), Ontario Student Assistance Program, The Government of Ontario. 2009-2010.

Graduate Research Scholarship (10,000$/1 year), The Scottish Rite Charitable Foundation of Canada. 2008-2009.

Winner (Honourable mention) - Best poster. Mechanism and Control of Mitosis (Abcam plc.). May 19th, 2008. Worcester, Massachusetts, USA.

Trainee of the Year Award. Children's Health Research Institute, London, Ontario, Canada. 2008.

Graduate Research Scholarship (10,000$/year, 1 year), The Scottish Rite Charitable Foundation of Canada. 2007-2008.

Chair's Research Award (1,000$). The Department of Biochemistry, The University of Western Ontario, 2007.

Graduate Thesis Research Award (1,250$), Schulich School of Medicine and Dentistry, The University of Western Ontario, 2007.

Related Work Experience:
Summer research project
Supervised by Dr. Nathalie Bérubé, Research Scientist, Children's Health Research Institute
Victoria Research Labs, London, Ontario, Canada

Publications:

1. CH Coschi, AL Martens, K Ritchie, SM Francis, S Chakrabarti, NG Berube, and FA Dick (2010) Mitotic chromosome condensation mediated by the retinoblastoma protein is tumor suppressive. *Genes & Dev.* 24: 1351-1363.
2. K Ritchie, C Seah, J Moulin, C Isaac, F Dick, and NG Bérubé (2008) Loss of ATRX leads to chromosome cohesion and congression defects. *J. Cell Biol.* 180(2): 315-324.